Investigating the role of mitochondrial damage-associated molecular patterns in the myeloma bone marrow microenvironment

By

Aisha Jibril, BSc

A thesis submitted for the degree:

Doctor of Philosophy

Norwich Medical School
Department of Molecular Haematology
The University of East Anglia, Norwich, UK

Date of submission: 3rd October 2022.

Declaration

I declare that the contents of this thesis entitled “Investigating the role of mitochondrial damage-associated molecular patterns in the myeloma bone marrow microenvironment” was carried out and completed by myself unless otherwise acknowledged and has not been submitted in support of an application for another degree or qualification in this or any other university or institution.

This thesis is approximately 40,000 words in length.

Aisha Jibril

Acknowledgements

Praises to Allah (swt) whose guidance and blessings have sustained me in this pursuit of knowledge. As I reflect on the past three years, I see a network of supportive, inspiring individuals who have seen me through this journey of unexpected challenges and rewarding experiences.

Firstly, I would like to express utmost appreciation to my supervisors Stuart and Kris, whose understanding and enthusiastic encouragement have been incomparable. You have fostered such a supportive lab environment, and I consider myself very fortunate to have been under your mentorship. To my fellow Rushworth lab members Jayna, Jamie, Charlotte, Rebecca, and Kat. Thank you for your invaluable teamwork and the many laughs that made long days in the lab an enjoyable experience. A special mention to Charlotte with whom I started this PhD journey, thank you for really looking out for me - the delicious bakes were a bonus! Notably, I would like to express my gratitude to the MM patients who generously donated research samples and the wonderful NHS staff at the NNUH who played an instrumental part in this PhD.

To my friends (Alice, Zara, Poppy, and Latife) who have provided the most joyous distractions from work, I'm truly grateful for your friendship. A special thanks to Zara, whose motivational pep talks were always just a FaceTime call away. To the support system that I am blessed to call my family, who are cast near and far and are too countless to name, but instrumental nonetheless, your prayers and steadfast belief in me have supported me during this process and for that I am thankful. A heartfelt shoutout to the G-Town clan for the constant source of quality entertainment and fierce encouragement, thank you for being the best hype team of siblings imaginable!

Finally, to Mama and Baba, your unwavering, unequivocal love and support have been a driving force my whole life. I am forever indebted to you for selflessly forging a life that afforded me the opportunities and experiences that have shaped me into who I am today, and so I dedicate this milestone to you.

Alhamdullilah, always.

Abstract

Mitochondrial damage-associated molecular patterns (mtDAMPs) encompass a group of mitochondrial-derived molecules such as proteins, lipids, metabolites, and DNA. Capable of activating innate immune system responses via pattern recognition receptors (PRRs), mtDAMPs possess immunoregulatory functions. Elevated levels of circulating mtDNA have been implicated in the pathogenesis of various diseases including cancer. Though the functional outcomes of the observation remain largely undefined. Multiple myeloma (MM) is an incurable haematological malignancy. A hallmark of MM is its homing to the bone marrow (BM) niche where MM cells are heavily reliant upon interactions with cells such as macrophages for their survival. Macrophages have been shown to interact with MM cells to promote disease progression. In this thesis, I investigated the role of mtDAMPs in the pro-tumoral BM microenvironment of MM.

This study identifies elevated levels of circulating mtDNA in the serum of MM patients compared to healthy controls. The use of an NSG xenograft mouse model of MM ascertained that circulating mtDNA is derived from MM cells. Functionally, mtDAMPs were shown to activate BM macrophages via the cGAS-STING signalling pathway. mtDAMPs activation induced a gene expression profile in macrophages that mediated pro-inflammatory and pro-chemotactic responses. Inhibition of STING led to reduced MM progression in the C57BL/KaLwRij mouse model. Moreover, mtDAMPs stimulated the upregulation of chemokines in BM macrophages which enhanced the migration of MM cells *in vitro.* Clodronate-mediated depletion of macrophages highlighted the crucial role of macrophages in facilitating MM cell homing to the BM. Furthermore, STING inhibition attenuated the pro-chemotactic signature in BM macrophages and resulted in the egress of MM cells from the BM into the peripheral blood circulation. Taken together, these findings establish the functional role of mtDAMPs in the activation of macrophages which promote MM disease progression and mediates BM homing and retention of MM cells in the BM niche.

Table of Contents

List of publications and conference papers

Jibril, A., Hellmich, C., Wojtowicz, E.E., Moore, J.A., Mistry, J.J., Maynard, R., Hampton, K., Bowles, K.M., Rushworth, S.A. Plasma cell-derived mtDAMPs activate the macrophage STING pathway which promotes myeloma progression. (Submitted to Blood).

Moore, J.A., Mistry, J.J., Hellmich, C., Horton, R.H., Wojtowicz, E.E., **Jibril, A**., Jefferson, M., Wileman, T., Beraza, N., Bowles, K.M., Rushworth, S.A. LC3-associated phagocytosis in bone marrow macrophages suppresses acute myeloid leukemia progression through STING activation. Journal of Clinical Investigation. (2022 Jan). DOI:10.1172/jci153157

Mistry, J. J., Hellmich, C., Moore, J. A., **Jibril, A**., Macaulay, I., Moreno-Gonzalez, M., Di Palma, F., Beraza, N., Bowles, K. M., Rushworth, S. A. Free fatty-acid transport via CD36 drives β-oxidation-mediated hematopoietic stem cell response to infection. Nature Communications. (2021 Dec). DOI: 10.1038/s41467-021-27460-9.

Mistry, J.J., Hellmich, C., Lambert, A., Moore, J.A., **Jibril, A**., Collins, A., Bowles, K.M., Rushworth, S.A. Venetoclax and Daratumumab combination treatment demonstrates pre-clinical efficacy in mouse models of Acute Myeloid Leukemia. Biomarker Research. (2021 May). DOI: 10.1186/s40364-021-00291-y.

Mistry, J.J., Moore, J.A., Kumar, P., Marlein, C.R., Hellmich, C., Pillinger, G., **Jibril, A**., Di Palma, F., Collins, A., Bowles, K.M., Rushworth, S.A. Daratumumab inhibits acute myeloid leukaemia metabolic capacity by blocking mitochondrial transfer from mesenchymal stromal cells. Haematologica. (2020 Mar). DOI:10.3324/haematol.2019.242974.

Malignant Plasma Cell Derived Mitochondrial Damps Activate Macrophages Via STING Signalling to Promote Myeloma Development. Abstract #351. **Oral presentation. American Society of Hematology Annual Meeting 2022. ASH abstract achievement award.**

Multiple Myeloma Derived Mitochondrial DAMPs Induce Inflammation in Bone Marrow Adipose Tissue Which Promotes Tumour Development. Abstract #2654. **Poster presentation. American Society of Hematology Annual Meeting 2021.**

Multiple Myeloma Derived Mitochondrial DAMPs Promote a Pro-Inflammatory Signature Within the Myeloma Bone Marrow Microenvironment. **Oral presentation. UK Myeloma Forum Autumn Day. UKMF/GSK bursary.**

Multiple Myeloma Derived Mitochondrial DAMPs Promote a Pro-Inflammatory Signature Within the Myeloma Bone Marrow Microenvironment. Abstract #S179. **Oral presentation with Live Q&A panel. European Hematology Association Virtual Congress. EHA participation grant.**

Multiple Myeloma Derived Mitochondrial DAMPs Induce a Pro-Inflammatory Signature in The Bone Marrow Microenvironment to Promote Pro-Tumoral Expansion. Abstract #2799. **Poster presentation. American Association of Cancer Research Annual Meeting 2021.**

Myeloma Derived Mitochondrial Damage Associated Molecular Patterns Promote Pro-Tumoral Expansion by Inducing a Pro-Inflammatory Signature in The Bone Marrow Microenvironment. Abstract #1348. **Poster presentation. American Society of Hematology Annual Meeting 2020. ASH abstract achievement award.**

Myeloma Derived Mitochondrial DNA Activates TLR9 Driven Pro-tumoral Expansion. Abstract #4228. **Poster presentation. American Association of Cancer Research Annual Meeting 2020.**

List of Figures

List of Tables

List of abbreviations

ALL	Acute lymphoblastic leukaemia
AML	Acute myeloid leukaemia
APRIL	A proliferation-inducing lingand
ARG-1	Arginase-1
ATP	Adenosine-5'-triphosphate
BCMA	B-cell maturation antigen
BM	Bone marrow
BMAT	Bone marrow adipose tissue
BMDM	Bone marrow derived macrophage
BMM	Bone marrow microenvironment
BMMΦ	Bone marrow macrophage
BMSC	Bone marrow stromal cell
C57BL/6	C57 Black 6
CAM-DR	Cell adhesion mediated drug resistance
CCL	C-C motif chemokine ligand
CCR	C-C motif chemokine receptor
cGAMP	2'3' cyclic GMP-AMP
cGAS	cyclic GMP-AMP synthase
CL	Cardiolipin
CLL	Chronic lymphocytic leukaemia
CLP	Common lymphoid progenitor
CML	Common myeloid leukaemia
CMP	Common myeloid progenitor
CNS	Central nervous system
CpG	5'-Cytosine-phosphate-Guanine-3' dinucleotide
Ct	Cycle threshold
CXCL	C-X-C motif chemokine ligand
CXCR	C-X-C motif chemokine receptor
DMEM	Dulbecco's Modifed Eagle's Medium
DMSO	Dimethyl sulfoxide
ECM	Extracellular matrix

FACS	Flouresence activated cell sorting
fMLP	N-formyl-methionyl-leucyl-phenylalanine
FMO	Fluorescence minus one
FPR	Formyl peptide receptor
FSC	Forward scatter
G-CSF	Granulocyte colony stimulating factor
gDNA	Genomic DNA
GFP	Green flourescent protein
GM-CSF	Granulocyte-macrophage colony stimulating factor
GMP	Granulocyte-macrophage progenitor
HSC	Haematopoietic stem cell
HSPC	Haematopoietic stem and progenitor cell
IFN	Interferon
Ig	Immunoglbulin
IL	Interleukin
IP	Intraperitoneal
IRF	Interferon regulator factors
ISG	Interferon stimulated genes
IV	Intravenous
LMPP	Lymphoid-primed multipotent progenitor
LT-HSC	Long-term haematopoietic stem cell
MAMΦ	Myeloma-associated macrophage
MEP	Megakaryocyte-erythrocyte progenitors
M-CSF	Macrophage-colony stimulating factor
MGUS	Monoclonal gammopathy of undetermined significance
miR	Micro RNA
MM	Multiple myeloma
MPP	Multipotent progenitor
mtDAMP	Mitochondrial damage-associated molecular pattern
mtDNA	Mitochondrial DNA
MSC	Mesenchymal stromal cell
NFP	N-formyl peptide
NOD	Non-Obese Diabetic

NSG	NOD SCID gamma mice
NK	Natural killer
ODN	Oligodeoxynucleotide
PAMP	Pathogen associated molecular pattern
PB	Peripheral blood
PRR	Pattern recognition receptor
qPCR	Real time quantitative polymerase chain reaction
RAGE	Receptor for advanced glycation end-products
RANKL	Receptor activator of nuclear factor kappa-B ligand
ROS	Reactive oxygen species
SCID	Severe Combined Immunodeficiency
SIRS	Systemic inflammatory response syndrome
SMM	Smouldering multiple myeloma
SNP	Single nucleotide polymorphism
SSC	Side scatter
ST-HSC	Short-term haematopoietic stem cell
STING	Stimulator of IFN genes
TAM	Tumour associated macrophages
TFAM	Mitochondrial transcription factor A
TLR	Toll-like receptor
VCAM	Vascular cell adhesion molecule
VEGF	Vascular endothelial growth factor

1 Introduction

1.1 The Bone and Bone Marrow

Bones are comprised of two types of osseous tissue, cortical bone and cancellous bone (Figure 1.1). Cortical bone is also known as compact bone, it is strong and dense and makes up the outer cortex of all bones. Cancellous bone, however, is light and spongy composed of bone projections in a mesh-like network of trabeculae that occupies the centre of the bone. Different bones contain different ratios of these two bone tissues in order to fulfil the unique flexibility and strength needs required of bones [1]. Bone marrow (BM) is the soft, spongy tissue which exists within the central cavities of bones, specifically the long and axial bones of the skeleton [2]. Bone marrow is comprised of both yellow marrow and red marrow. The bone marrow is the primary and largest haematopoietic organ, where new mature blood cells are made during a process called haematopoiesis. This process takes place in the aptly named red marrow, due to its high haem chromogen content [3]. At birth, the bone marrow consists of solely red marrow but with age more is converted to yellow marrow which contains a higher proportion of adipocytes [4]. This fatty yellow marrow has previously been dismissed as inert and only serving to fill space [5], however, in recent years research has shown that this adipocyte-rich marrow plays an important role in energy storage, bone metabolism, and endocrine function [6-8]. Under stressed conditions, when there is an increased haematopoietic demand yellow marrow can be converted to red marrow to support haematopoiesis [9]. The vascular arrangement of the bone marrow allows for the supply of nutrients to the marrow tissue. In long bone, these nutrients are supplied by a main nutrient artery which enters through the centre of the marrow cavity longitudinally, branching out towards the border of the surrounding bone as vascular vessels known as sinusoids. These sinusoids combine to form collecting venules which drain into a central vein that runs parallel to the nutrient artery. This creates a system whereby blood in the bone marrow flows from the centre of the bone towards the periphery and returns to the centre [10].

Consequently, there is a vast system of blood vessels present in the bone periphery. This results in a clear distribution of the two marrow tissue types with yellow marrow favouring the central cavity, and red marrow favouring the endosteal region closer to the cancellous bone [3].

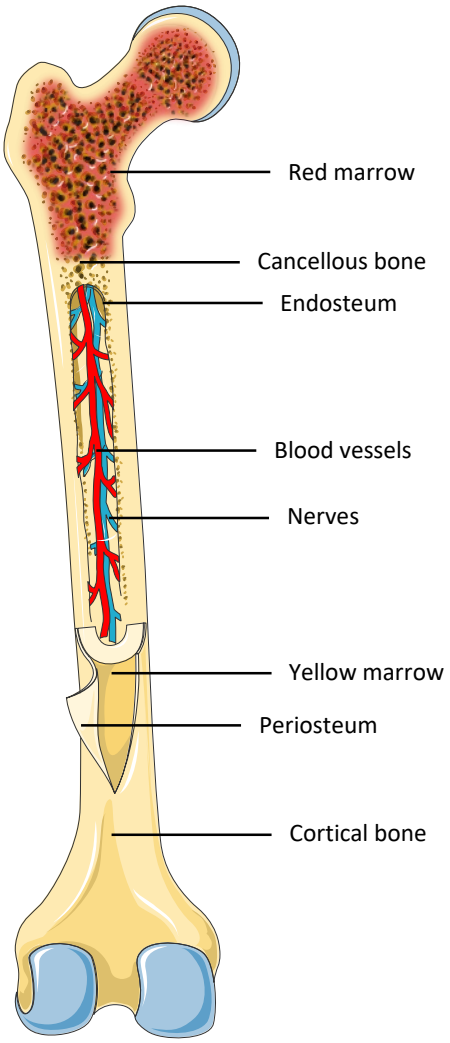

Figure 1.1. Structure and anatomy of long bones.

Comprised of cortical bone which makes up the outer shell of the bone, and cancellous spongy bone. The endosteum lines the inner cavity of long bones and encases the red marrow, blood vessels and nerve fibres. The periosteum is a thin layer of connective tissue that encases the yellow marrow.

The BM is innervated by a neural network comprised of 96% autonomic and 4% sensory nerve fibres [11], which help to regulate haematopoiesis and bone remodelling via the release of neuropeptides and neurotransmitters. Sympathetic noradrenergic nerve fibres can express tyrosine hydroxylase (TH) or neuropeptide Y (NPY). TH-expressing nerve fibres release noradrenaline which acts upon the β3 adrenergic receptors on mesenchymal stem cells (MSC) in the bone marrow to suppress the release of Haematopoietic stem cell (HSC) retention factor, C-X-C motif chemokine ligand 12 (CXCL12). It also causes the mobilisation and proliferation of haematopoietic stem and progenitor cells (HSPC) as well as the suppression of osteoblast function via β2 adrenergic receptors [12]. NPY nerve fibres also facilitate the mobilisation of HSPCs acting via Y1 receptors in osteoblasts to activate matrix metalloproteinase-9 (MMP-9) which degrades HSPC retention factors [13]. The parasympathetic nervous system opposes the sympathetic nervous system and thus, in the context of bone marrow innervation, acts to achieve HSPC retention. Parasympathetic choline acetyltransferase (ChAT) nerve fibres produce the neurotransmitter acetylcholine which acts upon nicotinic acetyl-cholinergic receptors on osteoblasts and osteoclasts to promote the proliferation of the former and the apoptosis of the latter [12]. Osteoblasts release osteopontin which HSPCs adhere to via β1 integrin, this results in the retention of HSPCs and the reduced expansion of the HSC pool in the bone marrow [14]. Neuropeptide substance P (SP) and calcitonin gene-related peptide (CGRP) are released by sensory nerve fibres. SP promotes HSPC retention by inducing the release of stem cell factor (SCF) and CXCL12 from MSC, whilst CGRP promotes MSC differentiation into osteoblasts [12]. Altogether, this displays the importance of the autonomic and sensory nerves in the regulation of HSPC homeostasis in the bone marrow.

1.2 Haematopoiesis

Haematopoiesis is an active and continuous process that occurs in the BM, by which all mature blood cells are produced. The process originates from the haematopoietic stem cells (HSC), multipotent cells which give rise to red blood cells and white blood cells [15]. On average, $5x10^{11}$ mature blood cells are produced by the bone marrow every day. With a daily output comprised of approximately $2x10^{11}$ red blood cells, $1x10^{10}$ white blood cells, and $4x10^{11}$ platelets [16, 17]. With such a large production volume, it is imperative to have an efficient process of blood cell production in order to maintain homeostasis.

During development, definitive haematopoiesis involves the multipotent HSCs which are found in the aorta-gonad-mesonephros (AGM) region of the developing embryo. HSCs are found in specialised microenvironments, or niches, within the bone marrow and their stemness is proven by their multipotency, quiescence and ability to self-renew [18]. The HSCs migrate to the foetal liver, spleen, and finally, the bone marrow, which is the primary site of haematopoiesis in adulthood [19]. However, under times of haematopoietic stress, infection or trauma where there is bone marrow failure, extramedullary haematopoiesis can occur in the spleen and liver [20].

The classical haematopoietic hierarchical model has been the traditional dogma for understanding the differentiation process of the HSC (Figure 1.2A). In this model, the HSC pool can be split into two populations based on their CD34 expression, $CD34^-$ long-term (LT)-HSCs and $CD34^+$ short-term (ST)-HSCs. LT-HSCs are a scarce and quiescent cell population, they differentiate into ST-HSCs which successively differentiate into multipotent progenitors (MPPs) [21]. These progenitors can branch off into two progenitor cell lineages, common myeloid (CMP) and common lymphoid progenitors (CLP). CMPs further branch and differentiate into megakaryocyte-erythrocyte progenitors (MEP) and granulocyte-macrophage progenitors (GMP) giving rise to megakaryocytes and erythrocytes, and granulocytes and monocytes respectively. On the other branch, CLPs differentiate into B-cells, T-cells and natural killer (NK) cells [22].

Through further study of the HSC population and its differentiation, it has now been identified that the MPP population can be further subdivided into four distinct progenitor phenotypes. MPP1 are very similar to the previously defined ST-HSCs, MPP2 is a megakaryocyte-biased MPP whereas MPP3 is a myeloid-biased MPP. MPP4 is lymphoid-biased and is thought to give rise to the lymphoid-primed multipotent progenitor (LMPP), a progenitor which differentiates and contributes to the GMP and the CLP population [22, 23]. This suggests that the HSC differentiation pathway may not be such a distinct step-by-step process. The heterogeneous nature of the HSC pool means that the process of haematopoiesis is complex and further study is still needed to fully uncover all the pathways of HSC differentiation. Landmark single-cell transcriptomics findings [24, 25] revealed snapshots of single HSPCs as they traversed differentiation landscapes, suggesting that cells differentiate along a trajectory that does not fit into a rigid branching tree model. Thus, triggering a shift in ideologies from the traditional hierarchical model towards a continuum of differentiation model (Figure 1.2B). This model states that HSCs may be able to give rise to fated cells without passing through distinct intermediate cell types [26-28]. Therefore, HSCs gradually progress from one cell population to the next, remaining highly flexible in order to meet variable blood demands which is advantageous in responding to stimuli such as stress, infection, and malignancy.

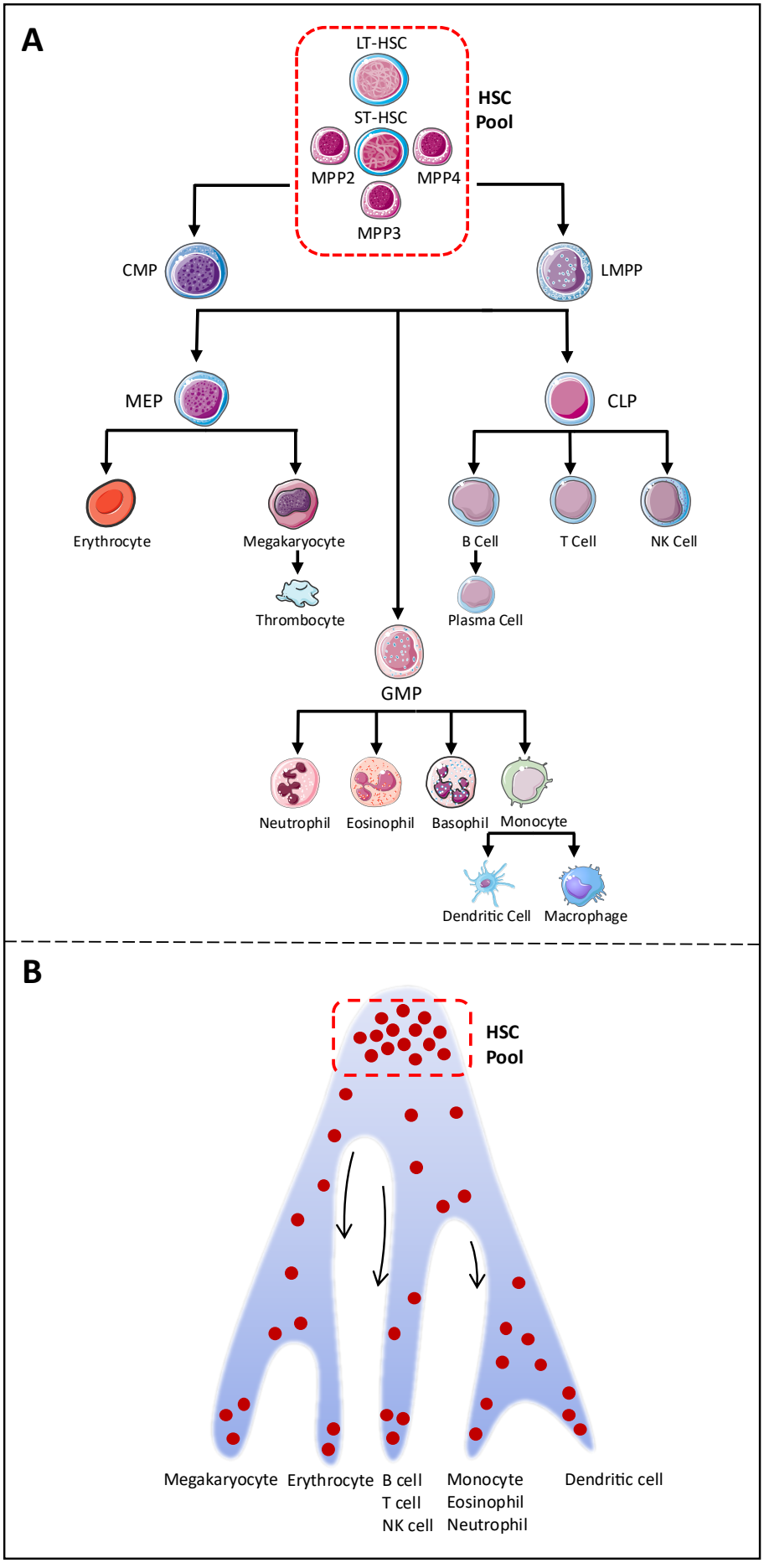
A
LT-HSC
ST-HSC
MPP2
MPP4
MPP3
HSC
Pool
CMP
LMPP
MEP
CLP
Erythrocyte
Megakaryocyte
B Cell
T Cell
NK Cell
Thrombocyte
Plasma Cell
GMP
Neutrophil
Eosinophil
Basophil
Monocyte
Dendritic Cell
Macrophage
B
HSC
Pool
Megakaryocyte
Erythrocyte
B cell
T cell
NK cell
Monocyte
Eosinophil
Neutrophil
Dendritic cell

Figure 1.2. Hierarchical models of haematopoiesis.

Haematopoiesis is the process of differentiation from haematopoietic stem cells to mature blood cells, passing through intermediate progenitor cell states. (A) The traditional haematopoietic tree model. The haematopoietic stem cell pool contains self-renewing HSCs of varied quiescence and maturity, with LT-HSCs being the most immature and quiescent. ST-HSCs and MPPs differentiate to give rise to megakaryocyte-erythrocyte (MEP), granulocyte-macrophage (GMP), and common lymphoid (CLP) progenitors which go on to differentiate into the cellular components of blood. (B) The continuum differentiation model. Advances in single-cell transcriptomic suggested that haematopoiesis occurs as cells gradually gain lineage bias as they differentiate, red dots represent single cells. (Adapted from Laurenti and Göttgens, 2018).

1.3 Bone Marrow Microenvironment

The main role of the bone marrow is to carry out haematopoiesis. Along with haematopoietic cells, non-haematopoietic cells within the bone marrow microenvironment (BMM) play an important role in facilitating this process by providing essential factors which support the HSC niche.

1.3.1 Bone marrow mesenchymal stromal cells

Bone marrow mesenchymal stromal cells (BMSC) also known as bone marrow stromal cells, play an important role in supporting the haematopoietic niche. BMSCs are highly heterogenous multipotent stem cells and different subgroups of BMSC exist within the BM niche. They have been shown to differentiate into other supportive cells of the BMM such as osteoblasts, endothelial cells, chondrocytes, and adipocytes [29]. In comparison to HSCs, the differentiation of BMSCs is less well-defined and various researchers have attempted to classify BMSCs via the identification of certain expression markers. A population of BMSCs have been found to express high levels of stem cell factor (SCF) and the HSC maintenance cytokine CXCL12 [30], and as such are named CXCL12 abundant reticular (CAR) cells [31]. Therefore, this subgroup of CAR-BMSCs plays an important role in the retention of HSCs within the BM niche and facilitates the regulation of HSC proliferation. BMSCs can be further classified by their expression of the melanoma adhesion molecule CD146 [32], nestin [33], and leptin receptor (LepR) [34]. These markers allow for the determination of the different BMSC population's spatial arrangement within the BM microenvironment and their effects on influencing HSC quiescence and proliferation. CAR and $CD146^+$ BMSCs are located near the sinusoids and blood vessels, whilst $nestin^+$ BMSCs reside in the perivascular region and are closely associated with HSCs [33, 35]. $LepR^+$ cells are found adjacent to sinusoids in the perisinusoidal niche and have been found to drive HSC proliferation. Conversely, $LepR^-$ cells contribute to the arterial niche residing close to small arterioles in the endosteal region and support HSC quiescence [36].

The multipotency of BMSCs leads to the generation of other BM stromal cells. These BMSC derivative cells support the BM microenvironment and provide their own contributions to the regulation and support of the HSC niche.

1.3.2 Adipocytes

BMSCs give rise to BM adipocytes which are the most abundant cell type within the adult BM [37]. In healthy adults, BM adipose tissue (BMAT) accounts for approximately 70% of bone marrow volume and 10% of total fat mass [38, 39]. Naturally with age BMAT accumulates, however, increased BM adiposity is also observed in clinical conditions including obesity, osteoporosis, type 1 diabetes, and cancer [40-43]. BMAT has unique features that distinguish it from white or brown adipose tissue found elsewhere in the body. There are two distinct populations of BMAT: regulated marrow adipose tissue (rMAT) located in proximal skeletal sites, is comprised of single adipocytes interspersed with red marrow and is thought to be actively involved in haematopoiesis. Constitutive marrow adipose tissue (cMAT) located in distal skeletal sites, contains large adipocytes and is thought to be inactive in haematopoiesis [44-46].

Adipocytes play an important role in bone marrow metabolism, they act as fat stores and contain lipid droplets filled with neutral lipids in the form of triglycerides which can be broken down into free fatty acids (FFA) and glycerol via a process known as lipolysis [47]. A key regulator for the differentiation of adipocytes is the activation of peroxisome proliferator-activated receptor gamma (PPARγ). Inhibition of this activation has been shown to impair adipocyte differentiation *in vitro* [48]. The CAAT- enhancer binding proteins (C/EBPs) are a family of transcription factors that are also key regulators of adipogenesis. Adipocytes are able to regulate haematopoiesis through cell-to-cell contact. Furthermore, they are able to prevent granulopoiesis via neuropilin-1 (NP1), which induces the inhibition of granulocyte colony-stimulating factor (G-CSF) [49]. They also arrest HSPCs in the G0 cell cycle phase and induce their apoptosis [50].

BM adipocytes also secrete certain haematopoietic regulatory cytokines and factors. For example, adipocytes secrete SCF [51] which promotes haematopoietic regeneration, whilst TGF-β1 acts as an inhibitor of haematopoiesis [52]. Lipocalin 2 (LCN2) and dipeptidyl peptidase 4 (DPP4) are both recently identified adipokines which are secreted by adipocytes and are able to negatively regulate haematopoiesis through the inhibition of erythroid progenitor differentiation and cleavage of essential haematopoietic cytokines, respectively [53, 54]. Adipocytes also secrete hormones to regulate HSCs. Adiponectin acts upon receptors AdipoR1 and AdipoR2 which are expressed on HSCs to induce their proliferation and maintain their undifferentiated state [55]. Leptin is secreted into the BMM by adipocytes and aids in the proliferation and differentiation of HSCs, whilst prostaglandin inhibits HSC proliferation and differentiation via apoptosis. The cytokine interleukin 6 (IL-6) is secreted by adipocytes to drive the differentiation of HSCs [56]. Therefore, adipocytes have a distinct role in modulating the HSC bone marrow niche.

1.3.3 Osteolineage cells

Osteolineage cells are derived from MSCs and play a role in HSC maintenance in the BMM, they have the capacity to differentiate into bone-forming cell types including pre-osteoblasts, mature osteoblasts, and osteocytes [57]. Osteoblasts secrete the growth factors and cytokines, osteopontin, G-CSF, and hepatocyte growth factor [58-60] which are important in inducing HSC mobilisation. By observing the maturation of osteoblasts, studies revealed that immature osteoblasts express high levels of runt-related transcription factor 2 (RUNX2) which correlates with an increase in haematopoiesis-enhancing (HEA) activity and is thought to act via CD166 [61]. This suggests that pre-osteoblasts have a role to play in the expansion and maintenance of HSCs. Whilst the idea remains that mature osteoblasts expressing lower levels of CD166 and RUNX2 are not essential to the regulation of HSCs [62].

Osteocytes are commonly described as terminally differentiated osteoblasts which are embedded within the bone matrix. They extend long dendritic processes which function to communicate with other osteolineage cells via intercellular gap junctions or by paracrine signalling [57].

An *in vivo* mouse study by Asada et al. revealed that in the absence of osteocytes, G-CSF failed to mobilise HSPCs into the circulation, indicating the role of osteocytes in G-CSF induced HSPC mobilisation [63]. Osteocytes have also been found to regulate haematopoiesis. In an *in vivo* mouse study by Sato et al., the ablation of osteocytes in mice led to drastic lymphopenia in the bone marrow, caused by a lack of lymphoid supporting stroma [64]. Though these cells are found rooted in the bone, they prove to play an important role in assisting the mobilisation of HSCs and supporting their haematopoietic differentiation.

1.3.4 Endothelial cells

Specialised endothelial cells called hemogenic endothelium, are found within the dorsal aorta where the first HSPCs derive from during embryonic development [65]. As a highly vascular tissue, endothelial cells are a major component forming the lining of the sinusoid-vascular niche within the bone marrow microenvironment. These vascular endothelial cells produce SCF and therefore contribute to HSC maintenance [34, 66]. Moreover, endothelial cells have been found to secrete IL-6, G-CSF, and granulocyte-macrophage colony-stimulating factor (GM-CSF). When co-cultured in direct contact with BM endothelial cells (BMECs), HSPCs were found to expand and generate progenitor cell populations for up to seven days [67]. This highlights that BMECs regulate HSPC proliferation via cytokine release.

E-selectin is an adhesion molecule specific to BMECs and has been shown to play a key role in regulating HSC proliferation, *in vivo* knock-out of E-selectin resulted in HSC quiescence [68]. Additionally, endothelial cells serve as a physical barrier at the BM-blood interface. BMECs express vascular cell adhesion molecule 1 (VCAM-1) [69, 70] which binds to its ligand very late antigen 4 (VLA-4) present on HSCs, this interaction is required in mediating the movement of HSPCs between the blood and bone marrow [71, 72].

Though they account for less than 2% of bone marrow cells [73], the current body of literature shows that endothelial cells are an important component of the BMM in the support of haematopoiesis.

1.3.5 Macrophages

Macrophages (MΦ) are derived from monocytes and have a phagocytic function which plays a crucial role in tissue homeostasis and both innate and adaptive immunity.

Monocytes circulate in the blood, bone marrow, and spleen remaining in circulation for 1-2 days [74]. When recruited to a tissue site they differentiate into macrophages for the purpose of phagocytosis whereby pathogens, cellular debris, apoptotic cells, malignant cells, or other targets are removed by engulfment and digestion [74, 75].

Macrophages play a crucial role in the enucleation process. Within the bone marrow erythroid niche, sites of erythropoiesis called erythroblastic islands consist of a central macrophage surrounded by erythroblasts [76]. Erythroblastic island macrophages are a unique erythropoietin receptor (EpoR) expressing sub-population. EpoR signalling is crucial for efficient erythropoiesis [77]. The role of these macrophages is to phagocytose the expelled nuclei, also known as a pyrenocyte, from committed erythroid progenitors in order to aid erythrocyte formation [78].

Macrophages also play a pivotal role in maintaining the endosteal HSC niche, $CD169^+$ macrophages promote HSC retention via promoting BM stromal cell release of the HSPC retention factor CXCL12 [79]. Depletion of these macrophages via clodronate-loaded liposomes or macrophage Fas-induced apoptosis, led to the mobilisation of HSPCs into the blood [80]. This finding indicates that macrophages play a crucial role in retaining HSPCs within the BM microenvironment. Therefore, suggesting that macrophages possess chemotactic functions which mediate BM homing and retention of various cells.

1.3.5.1 Macrophage activation

MΦ are highly plastic cells that are able to be polarised towards different phenotypes in response to environmental stimuli, which trigger their activation to meet specific situational needs (Figure 1.3). The most common phenotypic classification of these macrophages is modelled on the T helper 1/2 paradigm which states that macrophages can be polarised according to the cytokine production profile of T helper (T_H) lymphocytes [81]. T_H1 lymphocytes produce interferon-gamma (IFNγ) and polarise macrophages towards an M1 or "classically activated" phenotype, whereas T_H2 lymphocytes produce IL-4 which results in macrophages polarised towards an M2 or "alternatively activated" phenotype [82]. These distinct macrophage populations exhibit different functions.

1.3.5.2 Classically activated macrophages

M1 macrophages are stimulated by IFN-γ which is produced by T_H1 cells and natural killer cells, as well as macrophages themselves. M1 polarisation can also be activated by lipopolysaccharide (LPS), which makes up the outer membrane of gram-negative bacteria [83, 84]. These stimuli are detected via pattern recognition receptors (PRRs) that are involved in both innate and adaptive immunity. The IFN-γ receptor (IFNGR) is comprised of 2 subunits IFNGR-1 and IFNGR-2, receptor signalling recruits Janus kinase (JAK) adaptors which activates signal transducers and activators of transcription 1 (STAT1), which then activates interferon regulator factors (IRFs) and the transcription of interferon-stimulated genes (ISGs) [85]. Toll-like receptor (TLR) 4 recognises LPS and upon signalling the NF-κB pathway is activated which results in the production of pro-inflammatory cytokines such as (IL-6, IL-1β, IL-12, IL-18, and TNF-α) as well as chemokines (CCL2, CXCL10, and CXCL11) [86]. Recently, GM-CSF has also been recognised as a stimulator of M1 macrophage polarisation.

This signalling results in JAK2 recruitment and subsequent activation of STAT5, V-Akt murine thymoma viral oncogene homolog 1 (AKT), extracellular signal-regulated kinase (ERK), as well as the nuclear translocation of NF-κB and IRF5. This results in further regulation of the IFN-γ and NF-κB signalling pathways to further enhance cytokine production [87, 88]. Upon activation, M1 macrophages express CD16/32, CD80, and CD86, the expression of these cell surface markers aids in characterising macrophage populations.

Macrophages can also be characterised by their ability to secrete a range of chemokines, and pro-inflammatory cytokines, as well as the generation of nitric oxide (NO) via inducible nitric oxide synthase (iNOS) production and reactive oxygen species (ROS) [89]. As such, M1 macrophages mediate pro-inflammatory responses which aid in pathogen clearance, microbial defence and tumoricidal activity (Figure 1.3).

However, dysregulation of M1 polarisation has been implicated in the pathology of some autoimmune diseases. Synovial inflammation in rheumatoid arthritis has been shown to be exacerbated by M1 macrophages [90], this inflammation was resolved by reducing the levels of pro-inflammatory M1 macrophages in favour of anti-inflammatory M2 macrophages via manganese ferrite and ceria nanoparticle-anchored mesoporous silica nanoparticles (MFC-MSNs) which act by down-regulating the production of hypoxia-inducible factor (HIF-1α) [91].

However, sometimes the flexibility of the macrophage polarisation paradigm can be exploited by the very targets it aims to overcome. For example, the opportunistic fungus *Candida albicans* induces an M1 to M2-like phenotype switch in macrophages. This reduces NO production in favour of macrophage arginase activity, thereby reducing the microbicidal function and mediating *C. albicans* survival [92, 93].

Overall, the classical activation of macrophages is required for microbial defence. This form of polarisation is tailored to allow macrophages to respond in an appropriate fashion to achieve this function.

1.3.5.3 Alternatively activated macrophages

M2 macrophages can be characterised by their cell surface expression of CD163 and CD206 [94]. These cells were first shown to be polarised by IL-4 and IL-13 produced by T_H2 cells, basophils, eosinophils, or macrophages themselves [95, 96]. Whilst the cytokines share functional receptors, the receptors for IL-4 are mainly expressed on haematopoietic cells, whereas IL-13 receptors are present on non-haematopoietic cells [94]. The IL-4 receptor is comprised of two transmembrane proteins, IL-4 has an affinity for the IL-4Rα chain which can then recruit either the common gamma chain (γC) to form the type I receptor complex or dimerise with IL-13Rα1 to form the type II receptor complex which is the IL-4 receptor found exclusively on non-haematopoietic cells [97, 98]. IL-13 on the other hand binds to IL-13Rα1 before heterodimerisation with IL-4Rα to form a functional type II receptor complex [99]. However, it has also been shown that IL-13 can be bound with high affinity to IL-13Rα2 which is regarded as a decoy receptor which inhibits IL-13 binding to IL-13Rα1 and thereby functional type II complex formation [100]. The IL-4/IL-13 signalling pathways result in the phosphorylation and subsequent translocation of STAT6 to the nucleus where it regulates gene transcription [98, 101].

M2 macrophages produce IL-10, arginase 1 (ARG1), resistin-like molecule α (FIZZ1), and chitinase-like protein (YM1) [102]. IL-10 is another M2 polarising cytokine, it signals via the IL-10 receptor and activates STAT3-mediated gene expression of anti-inflammatory and immunosuppressive cytokines IL-10 and TGF-β [103]. IL-10 is a potent inhibitor of inflammation as it is able to inhibit pro-inflammatory cytokine production and activity by M1 macrophages, as such, M2 macrophages play an important regulatory role in the pro-inflammatory response. The gene expression profile of M2 macrophages also suggests a host protective function in contributing to the clearance of nematodes and helminths via ARG1 production [104, 105].

Furthermore, YM1 and other chitinase-like molecules have been shown to possess carbohydrate and extracellular matrix-binding activity, which would suggest that M2 macrophages play a role in wound healing and tissue repair homeostasis [106].

However, the functions of these alternatively activated macrophages can become detrimental when dysregulated. For example, in cases of chronic schistosomiasis caused by the parasitic worm *Schistosoma mansoni,* the pathological liver fibrosis that occurs is a result of the uncontrolled activation of M2 macrophages and their ARG1 mediated wound-healing capabilities. This pathology failed to be induced when ARG1 activity was inhibited in IL-4/IL-13 deficient mice [107]. Furthermore, M2 macrophages have been implicated in asthma pathogenesis and have been shown to mediate allergic lung pathology [108].

As our understanding of macrophage polarisation expands, further subsets of M2 macrophages have been described which differ dependent on the stimuli (Figure 1.3). M2a macrophages are stimulated by IL-4 or IL-13, M2b macrophages are stimulated by LPS or IL-1β, and M2c macrophages are stimulated by IL-10 [89]. All of these subsets produce minimal to null levels of pro-inflammatory cytokines and high levels of IL-10. However, M2a macrophages are characterised by high CD86 and CD200R expression, and they produce CCL13, CCL17, and CCL22. M2b macrophages are characterised by high CD80 and CD14 expression. M2c macrophages were characterised by high CD163 expression and CCL16 and CCL18 expression [109]. Finally, a novel M2d macrophage subset that can inhibit M1 macrophage activity has been proposed as a tumour-associated macrophage (TAM) phenotype [110].

1.3.5.4 Tumour-associated macrophages

Macrophages are heavily involved in the remodelling of the inflammatory tumour microenvironment, this invasive cell population are termed tumour-associated macrophages [111]. TAMs are usually associated with having a similar phenotype to M2 macrophages and are influenced by the tumour microenvironment to promote angiogenesis, tumour growth, immune evasion, and metastasis [112, 113]. M1 macrophages are notably considered tumour-killing macrophages as they release cytotoxic NO and ROS, therefore the ideal route for therapeutic intervention would involve converting pro-tumoral M2-TAMs to an anti-tumoral M1-TAM phenotype [114]. Characterisation of TAMs makes their pro-tumorigenic functions clear. TAMs express high levels of the anti-inflammatory cytokine IL-10 which has been shown to inhibit pro-inflammatory cytokine production by M1 macrophages [103, 110]. They also have poor antigen-presenting capabilities and prevent T-cell activation which aids in immune evasion [115]. Furthermore, they produce vascular endothelial growth factor (VEGF), platelet-derived endothelial cell growth factor (PDGF), and matrix metalloproteinases (MMPs) which contribute to tumour cell angiogenesis, proliferation, and survival [110, 116].

Whilst the classification of macrophages into discrete sub-categories is convenient, there are instances in which this has been proven to be an oversimplification. For example, this has been demonstrated in systemic sclerosis-related interstitial lung disease, where a population of macrophages that expressed both M1 and M2 markers were found to be implicated in the pathogenesis of the disease [117]. Taken together, it is evident that the macrophage is a highly complex cell type, the plasticity of macrophage functions suggests that polarisation occurs on a transitionary spectrum and that the M1/M2 paradigm may not be sufficient to encompass the variation in macrophage phenotypes (Figure 1.3).

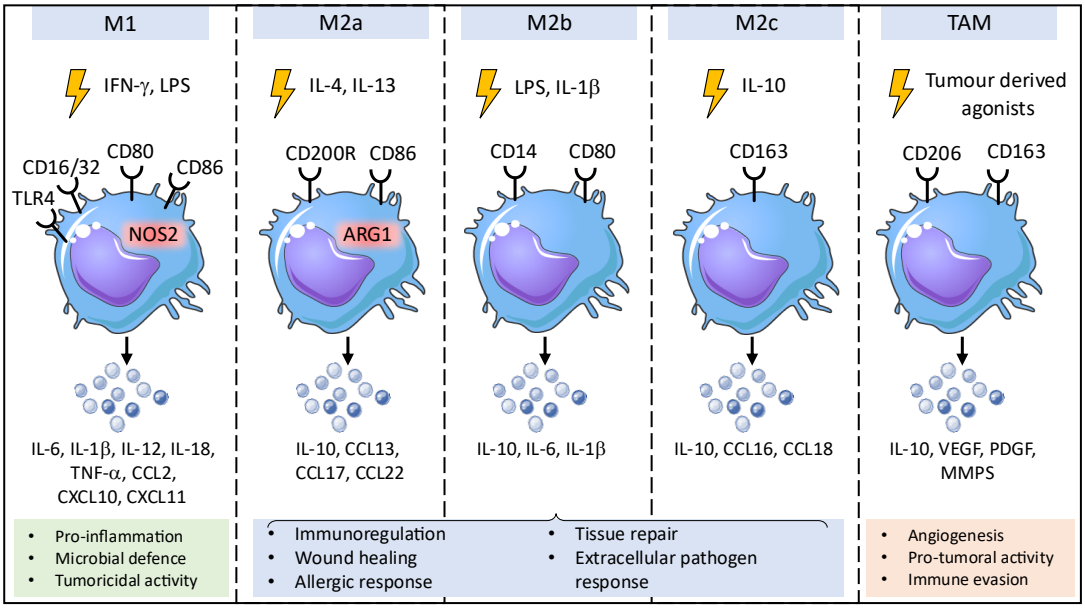

Figure 1.3. Polarisation of different macrophage subsets.

Depending on external stimuli, macrophage polarisation can be triggered to alter their gene expression profiles to carry out specific functions. M1 macrophage polarisation is triggered by LPS and IFN-g and results in pro-inflammatory and anti-tumoral responses. M2 macrophages are responsible for a range of immunoregulatory functions. M2a macrophages are polarised by IL-4 and IL-13. M2b macrophages are induced by LPS and IL-1b. M2c macrophages are polarised by IL-10. Tumour-associated macrophages (TAM) are polarised by tumour-derived intermediates and promote functions that support tumour progression processes such as angiogenesis and immune evasion.

1.4 Malignancy

Malignancy is defined as a group of diseases, also termed cancer, whereby abnormal malignant cells divide uncontrollably invading nearby tissues and metastasising to other parts of the body [118]. In most cases, this aberrant behaviour is caused by the accumulation of genetic alterations that affect the cell cycle such as the activation of oncogenes and/or the deactivation of tumour suppressor genes as well as epigenetic changes that can also induce pro-cancer genetic alterations [119, 120]. The transformation of normal cells into malignant cells is a multi-step process that encompasses six biological capabilities, or “hallmarks” of cancer, that are acquired by the cells. These hallmarks include the ability to sustain proliferative signalling, the evasion of growth suppressors, resistance to programmed cell death, the acquisition of replicative immortality, the induction of angiogenesis, and the activation of invasion and metastasis [118]. Hanahan et al. further proposed the characteristics of energy metabolism reprogramming and immune system evasion as two additional hallmarks [121]. Collectively, these functional capabilities facilitate the proliferation, survival, and dissemination of cancer cells in the body.

1.4.1 Bone marrow malignancy

Bone marrow malignancies describe a range of cancers that arise in the bone marrow. These include leukaemia and multiple myeloma. Leukaemia is characterised by an abnormal accumulation of malignant white blood cells in the bone marrow and blood. Leukaemia can be split into four different subtypes based on how aggressive the cancer is, chronic or acute, and the haematopoietic lineage that is affected, myeloid or lymphoid. Chronic disease is associated with the malignancy of mature leukocytes, whereas the acute form stems from the malignancy of immature leukocytes and has a rapid progression.

1.4.2 Chronic Lymphocytic Leukaemia

Chronic lymphocytic leukaemia (CLL) diagnosis is characterised by the presence of >5 x 10^9 CD19 positive B lymphocytes/L in the peripheral blood with the immunophenotypic profile of CD5, CD23, and low CD20 expression [122]. In adults, CLL is the most prevalent leukaemia, with more incidences occurring in older adults as the median age of diagnosis is 72 [123]. IL- 6 and IL-10 serum expression is elevated in CLL patients and correlates with poor disease prognosis [124]. As with most malignancies, the progression of CLL is reliant upon the support of a suitable tumour microenvironment. Within the bone marrow microenvironment, CLL cells require cell-to-cell interaction with endothelial cells via β1 and β2 integrins which promote the survival and chemoresistance of the disease [125]. LYN kinase and Bruton's tyrosine kinase (BTK) expression on monocytes/macrophages have been shown to be important in the survival of CLL [126]. Thus, the BMM is important in the progression of CLL and cellular interactions prove to be advantageous to the progression of this leukaemia.

1.4.3 Acute Lymphocytic Leukaemia

Acute lymphocytic leukaemia (ALL) is a malignancy of immature lymphocytes that can affect either B-cell or T-cell progenitors and is the most common form of cancer in children [127]. Approximately 80% of patients will have B-cell ALL and the rest T-cell ALL [128]. ALL has been shown to cause changes to the BMM creating favourable conditions for the leukaemia to progress. ALL cells secrete receptor activator of nuclear factor kappa-B ligand (RANKL) which is responsible for osteoclast-mediated bone loss and reduction of osteoblast and adipocyte numbers [129] which disrupts the normal homeostasis of haematopoiesis within the BM. β1 integrins VLA-4/ α4β1 and VLA-5/ α5β1 mediate BM homing in ALL and CXCL12/CXCR4 interaction enhances this integrin-adhesion which assists in the engraftment of ALL cells in the BM [130]. Thus, ALL can strategically shape the BM microenvironment to aid tumour survival and progression.

1.4.4 Chronic Myeloid Leukaemia

Chronic myeloid leukaemia (CML) is a myeloproliferative disease that results in the malignancy of the granulocyte lineage. It is a rarer form of leukaemia that has an incidence rate of approximately 1-2 per 100,000 per year [131]. Most cases of CML are caused by a chromosomal abnormality called the Philadelphia chromosome, a reciprocal translocation of the ABL1 gene on chromosome 9 to the BCR gene on chromosome 22, creating a new BCR-ABL1 fusion oncogene [132]. This oncogene results in the production of a non-receptor tyrosine kinase which is constitutively active, this results in signalling cascades that confer cell survival and resistance to cell death via the P13K pathway, and cell proliferation via the JAK/STAT and RAS signalling pathways [131]. BCR-ABL1 also affects the BMM by causing the overexpression of osteopontin [133], which suppresses the proliferation of HSCs within the BM. These interactions contribute to the favourable BMM conditions which allow for the survival and progression of CML.

1.4.5 Acute Myeloid Leukaemia

Acute myeloid leukaemia (AML) is the most common form of acute leukaemia and is predominantly observed in older adults, with the incidence rate increasing from 1.3 cases per 100,000 in those under 65 to 12.2 per 100,000 in those over the age of 65 [134] according to US 2016 figures. AML is a malignancy of the myeloid lineage progenitors and as such is a heterogeneous disease which contributes to its complexity and lethality. 70% of over 65s who are diagnosed with AML die within a year of their diagnosis [134]. Genetic mutations have been associated with AML and have been shown to affect the disease prognosis such as FMS-like tyrosine kinase 3 (FLT3), tumour protein 53 (TP53), and nucleophosmin 1 (NPM1) [135]. AML also manipulates the BM microenvironment to create favourable conditions for leukemic survival. AML cells adhere to endothelial cells in the BMM via E-selectin, P-selectin and vascular adhesion molecule (VCAM)-1, these interactions promote angiogenesis through the Notch/Dll4 pathway which is important for the survival and proliferation of AML [8]. AML has also been shown to promote MSC differentiation to create a “pre-osteoblast-rich” BM niche, they also inhibit adipogenic differentiation which promotes the expansion of AML [136]. Thus, the crosstalk between AML and the BMM is very important in the progression of the disease.

1.4.6 Multiple Myeloma

Multiple myeloma (MM) is a clonal plasma cell malignancy arising from mutations in memory B-cells. According to 2016 American Cancer Society statistics, MM accounts for 10% of all haematological malignancies with an incidence rate of 6.2 per 100,000 individuals [137, 138]. MM is strongly linked to age as a risk factor, with half of the new cases occurring in those 75 years of age and above. The average five-year survival rate for MM is 52.3% although this can vary from 74% to 24% depending upon the age of diagnosis [139].

The malignant plasma cells primarily reside in the protective environment of the BM niche. The cells also secrete abnormal immunoglobulin (Ig) as well as an excess of light chains; these proteins are called monoclonal proteins (M-protein) or paraproteins. In most cases, these immunoglobulins are IgG or IgA however, in 20% of myeloma cases the cells only secrete monoclonal free light chains [137]. The presence of paraprotein can be detected in the blood serum and urine by electrophoresis and used to diagnose and monitor the progression of MM.

Multiple myeloma is preceded by two premalignant precursor disease states. The first is monoclonal gammopathy of undetermined significance (MGUS). Clinically, MGUS is characterised by M-protein levels of < 3g/dL, the presence of <10% plasma cells in the bone marrow, and a lack of the symptoms associated with MM. Smouldering multiple myeloma (SMM) also presents asymptomatically but is characterised as the presence of >3g/dL M-protein and >10% plasma cell presence in the bone marrow [140]. The onset of MGUS is thought to be partially caused by chromosomal aberrations, the most common being t (11;14), a translocation of the Ig heavy-chain (IgH) gene on chromosome 14 and the gene encoding cyclin D1 on chromosome 14, as well as deletion of chromosome 13 [141]. Sequencing of the IgH gene in MM cells has shown that the primary oncogenic event occurs in the germinal centres of the lymph nodes during plasma cell development [142]. These initial genetic mutations are detectable in MGUS patients suggesting that further oncogenic events are required for the progression of MGUS to a malignant state.

However, it is important to note that there is only a small risk, 1% per year, that MGUS patients progress to MM whilst SMM has a 10% risk per year, but that all MM cases are preceded by the premalignant phase [142]. MM is defined by the presence of end-organ damage known as CRAB features, they include hyperCalcaemia, Renal failure, Anaemia, and Bone lesions, as well as elevated levels of M-protein. In 2014, the diagnostic criteria were updated to account for cases where CRAB features were not present. These include a clonal plasma cell presence of >60% in the bone marrow, an elevated serum free light chain ratio, and one or more focal lesions on an MRI [143].

A range of treatment options are available for clinical use in the management of MM disease. Regimens combining multiple drugs are often the first line of treatment in newly diagnosed myeloma, the most common being a combination of bortezomib, lenalidomide, and dexamethasone (VRd), or daratumumab, lenalidomide, and dexamethasone (DRd). VRd is the preferred therapy option due to the low overall cost and the strong track record of high complete response rates [144]. In eligible patients, usually younger than 65 with no serious comorbidities, autologous stem cell transplantation is a standard of care as it provides a long remission period and improves overall survival by approximately 12 months [144, 145]. Despite a MM treatment standard of care consisting of four or more lines of therapy, including a proteasome inhibitor, an immunomodulatory drug, anti-CD38 monoclonal antibodies, and corticosteroids, patients often become resistant to these treatments and are classed as relapsed or refractory MM patients [146]. As such, MM remains incurable.

However, for patients with relapsed or refractory MM who have exhausted their treatment options, Chimeric antigen receptor (CAR) T-cell therapy provides an encouraging possibility for delaying disease progression and extending survival. CAR T-cell therapy is an immunotherapeutic approach that is rapidly developing and proving highly promising, with the U.S Food and Drug Administration (FDA) approved anti-CD19 CAR T-cell products to be used for the treatment of ALL (tisagenelcleucel/Kymriah) and diffuse large B-cell lymphoma (axicabtagene ciloleucel/Yescarta) in 2017 [147]. CAR T-cell therapy involves genetically engineering patient's T-cells so that they express chimeric antigen receptors specific to the target antigen of choice expressed on the cancer cell, this essentially reprogrammes the patient's immune system and redirects T-cell function to attack tumour cells via the cytolytic granzyme and perforin axis, and cytokine production [148, 149].

The most widely researched CAR target in MM is BCMA, which is present in all MM cells and whose overexpression is indicative of poor prognostic outcomes [150, 151]. In March 2021, idecabtagene vicleucel (Abecma) became the first BCMA-targeted CAR T-cell therapy to be FDA-approved for the treatment of relapsed or refractory MM [152]. Furthermore, in February 2022, following the success of the pivotal CARTITUDE-1 study, the FDA also approved another BCMA-directed CAR T-cell therapy ciltacabtagene autoleucel (CARVYKTI™) for the treatment of adults with relapsed or refractory MM [153, 154]. So far, CAR T-cell therapy has deservedly been regarded as a breakthrough development in cancer immunotherapy however, it is not without its drawbacks [147, 155]. Therapeutic resistance is still a possibility with CAR T-cell therapy caused by antigen escape due to the biallelic loss of BCMA expression on MM cells upon disease relapse after the first CAR T infusion [156]. Furthermore, due to the off-target effects of activated T-cells, the therapy can be toxic and there is a high incidence of cytokine release syndrome (CRS) as a side effect which can range from manifesting as mild flu-like symptoms to resulting in hypotension, liver failure, and cardiac arrest in extreme cases [157]. Neurotoxicity is another side effect that can vary from mild confusion to life-threatening seizures and cerebral edema [158]. Despite this, CAR T-cell therapy is a personalised immunotherapeutic that has come a long way in the treatment of MM with current CARs being optimised for functionality, efficiency and specificity. Furthermore, other non-BCMA antigen targets are being explored and undergoing pre-clinical and clinical trials [147].

Whilst there are exciting developments in the treatment of MM, relapse is still the probable outcome. This further emphasises the ongoing need for further research into understanding the pathogenesis of MM and its microenvironment in order to identify potential avenues for therapeutic intervention and expand the arsenal of treatment options available for MM patients.

1.4.6.1 Multiple Myeloma Microenvironment

The bone marrow microenvironment (Figure 1.4) plays an important role in the development and progression of MM [159]. The BMSC is an integral component for creating a favourable niche. VCAM-1 is expressed on the surface of BMSCs and interacts with $\alpha 4\beta 1$ integrin expressed on the myeloma cell, activating the NF-κB and mitogen-activated protein kinase (MAPK) signalling pathways. This causes the BMSC secretion of cytokines which are pro-proliferative and anti-apoptotic, such as IL-6, CXCL12, and vascular endothelial growth factor A (VEGFA) [142]. BMSCs are the main source of IL-6 in MM, a pro-inflammatory cytokine which promotes MM cell proliferation and survival [160]. CXCL12 binds to CXCR4 on the myeloma cell and is important for myeloma cell homing and migration towards sites of metastatic disease, where CXCL12 is highly expressed [161]. CXCL12 signalling also induces the secretion of IL-6 and VEGF.

VEGF is responsible for promoting angiogenesis [142]. BMSCs also express Jagged which activates Notch on MM cells, this has been shown to mediate resistance to de novo chemotherapeutic drugs [162, 163]. MM cells are capable of taking up microRNAs (miR) contained in exosomes released by BMSCs, it has been shown that these miRs help mediated drug resistance as well [164]. BMSCs promote the release of cyclophilin A (eCYPA) from BM endothelial cells (BMEC) via VEGFA which binds to its receptor VEGFR on the surface of BM endothelial cells. eCYPA binds to CD147 on the MM cell surface and promotes the proliferation and homing of MM [137, 165]. MM cells also express elevated levels of macrophage inhibitory factor (MIF), which causes BMSCs to release pro-inflammatory cytokines IL-6 and IL-8, and also aids in myeloma adhesion in the bone marrow and chemotherapy resistance [166, 167].

The extracellular matrix (ECM) is a component of the BM niche comprised of structural proteins such as collagen, laminin and fibronectin. MM cells express CD138, also known as syndecan-1, on their surface which binds to ECM proteins and mediates adhesion to MM cells, growth, and myeloma cell-cell adhesion [168]. MM cells also express the β1 integrins, α4β1 and α5β1 which bind to fibronectin in the ECM and cause cell adhesion mediated drug resistance (CAM-DR) [169].

Additionally, MM cells express programmed cell death ligand 1 (PDL1) which interacts with programmed death 1 receptor (PD1) on T cells, causing down-regulation of T cell function so that myeloma cells can evade the immune system. It was also recently discovered that the PD1/PDL1 pathway is a mechanism used by tumour-associated macrophages (TAM) and natural killer (NK) cells to confer MM tumour immunity [170-172]. TAMs secrete the pro-MM cytokines IL-1β, TNF-α, and IL-10 which support immune evasion via the suppression of T-cell function, they also secrete VEGFA which supports the process of angiogenesis [142].

Bone disease is a pathological feature of MM for which increased osteoclastogenesis is responsible. Interaction between RANK receptors on pre-osteoclasts and RANKL released by pre-osteoblasts and T-cells promotes osteoclast differentiation, this, in turn, decreases the number of osteoblasts in the BM niche. In normal conditions, pre-osteoblasts secrete osteoprotegerin (OPG) a soluble decoy of RANKL which would prevent the activation of osteoclasts. Consequently, in MM this protein is significantly under-expressed and thus osteoclast formation is favoured [142, 173]. Osteoclast differentiation and subsequent bone resorption are also driven by the chemokine CCL3 also known as macrophage inflammatory protein-1α (MIP-1α), which is highly expressed by MM cells, interacting with its receptor CCR1 found on pre-osteoclasts [174]. Osteoclasts secrete a proliferation-inducing ligand (APRIL) which binds to B-cell maturation antigen (BCMA) on MM cells and plays a vital role in the growth and survival of myeloma cells [160].

Osteolytic bone disease and its mechanism is well-defined as being due to the dysregulation of osteoblast and osteoclast function and homeostasis in the MM BMM. Adipocytes have also been shown to contribute to myeloma-associated bone disease via a reduction in the adipokine peroxisome proliferator-activated receptor γ (PPARγ) which suppresses osteoblastogenesis and enhances osteoclastogenesis [175]. Not only does MM impair osteoblastogenesis, but a study showed that osteoblast differentiation potential is shifted towards adipogenesis via increased heparanase production [176].

In MM there is an increased number of pre-adipocytes and larger mature adipocytes [177]. As endocrine cells, bone marrow adipocytes have been shown to play a key role in shaping the BMM via the secretion of soluble molecules. Adipocytes have been shown to secrete pro-MM cytokines such as osteopontin (OPN), VEGF, and IL-6 which all promote MM growth and progression [177]. Furthermore, mature adipocytes are able to provide chemotherapy resistance to MM cells via autophagy activation, which can be used by cancer cells as a survival mechanism to evade microenvironmental stressors such as radiation or chemotherapy [178, 179].

A key feature of MM is the localisation and retention of MM cells in the BM microenvironment [180]. Much like the homing of normal lymphocytes, BM homing in MM is a multistep process that firstly involves adhesion molecules to allow the MM cells to navigate the BM endothelium [181]. Adhesion molecules CD44, VLA-4, and ICAM-1 have been reported to mediate the binding of MM cells to the BM endothelium to facilitate both BM homing and the extravasation of MM cells during metastasis [182, 183]. Stem cell-derived factor 1 (SDF-1) is a chemokine that upregulates VLA-4 and within the BM microenvironment, it regulates MM cell adhesion to fibronectin further aiding MM localisation in the BM [182].

Furthermore, chemotactic molecules are crucial in the BM homing process via the migration of MM cell surface chemokine receptors towards their ligand. MM cells express CCR1, CCR2, CXCR4, CXCR3, and CCR5 [184-188]. MM cells were shown to migrate in the presence of the corresponding chemokine ligands; MIP-1α for receptors CCR1 and CCR5, monocyte chemotactic protein (MCP)-1, -2, and -3 for the CCR2 receptor, CXCL9, 10, and 11 for CXCR3, and SDF-1 for CXCR4 [189]. In new metastatic bone sites, adipocytes also play a role in promoting MM homing via the secretion of chemoattractant molecules such as MCP-1, SDF-1α, and pre-adipocyte factor 1 (Pref-1) [177]. Macrophages have also been implicated in the homing of MM most likely by the secretion of chemotactic molecules, a study found that depletion of BM macrophages via clodronate treatment impairs homing and inhibits MM tumour establishment [190].

Together, it is clear that the BM niche and the cellular interactions that occur within it play a key role in creating a supportive microenvironment for myeloma growth and survival.

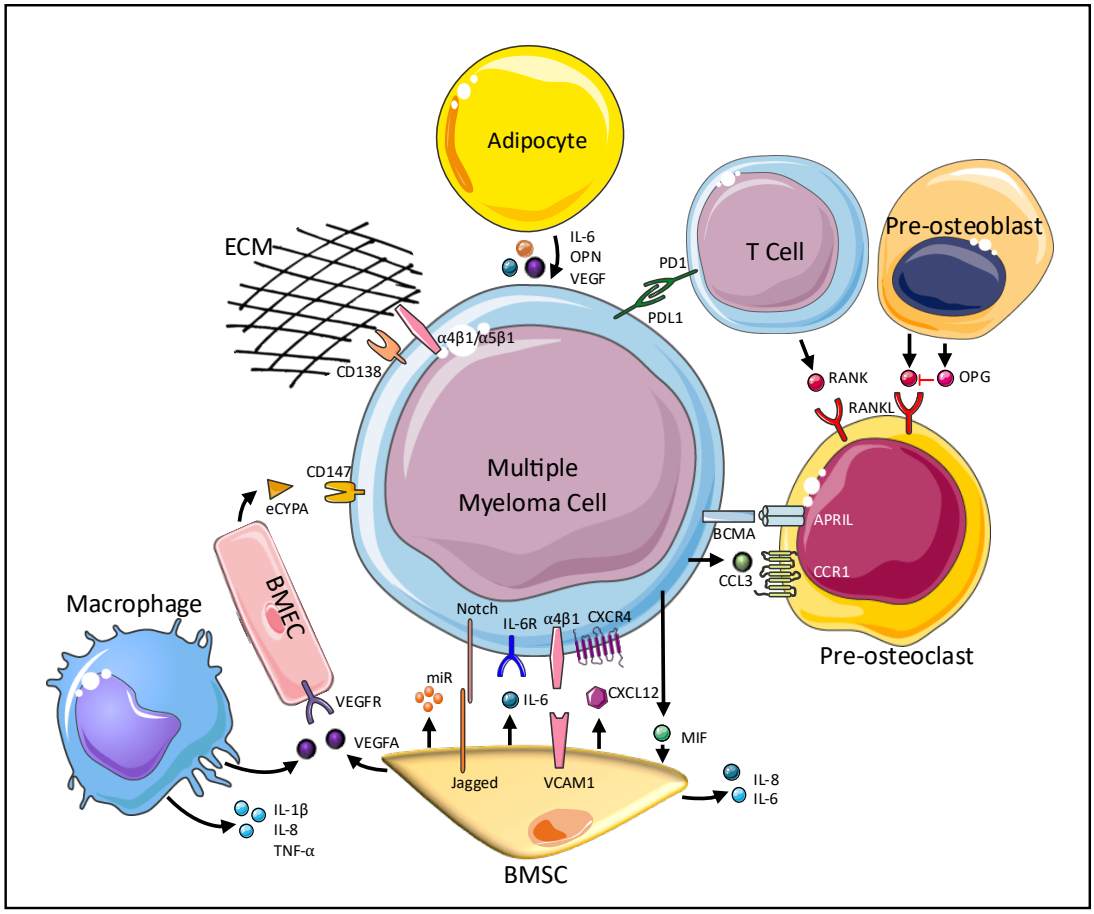

Figure 1.4. Multiple myeloma cellular interactions within the bone marrow microenvironment.

BMSCs express proteins such as Jagged and VCAM1, which interact with their ligands Notch and a4b1 to promote drug resistance and pro-inflammatory cytokine release. BMSCs secrete IL-6 CXCL12, miR, and VEGFA. Macrophages secrete VEGFA as well as pro-inflammatory cytokines, IL-1b, IL-8, and TNF-a. VEGFA causes the release of eCYPA from BM endothelial cells (BMEC), which binds CD147 on MM cells promoting MM proliferation. CD138 and $\alpha 4\beta 1/\alpha 5\beta 1$ integrins bind to proteins in the ECM. MM negatively affects T cell activation through PDL1 / PD1 interaction. BCMA binds to APRIL on pre-osteoclasts and drives myeloma survival and growth. CCL3 which binds to CCR1 on pre-osteoclasts driving osteoclast differentiation. Pre-osteoclasts express which binds RANKL secreted by T cells and pre-osteoblasts and promotes osteoclast differentiation. Adipocytes secrete OPN, VEGF, and IL-6 which support MM cell growth. MM secretes MIF causing IL-6 and IL-8 release from BMSCs, driving MM chemoresistance and adhesion.

1.5 Origin and role of mitochondria

Mitochondria are the organelles most commonly described as the 'powerhouses' of the cell which are responsible for generating adenosine-5'-triphosphate (ATP) via oxidative phosphorylation and glycolysis using the electron transport chain [191].

Mitochondria are double-membraned organelles, comprised of the outer and inner mitochondrial membrane. The inner mitochondrial membrane has a large surface area due to the invaginations called cristae, it houses the complexes of the electron transport chain [192]. The space between the inner and outer mitochondrial membrane is called the intermembrane space, and the inner mitochondrial membrane encloses the matrix. The Krebs cycle produces NADH and $FADH_2$, which donate a pair of electrons to complex I and complex II respectively. The electrons are then transferred to coenzyme-Q which transports them to complex III. Cytochrome c further transfers the electrons to complex IV, which then facilitates the transfer of the electrons to molecular oxygen resulting in the formation of water. The process of electron transfer is coupled with the transfer of protons from the cell matrix into the intermembrane space [193]. This results in a proton gradient leading to the flow of protons back into the matrix via complex V or ATP synthase which converts ADP to ATP [194, 195].

Mitochondria are thought to have originated from ancient proteobacteria being absorbed into another prokaryotic cell, this hypothesis was put forward by Lynn Margulis (Lynn Sagan at the time of publication) and is now widely accepted and known as the endosymbiotic theory [196]. As such, mitochondria have retained many characteristics of their ancestral bacterial origins. These features include mitochondria being approximately the same size as bacteria, the presence of a double membrane, and the way the mitochondrial genome is packaged as 16kb circular DNA, much like bacterial plasmids. The mitochondrial genome is also rich in unmethylated CpG motifs, regions of DNA where a cytosine nucleotide is followed by a guanine nucleotide [197].

Bacteria are able to activate the innate immune system through the recognition of molecular motifs called pathogen-associated molecular patterns (PAMPs), these are recognised by the body's pattern recognition receptors (PRRs) which trigger a response against the pathogen (Figure 1.5). Mitochondria contain damage-associated molecular patterns (DAMPs) also known as alarmins which signal through the same PRRs as bacterial PAMPs. Given the bacterial origin of mitochondria and their conserved evolutionary motifs, mitochondrial DAMPs have been shown to elicit an immunogenic response in a similar fashion to bacterial PAMPs, as was observed in the pathological similarities between sepsis and systemic inflammatory response syndrome (SIRS) caused by injury and trauma [198].

1.6 Mitochondrial DAMPs

In normal circumstances, mitochondrial damage-associated molecular patterns (mtDAMPs), which comprise of molecules such as proteins, lipids, and DNA, are shielded from the immune system by cell compartmentalisation and cell membranes. Furthermore, the leakage of mitochondrial molecules into the extracellular space and cytosol is prevented by a process called mitophagy, the selective degradation of damaged mitochondria by autophagy [199]. However, this homeostatic system may be overwhelmed in times of major trauma or stress and result in the release of mtDAMPs into the extracellular space (Figure 1.5). This phenomenon can be implicated in the pathogenesis of numerous diseases.

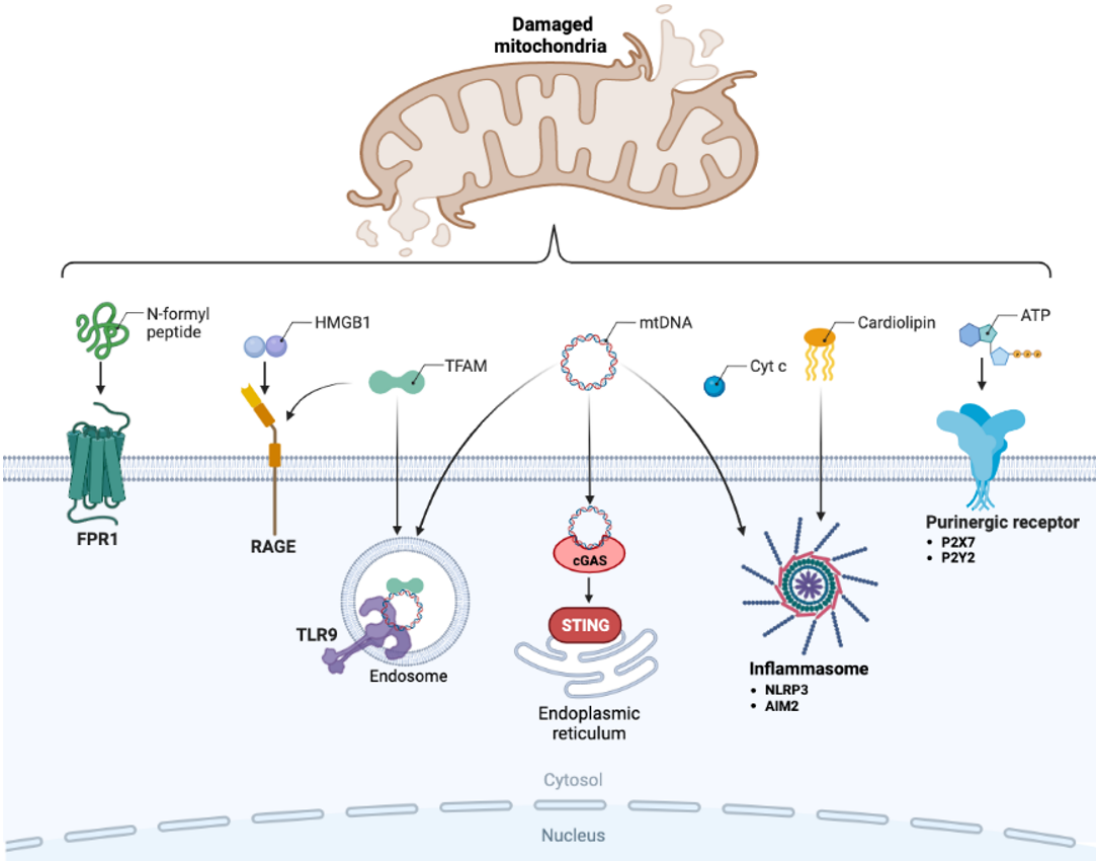

Figure 1.5. Mitochondrial damage-associated molecular pattern signalling receptors.

A schematic showing the mtDAMPs released from damaged mitochondria and their corresponding pattern recognition receptors (PRR). N-formyl peptides are sensed by formyl peptide receptor 1 (FPR1). High mobility group box 1 (HMGB1) is detected by the receptor for advanced glycation end-products (RAGE). Mitochondrial transcription factor A is also detected by RAGE and Toll-like receptor 9 (TLR9). Mitochondrial DNA is detected by 3 PRRs; TLR9, the cyclic GMP-AMP synthase (cGAS)- stimulator of interferon genes (STING) pathway, and by inflammasomes including NOD, leucine-rich repeats, and pyrin domain-containing protein 3 (NLRP3) and absent in melanoma 2 (AIM2). Cardiolipin also signals via inflammasomes. ATP is detected by P2 purinergic receptors P2X7 and P2Y2. The exact PRR signalling mechanism for cytochrome c is to be determined but its involvement as a mtDAMP in disease is well-documented. Created with BioRender.com.

1.6.1 Mitochondrial DNA

Mitochondrial DNA (mtDNA) is a double-stranded circular genome of 16,569 base pairs and contains 37 genes which encode for 2 ribosomal RNAs, 22 transfer RNAs, and 13 proteins which are the essential subunits of the oxidative phosphorylation system [200]. mtDNA is coated by mitochondrial transcription factor A (TFAM), a DNA binding protein which packages the genome into DNA-protein complexes called nucleoids thus, protecting the genome from oxidative damage [201]. Every cell of the body, except for erythrocytes which lack mitochondria, contains hundreds to thousands of copies of mtDNA [202].

Mitochondrial DNA is recognised mainly by the PRR toll-like receptor 9 (TLR-9), which is able to detect the unmethylated CpG repeat motifs as it would in the context of bacterial DNA detection. This was demonstrated by Hemmi et al., where TLR9 knockout mice did not mount an immune response to CpG DNA [203]. mtDNA is also recognised by cytosolic inflammasomes and the type I interferon response.

There are two key inflammasomes involved in the sensing of mtDNA. The NOD, leucine-rich repeats, pyrin domain-containing protein 3 (NLRP3) inflammasome, and the absent in melanoma 2 (AIM2) inflammasome. mtDNA can also be sensed by the cyclic GMP-AMP synthase (cGAS) and stimulator of interferon genes (STING) pathway in order to trigger type I interferon (IFN) response [204, 205]. Overall, this data suggests that mtDNA is an abundant DAMP that acts as a mediator of the systemic inflammatory response.

1.6.2 ATP

The intracellular role of ATP as the universal energy source for cellular functions and metabolism has long been recognised, however, its extracellular functions have also been linked to the processes of vascular tone, platelet aggregation, neurotransmission, and cardiac and muscle contraction [206]. Extracellularly, ATP release from damaged or dying cells has also been shown to act as a DAMP alerting the immune system to tissue damage through binding to P2 purinergic receptors, ligand-gated ion channels P2X receptors, and G-protein-coupled P2Y receptors [207].

P2Y2R is the most studied P2Y receptor. P2Y2R and ATP interaction acts as a 'find me' signal to mediate macrophage phagocytosis [208] and neutrophil chemotaxis [209], and so has been associated with wound healing and mucociliary and bacterial clearance. ATP-P2Y2R signalling has been shown to contribute to a pro-inflammatory response in chronic inflammatory diseases. This signalling induces the release of pro-allergic mediators such as IL-33, IL-8, and eosinophil cationic protein (ECP) from airway epithelial cells and eosinophils during allergic airway disease and asthma [210, 211].

P2X receptors also bind extracellular ATP and have seven subtypes, characterised 1-7. The P2X7 receptor has been shown to play an important role in the regulation of inflammatory and immunological responses against pathogens such as tuberculosis and toxoplasmosis, and cancer cells [212]. The innate immune response against bacterial infection involves ATP-P2X7 signalling, which results in bacterial clearance via reactive oxygen species (ROS) generation [213], improved phagosome and lysosome fusion [214], and apoptosis [215]. This signalling pathway has also been implicated in tumour suppression, via the activation of the NLRP3 inflammasome and the subsequent release of IL-1β, which is capable of priming CD8+ T-cells and thus promotes the clearance of cancer cells [216].

Despite its important role as an inflammatory defence mechanism, inappropriate activation of the ATP-P2X7 axis can contribute to chronic inflammation and related disorders such as allergic contact hypersensitivity, asthma, transplant rejection, and the intestinal inflammation observed in inflammatory bowel disease [217]. Collectively, ATP is more than a molecule that provides energy for cellular biochemical reactions, as a DAMP it is important in the activation of both innate and adaptive immune responses.

1.6.3 Mitochondrial transcription factor A / High mobility group box 1

TFAM is a ubiquitous mtDNA-binding protein that belongs to the high mobility group box (HMGB) family, which regulates mitochondrial genome packaging, transcription and mtDNA copy number [218]. An *in vivo* study by Chaung et al. demonstrated that levels of extracellular TFAM in blood serum were increased after haemorrhagic shock and that TFAM can act as a pro-inflammatory mediator, upregulating the levels of pro-inflammatory cytokines in the circulation [219]. It was also shown that TFAM can work in the presence of N-formyl peptides to activate monocytes and cause them to secrete significant levels of IL-8 [220]. Furthermore, TFAM that remains associated with mtDNA increases the release of TNF-α from TLR-9 expressing plasmacytoid dendritic cells (pDCs) through the engagement of receptor for advanced glycation end-products (RAGE) [221].

HMGB1 is another DNA chaperone protein that, due to its potent inflammation modulatory effects, has also been identified as a DAMP released as a result of cell damage or death [222]. HMGB1 secretion is mediated by the NLRP3 inflammasome [223], since TLR signalling primes NLRP3 formation, it has been suggested that HMGB1 could prime NLRP3 itself via binding to TLR2/4 [224]. Like TFAM, HMGB1 signals through RAGE, which activates the NF-κB [225], and MAP/ERK (extracellular signal-related) kinase pathways [226].

HMGB1 has also been shown to bind to toll-like receptors including TLR-9 which enhances cytokine production in pDCs [227], TLR-2 when bound to nucleosomes which activate pDCs and macrophages [228], and TLR-4 which is the most studied. HMGB1-TLR-4 signalling has been implicated in driving inflammation via pro-inflammatory cytokine production [229].

Overall, DNA chaperone proteins, TFAM and HMGB1 are mtDAMPs that have been shown to play important roles in stimulating pro-inflammatory cytokine production through signalling via various receptor pathways.

1.6.4 N-formyl Peptides

N-formyl peptide (NFP) or, N-formyl-methionyl-leucyl-phenylalanine (fMLP) is recognised by formyl peptide receptors (FPR), specifically, FPR1 which belongs to the family of seven transmembrane G-protein coupled receptors and are highly expressed on polymorphonuclear and mononuclear phagocytes, and also platelets [230, 231]. NFP is found to be released from mitochondrial proteins of damaged or dying cells, and also in the membrane of bacterial cells such as E.coli [230]. Therefore, NFP plays a role in the host's defence against bacterial infection and in clearing damaged cells. NFP is implicated in the chemoattraction of neutrophils via FPR1 binding and the consequent increase in IL-8 secretion, which is a potent neutrophil chemoattractant [198, 220]. As such, NFPs have been implicated in the induction of lung neutrophil infiltration which causes airway constriction and lung inflammation [232], resulting in the respiratory failure that presents in systemic inflammatory response syndrome (SIRS) patients.

Overall, NFPs are effective chemoattractants that are capable of driving immune activation which leads to the clearance of microbial and dead cells. However, the aberrant release of NFPs is also associated with disease pathology.

1.6.5 Cardiolipin

Cardiolipin (CL) is a phospholipid dimer comprised of a glycerol head and two phosphatidyl groups. It is an essential component of the mitochondrial membrane, predominantly the inner membrane where it constitutes up to 20% of the total lipids, compared to the outer membrane where it only accounts for 3% of the total lipid content [233]. Cardiolipin functions to regulate mitochondrial respiration and biogenesis and is vital in providing the structural integrity of membrane translocases which are necessary for mitochondrial protein transport [233].

Cardiolipin is also found in the bacterial cell wall, therefore it can also elicit an immune response. CL has been shown to induce an inflammatory response via direct binding to the NLRP3 inflammasome, this was proven as interfering with the synthesis of CL leads to the inhibition of NLRP3 activation [234]. Cardiolipin is able to act as a ligand for CD1d and activates $\gamma\delta$T cells [235]. CL has also been shown to regulate mitochondrial outer membrane permeability and cytochrome c release into the cytoplasm where it can induce apoptosis [236].

Ultimately, CL is integral to the stability of the mitochondrial membrane and provides functional support to facilitate the process of oxidative phosphorylation. As a DAMP, externalised cardiolipin can initiate an inflammatory cascade that results in the activation of the adaptive immune system.

1.6.6 Cytochrome C

Cytochrome c is crucial for mitochondrial respiratory function. It is an electron carrier located in the inner mitochondrial membrane where it mediates the transfer of electrons from complex III to complex IV in the electron transport chain [237]. As previously discussed, cytochrome c is maintained within the inner mitochondrial membrane via close association with cardiolipin, and once released into the cytosol under pro-apoptotic signals it activates apoptosome complex formation with apoptotic protease activating factor-1 (Apaf-1) which triggers a caspase cascade resulting in cell apoptosis [236, 238, 239]. Cytochrome C has also been found to be elevated in the serum of patients with SIRS [240] indicating that the inflammatory response is triggered through this signalling pathway.

1.7 Mitochondrial DAMP Recognition Receptors

mtDAMPs are recognised by pattern recognition receptors expressed on immune and non-immune cells triggering the activation of the innate immune system and subsequent downstream signalling of pro-inflammatory responses. Different PRRs are involved in the sensing of specific mtDAMPs and eliciting various responses (Figure 1.5).

1.7.1 Toll-Like Receptors

Toll-like receptors (TLR) are type I transmembrane domain glycoproteins that are comprised of an amino (N)-terminal ectodomain containing leucine-rich repeats which mediates ligand recognition, a transmembrane domain that regulates cellular localisation, and a carboxyl (C)-terminal globular cytoplasmic toll/interleukin-1 receptor (TIR) domain that facilitates downstream signalling [241].

After the characterisation of the first mammalian toll-like receptor, TLR-4, a whole family of structurally related proteins was identified [242]. The mammalian TLR family is large and consists of 11 members, with TLR1-9 being conserved in mice and humans, whilst TLR10 and TLR11 are only functional in humans and mice respectively [241]. TLRs can be divided into two groups based on their cellular localisation, cell surface TLRs (TLR-1, -2, -4, -5, -6, and -10) and intracellular endosomal TLRs (TLR-3, -7, -8, -9, and -11) [243]. Cell surface TLRs mainly recognise and respond to microbial membrane components such as lipoproteins and lipids, and intracellular TLRs recognise bacterial and viral nucleic acids.

As established above, mtDNA acts as a TLR-9 agonist. Binding and recognition of mtDNA to TLR-9 occurs in the endolysosome, this results in the recruitment of the signal transduction adaptor protein myeloid differentiation primary response 88 (MyD88) [244]. MyD88 is able to link members of the TLR family to IL-1R associated kinases (IRAK), activation of IRAK leads to the activation of NF-κB and MAPK. This in turn causes the transcription of pro-inflammatory cytokines, mtDNA has also been shown to activate polymorphonuclear neutrophils via p38 MAPK [245]. TLR9-dependent activation of NF-κB is also considered a priming step for the activation of the NLRP3 inflammasome [246, 247]. mtDNA bound to TFAM is able to elicit a stronger activation of NF-κB as the plasma membrane receptor RAGE is able to deliver the mtDNA to TLR-9 [221].

Overall, toll-like receptors are a diverse family involved in the recognition of a wide range of PAMPs and DAMPs. As such, they are important mediators of the innate and adaptive immune systems. In relation to mtDAMPs specifically, TLR-9 is the best characterised as an mtDNA sensing receptor that mediates the production of pro-inflammatory cytokines.

1.7.2 Inflammasomes

Inflammasome activation is mediated by the innate immune system. Inflammasomes are multimeric protein complexes that assemble in the cytosol following PAMP or DAMP sensing [248]. NOD, leucine-rich repeats, and pyrin domain-containing protein 3 (NLRP3) is the best-characterised inflammasome. The inflammasome is a protein complex comprised of the NLRP3 sensing protein, an adapter protein ASC, and the caspase-1 inflammatory protease. The priming and activation of this inflammasome results in the maturation and secretion of pro-inflammatory cytokines [249]. It has been shown that mtDNA in the cytosol can activate NLRP3 inflammasome mediated caspase-1 activity which leads to the secretion of IL-1β and IL-18 [250-252]. mtDNA also activates another inflammasome, absent in melanoma 2 (AIM2). AIM2 belongs to the pyrin and HIN domain-containing protein (PYHIN) family and is a receptor for double-stranded cytosolic DNA which also associates with ASC to activate caspase-1 activity and cleave the immature pro-forms of the IL-1β and IL-18 cytokines [253]. On the whole, inflammasomes are key PRRs that sense and respond to mtDNA in a manner that results in the production of pro-inflammatory cytokines.

1.7.3 RAGE

The receptor for advanced glycation end-products (RAGE) is a type I single-pass transmembrane protein comprised of an extracellular domain, a hydrophobic transmembrane spanning domain, and a cytoplasmic tail [254]. The extracellular domain can bind the mtDAMP HMGB1 [255]. Upon ligand binding, RAGE activates multiple signalling pathways such as extracellular-signal-related-kinase 1/2 (ERK 1/2), Akt, and NFκB [256]. RAGE binding to HMGB1-DNA complexes results in the internalisation of the receptor to the cytosol and interaction with endosomal TLR-9 which augments MyD88-dependent type I IFN production [227].

Overall, RAGE activation is capable of initiating multiple signalling pathways that act to promote the expression of a range of pro-inflammatory cytokine genes.

1.7.4 FPR1

The formyl peptide receptor 1 belongs to a family of G-protein-coupled receptors which are able to recruit immune cells and promote inflammatory responses [257]. Upon binding of N-formyl peptides to the FPR1 receptor, the p38 MAPK signalling pathway, as well as the extracellular-signal-related-kinase 1/2 (ERK 1/2) pathway, is activated and this is the mechanism involved in inducing neutrophil activation [258, 259]. In brief, FPR1 recognition of NFPs and subsequent signalling serves to guide phagocytic cells to sites of inflammation and injury.

1.7.5 Stimulator of Interferon Genes

A crucial immune molecule in the detection of cytoplasmic or nuclear DNA is organised by the cyclic GMP-AMP synthase (cGAS) - stimulator of interferon genes (STING) pathway [260]. The cGAS DNA sensor forms a dimeric cGAS-DNA complex upon recognition of double-stranded DNA such as mtDNA, it then synthesises 2'3' cyclic GMP-AMP (cGAMP) from ATP or GTP (Figure 1.6). The cGAMP binds to STING in the endoplasmic reticulum (ER) [261]. STING is an endoplasmic reticulum resident transmembrane protein [262], once activated STING dimerises and translocates from the ER to the ER-Golgi intermediate compartment (ERGIC) and then onto the Golgi apparatus. During this process STING co-immunoprecipitates with TANK-binding kinase 1 (TBK1) which leads to the phosphorylation of STING and subsequent phosphorylation and activation of interferon regulatory factors (IRF) 3 and 7 and the up-regulation of IFN-stimulated genes (ISG) [262, 263].

In the presence of IκB kinase (IKK), STING activates NF-κB by phosphorylating its inhibitor, IκB. NF-κB then translocates to the nucleus and induces transcription of pro-inflammatory factors such as IL-6, IL-1β, TNF-α, and type I IFN [262].

Type I interferon production is one of the most studied and well-documented functions of downstream cGAS-STING signalling. Type I IFNs are cytokines that signal via JAK-STAT signalling to induce the transcription of ISGs such as guanylate-binding protein 2 (GBP2) and IFN-induced protein with tetratricopeptide repeats 3 (IFIT3) [264, 265] which confer antiviral immunity

In summary, cGAS-STING is an essential cytoplasmic DNA sensor that plays an important role in the induction of both pro-inflammatory cytokine release and the activation of the type I IFN response (Figure 1.6).

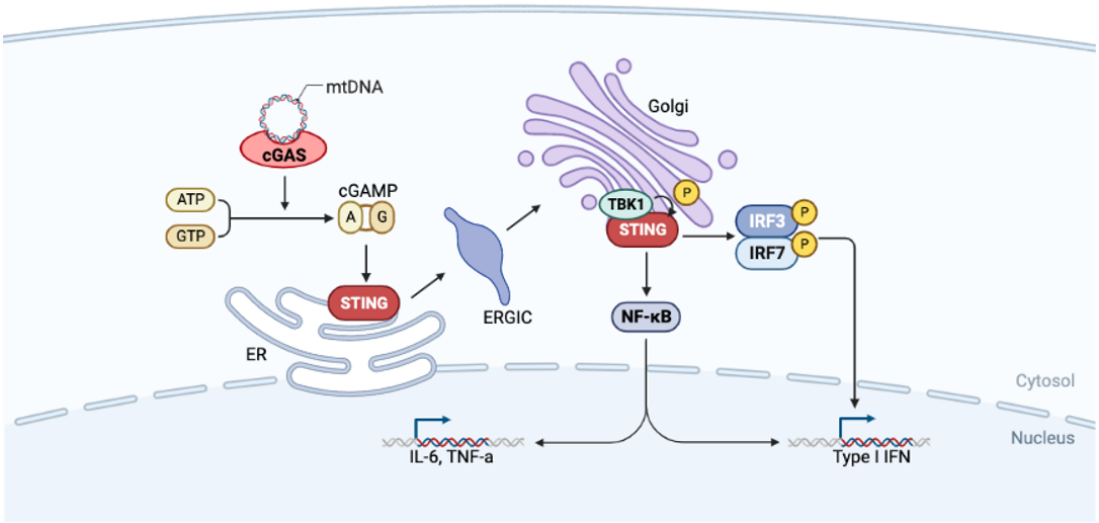

Figure 1.6. The cGAS-STING signalling pathway.

A schematic overview showing the activation of GMP-AMP synthase (cGAS) upon binding of mtDNA. This results in the synthesis of 2'3' cyclic GMP-AMP (cGAMP). cGAMP binds to stimulator of interferon genes on the endoplasmic reticulum (ER). Conformational changes occur and STING dimerises, before passing through the ER-Golgi intermediate compartment (ERGIC) to the Golgi where TANK-binding kinase 1 (TBK1) is recruited, leading to the phosphorylation of STING and interferon regulatory factor 3 and 7 (IRF3/7), which translocates to the nucleus where it induces the transcription of type I interferon (IFN) genes. STING also activates NF-κB which induces the transcription of pro-inflammatory genes. Created with Biorender.com.

1.8 Mitochondrial DAMPS in Disease

In recent years, there has been some focus on the pro-inflammatory properties of circulating mitochondrial molecules and their role in triggering innate immune responses. There is a growing body of literature that implicates the role of mitochondrial DAMPs in the pathogenesis of various human diseases. They are able to be detected in various human body fluids suggesting their potential use as biomarkers for diseases and yet, their role remains largely unknown, highlighting a need for further research of mtDAMPs in the context of disease.

1.8.1 Mitochondrial DAMPs in inflammatory disorders

Systemic inflammatory response syndrome (SIRS) is a condition where immune cell activation spreads throughout the whole body rather than being localised, it is often associated with an exaggerated response to pathogenic infection [266]. However, some SIRS patients present without such infection which suggests that other factors are at play in the development of SIRS [267]. Studies have shown that an elevation in plasma mtDNA is associated with the clinical outcomes of severe trauma, injury, septic shock, and major surgery [198, 245, 268-270] and is present in SIRS and sepsis development [271-273].

N-formyl peptides have also been reported to be elevated in the peripheral blood serum of trauma patients with SIRS or sepsis compared to a control trauma group [257]. This suggests that mtDAMPs released as a result of trauma activate systemic inflammatory responses via inflammation-associated signalling pathways. Cytochrome c has been identified as a prognostic marker in cases of SIRS [240] and has also been implicated in the induction of rheumatoid arthritis [274]. Rheumatoid arthritis is a systemic autoimmune disease that causes inflammation of the synovial membrane of joints [275]. Elevated levels of mtDNA were found in the plasma and synovial fluid of patients with rheumatoid arthritis [276].

The mtDAMP HMGB1 has also been implicated in the pathogenesis of RA as levels were increased in the serum and synovial fluid of RA patients [277]. It is assumed that HMGB1 contributes to joint inflammation via the production of pro-inflammatory cytokines [278]. Additionally, HMGB1 involvement in RA pathogenesis is further substantiated by a study where the use of a monoclonal anti-HMGB1 antibody ameliorated RA in two animal models [279]. Another chronic autoimmune disease that causes widespread inflammation is systemic lupus erythematosus (SLE), which affects multiple organs. HMGB1 was found to be increased in SLE patients, particularly those with renal dysfunction, which is a characteristic feature of many autoimmune diseases, thus implicating the involvement of mtDAMPs in the development of these diseases [280].

Furthermore, chronic inflammation is implicated in the pathophysiology of sickle cell disease (SCD). Recently, circulating mtDNA has been shown to be elevated in the plasma of SCD patients and triggers neutrophil extracellular trap (NET) expulsion [281, 282]. The activation of the cGAS-STING pathway is likely the mechanism behind this pathological inflammation as inhibition of TBK1 significantly reduced NET formation [281].

Overall, a range of mtDAMPs have been implicated in the inflammation that is associated with the pathogenesis of various diseases. Understanding the underlying mechanisms responsible for driving these inflammatory states will be essential in advancing our comprehension of pathologies and may elucidate potential therapeutic targets.

1.8.2 Mitochondrial DAMPs in respiratory diseases

Acute respiratory distress syndrome (ARDS) and acute lung injury (ALI) are leading causes of intensive care mortality, with the hyperinflammatory ARDS phenotype associated with higher mortality [283]. As a key activator of inflammation, elevated plasma mtDNA has been associated with the pathogenesis of ALI/ARDS [284, 285].

Cardiolipin has been associated with bacterial pneumonia. It was found that levels of CL were elevated in bronchoalveolar lavage fluids (BALF) of bacterial pneumonia patients and mice, and intratracheal administration of CL in mice resulted in the clinical reproduction of pneumonia [286]. CL has also been found to be the only phospholipid to be significantly increased in the BALF of patients with chronic obstructive pulmonary disease (COPD) [287]. CL was found to be responsible for suppressing the anti-inflammatory cytokine IL-10 in lung myeloid-derived suppressor cells (MDSCs), which drives lung inflammation. This IL-10 suppression is caused by CL-mediated PPARγ S112 phosphorylation, all in all, this results in impaired lung inflammation resolution in bacterial pneumonia [288].

TFAM levels were found to be decreased in the skeletal muscle of patients with chronic obstructive pulmonary disease (COPD), suggesting that the under-expression of TFAM is implicated in the skeletal muscle dysfunction that is a characteristic of COPD [289]. ATP is a mtDAMP that has been widely explored in COPD. Increased levels of extracellular ATP have been reported in the BALF of COPD patients, and smokers [290]. In a separate mouse study, they also found that the ATP receptor P2X7 was upregulated in blood and airway neutrophils, alveolar macrophages, and lung tissue, indicating that ATP-mediated signalling in these cells is upregulated [291]. ATP has also been identified as a mtDAMP in asthma, as purinergic receptor activation leads to allergic airway inflammation, the recruitment of lung dendritic cells and enhancement of allergen-induced Th2 cytokine production [211].

To summarise, mtDAMPs are heavily implicated in the pathology of respiratory diseases, they drive immune cell recruitment which exacerbates the inflammatory phenotype of respiratory diseases and impairs the resolution of inflammation.

1.8.3 Mitochondrial DAMPs in cardiovascular disease

mtDAMPs also play a role in the induction of the inflammatory cascades that are involved in the initiation and progression of cardiovascular diseases. Atherosclerosis is a significant burden on healthcare systems globally, the condition results from a build-up of atherosclerotic plaques which clog coronary vessels restricting blood flow and can result in myocardial infarction. Increased levels of cytochrome c have been reported in patients with myocardial infarction [292]. Furthermore, a study found that overexpression of human TFAM in mice enhanced cardiac dysfunction seen in myocardial infarction and also increased the amount of mitochondrial DNA [293]. Plasma levels of mtDNA have been reported to be elevated in patients with myocardial infarction and acute ischaemic stroke patients [294, 295]. Extracellular ATP has also been implicated in atherosclerosis and vascular inflammation via P2Y2 signalling in mice [296].

Taken together, these studies highlight that mtDAMPs do play an important role in the pathogenesis of cardiovascular diseases and pose the idea that mtDAMPs could be used as diagnostic/prognostic biomarkers.

1.8.4 Mitochondrial DAMPs in neurodegenerative disease

In the central nervous system (CNS), microglial cells act as innate immune system sentinels and are responsible for maintaining CNS homeostasis and facilitating neuroinflammation which can be exacerbated by excessive pro-inflammatory activation of microglial cells. This neuroinflammation mediates neuron cellular stress and death. Due to the limited regenerative capabilities of neurons, this cell death can lead to pathological disease states [297].

Studies have shown a correlation between mtDAMPs and the underlying neuroinflammation that is observed in the neurogenerative conditions of Alzheimer's and Parkinson's disease [298, 299].

HMGB1 and soluble RAGE are elevated in the serum of patients with Alzheimer's disease, which suggests activation of the pro-inflammatory HMGB1-RAGE signalling pathway. HMGB1 signalling triggers inflammation and blood-brain barrier dysfunction [300]. In Parkinson's disease, HMGB1 was again implicated in the chronic inflammation that is characteristic of the disease [301]. HMGB1 levels were elevated in the serum of patients with Parkinson's disease [302]. This finding was substantiated by a study in a rat model of Parkinson's where treatment with an anti-HMGB1 monoclonal antibody reduced the secretion of pro-inflammatory cytokines thereby attenuating inflammation and maintaining the integrity of the blood-brain barrier [303]. NFPs have also been implicated in the CNS inflammatory process that drives Parkinson's disease pathogenesis, they are thought to activate microglia resulting in dopaminergic neurotoxicity via NADPH-dependent superoxide production [304]. In brief, the inflammation observed in the pathology of neurological diseases is in part mediated by mtDAMPs. Elucidating the mechanisms of action and release of these mtDAMPs will be crucial in gaining a better understanding of the role that they play in neurodegenerative conditions.

1.8.5 Mitochondrial DAMPs in cancer

The normal functions of inflammatory responses are to respond to infection and promote wound healing and tissue regeneration. These functions serve a much more innate and evolutionary purpose than the clearance and avoidance of tumorigenesis. In instances of injury or infection, the immune system responds through the recruitment of local tissue macrophages and dendritic cells, and bone marrow-derived immune cells such as monocytes and neutrophils. This recruitment leads to the release of cytokine inflammatory mediators in an effort to be rid of the pathogen and activate epithelial cell proliferation to repair injuries. As a result, normal tissue homeostasis is restored [305].

However, if the initial insult to epithelial cell homeostasis is caused by an oncogenic event or the presence of danger signals in the cancer microenvironment, though an inflammatory response will be mounted it will not result in the correction of this imbalance as cancer and growing tumours result in persistent cell damage/death signals that feed into a negative feedback loop of inflammatory cell recruitment and inflammatory signalling driving proliferation and facilitating tumour growth [306]. As such, tumours have been described as wounds that never heal. Therefore, there is a compromising trade-off between the role of inflammation in normal physiological circumstances and inflammation in cancer.

Inflammation has been shown to contribute to tumour promotion, a study by Greten et al. 2004 first demonstrated this link [307]. The transcription factor NF-κB is a key inflammatory mediator that induces the expression of pro-inflammatory cytokines and chemokines [308]. In a colitis-associated cancer model, inactivation of the inhibitor of nuclear factor-κB kinase (IKKβ)/ NF-κB pathway through ablation of IKKβ resulted in a significant reduction in tumour growth [307]. Inflammation has also been linked to promoting the process of epithelial-mesenchymal transition (EMT), a process co-opted by cancer cells by which cell-cell and cell-extracellular matrix adherence complexes are loosened and cells gain enhanced migratory and invasive abilities which are used to enable cancer metastasis [309]. Inflammatory mediators such as TNF-α, TGF-β1, IL-1β, and IL-6 have been shown to promote the acquisition of EMT features in various cancer cell types *in vitro* [309, 310]. Conversely, these cancer cells also produce pro-inflammatory mediators further fuelling the low-grade inflammation (para-inflammation) that is prevalent in cancer [311].

The current body of literature strongly recognises the role of chronic unresolved inflammation in cancer development and the inflammatory tumour microenvironment as a hallmark of cancer [312]. Meanwhile, mitochondrial DAMPs have been implicated in both sterile and infection-associated inflammation. Therefore, there is an interplay between mtDAMPs and the inflammatory cancer tumour microenvironment.

Circulating mitochondrial DNA in recent years has become a focus in cancer, due to the non-invasive nature and ease of detection in plasma and serum. As such, it is an attractive candidate to serve as a liquid biopsy as a diagnostic and prognostic biomarker in various cancer types [313]. The levels of mtDNA are higher in patients with urological malignancies [314] such as bladder cancer, renal cell carcinoma, and prostate cancer [315]. mtDNA is also elevated in the plasma of ovarian cancer patients [316]. However, decreased plasma levels of mtDNA are observed in patients with Ewing sarcoma [317] and breast cancer [318]. Therefore, it is likely the case that changes in levels of circulating mtDNA may be dependent upon the type of cancer in question. Measuring the serum levels of cytochrome c has also been shown to have the potential to be used as a biomarker and a prognostic tool in instances of identifying malignant tumours in patients [319], and in determining the prognosis of patients with non-small cell lung cancer [320].

However, the majority of reported findings on mtDAMPs and malignancies are focused towards identifying potential biomarkers of disease but the functional purpose behind the varying levels of mtDAMPs presence is largely unknown. Interestingly, a study identified that activation of BM macrophage LC3-associated phagocytosis activated the mtDNA-mediated STING signalling pathway resulting in the suppression of AML tumour growth in mice [321]. This study offers insight into a possible mechanism of function of mtDAMPs signalling.

To summarise, mtDAMPs research is an emerging field that holds a lot of promise for providing potential biomarkers for disease progression as well as opening up novel avenues for therapeutic targets in various cancers. Nevertheless, the field is still in its infancy and further research is needed to understand the complex role that mtDAMPs play in malignant microenvironments.

1.9 Rationale

Multiple myeloma is a bone marrow malignancy that is currently incurable. Whilst many treatment options are available with new treatment strategies and therapeutics being developed all the time, refractory disease and relapse are all but inevitable for MM patients. As such, further research into potential therapeutic avenues is necessary to improve survival outlooks for MM patients. MM is heavily dependent on cellular interactions within the BM microenvironment for its growth, progression, and survival. Therefore, understanding the BM microenvironment of MM is likely to shed light on potential interactions that can be exploited for generating novel MM treatments.

Mitochondrial DAMPs play a crucial role in sterile inflammation and the pathogenesis of various diseases. mtDAMPs have been detected in various cancers at levels significant enough to be considered diagnostic and prognostic biomarkers. mtDNA is the mtDAMP that has been the most widely researched and implicated in the widest range of disease states. However, the mechanisms that underpin the relationship between mtDNA and the cancer microenvironment, particularly in the context of blood malignancies, are not fully understood.

This study intends to fill that gap by gaining an understanding of the functional purpose of the increased circulating mtDNA levels, in the context of MM. Furthermore, the study will explore the effects that mtDAMPs cause on the cells of the bone marrow microenvironment, allowing us to understand how these mtDAMPs can drive a response which creates favourable conditions in the bone marrow for the survival, growth, and progression of multiple myeloma.

1.10 Hypothesis

I hypothesise that MM cells release mtDAMPs into the BM microenvironment where they promote a pro-inflammatory and pro-tumoral state. Since macrophages have been evidenced to sense and respond to mtDAMPs, I also hypothesise that mtDAMPs-driven BM macrophage activation further supports MM progression and survival. Therefore, this study aims to determine MM cell mtDNA release and understand the functional role that mtDAMPs play in the disease progression of MM.

1.11 Aims and Objectives

The following objectives are proposed to address the research aim:

1. To investigate the associations between mtDAMPs and MM, using mtDNA as a surrogate marker for mtDAMPs, and determine the prognostic biomarker potential of mtDNA in MM.

2. To determine the mechanism of mtDAMPs signalling in BM macrophages.

3. To explore the role of mtDAMPs mediated macrophage activation in MM disease progression and survival.

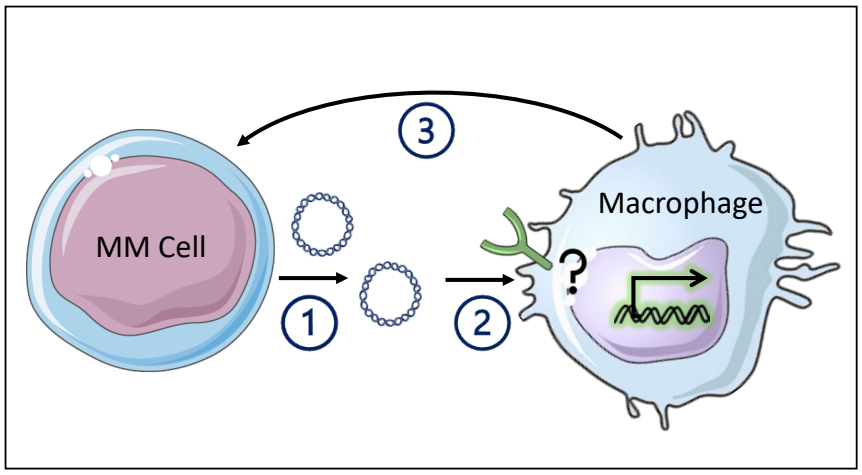

Figure 1.7. Graphical representation of aims and objectives.

Using a combination of in vivo and in vitro (human and mouse) methodologies this thesis aims to investigate: (1) MM cell derived mtDNA (a surrogate marker for mtDAMPs) as a potential biomarker of myeloma disease, (2) the signalling mechanism used in mtDAMPs and BM macrophage interaction, (3) how BM macrophages activated by mtDAMPs mediate MM disease progression.

2 Materials and methods

2.1 Materials

All reagents and materials used in this study are disclosed below in Table 2.1 and in the subsequent Methods section.

Table 2.1. Reagents with the manufacturer and catalogue number details.

Product	Manufacturer	Catalogue Number
8µm Transwell 24-well plate	Fisher Scientific	10167000
26G Butterfly Needles	Medisave UK Ltd	2674829
26G Needles	Fisher Scientific	12349189
Amicon® Ultra-15 Centrifugal Filter	Merck Life Science	UFC910008
Bovine Serum Albumin	Fisher Scientific	BP1600-100
Busulfan	Sigma Aldrich	B2635
Cellometer SD100 counting chamber	Nexcelom Bioscience	CHT4-SD100-002
CellTrics 40µm filter	Wolf Laboratories	04-0042-2316
Combo: Clophosome®-A and Control Liposomes	Stratech Scientific	F70101C-AC-FOR
D-Luciferin	Fisher Scientific	8829
DMEM Medium	ThermoFisher	10566016
DMSO	Fisher Scientific	BP231-100
EDTA	Sigma Aldrich	E9886
Fetal Bovine Serum	ThermoFisher	105000056
GenElute Mammaliam Genomic DNA Miniprep Kit	Sigma Aldrich	G1N70
H-151 STING Inhibitor	Invivogen	INH-H151
Heparin	Sigma Aldrich	H3393
Histopaque-1077	Sigma Aldrich	10771
IsoFlo (Isoflurane)	Zoetis	DMU (in house)
MEM Non-Essential Amino Acids	ThermoFisher	11140050
Mitochondria Isolation Kit for Tissue	ThermoFisher	89801
Murine mCSF	PrepoTech	315-02

Table 2.1. (continued).

Product	Manufacturer	Catalogue Number
ND1 TaqMan Gene Expression Assay Human	ThermoFisher	4331182_Hs02596873
ND1 TaqMan Gene Expression Assay Mouse	ThermoFisher	4331182_Mm04225274
ODN 1826	Invivogen	Tlrl-1826
ODN 2088	Invivogen	Tlrl-2088
OneComp eBeads™ Compensation Beads	ThermoFisher	01-111-42
PCRBIO 1-Step Go RT-PCR Kit	PCR Biosystems	PB10.53-10
Penicillin-Streptomycin	GE-Healthcare	SV30010
Proteome Profiler™ Mouse Cytokine Array Panel A	R&D Systems	ARY006
qPCRBIO cDNA Synthesis Kit	PCR Biosystems	PB30.11-10
qPCRBIO SyGreen Mix	PCR Biosystems	PB20.12-51
ReliaPrep RNA Cell Miniprep System	Promega	Z6012
rLV.EF1.AcGFP-Mem9	Clontech	0019VCT
rLV.EF1.mCherry-Mito-9 lentivirus	Clontech	0024VCT
RPMI-1640 Medium	ThermoFisher	11875093
Sodium Pyruvate	Fisher Scientific	11501871
TaqMan Human Tert	ThermoFisher	4403316
TaqMan Mouse Tert	ThermoFisher	4458368
TaqPath ProAmp Mastermix	ThermoFisher	A30865
Trypan Blue	Sigma Aldrich	T8154
Trypsin-EDTA	ThermoFisher	25200056
Tween-80	Fisher Scientific	T164-500

BioLegend (San Diego, CA, USA), Clontech Takara Bio (Saint-Germain-en-Laye, France), Fisher Scientific (Hampton, New Hampshire, USA), GE Healthcare (Little Chalfont, UK), InvivoGen (San Diego, CA, USA), Medisave UK Ltd (Weymouth, UK), Merck Millipore (Burlington, MA, USA), Miltenyi Biotec (Bergisch Gladbach, Germany), Nexcelom Bioscience (Lawrence, MA, USA), PCR Biosystems (London, UK), Peprotech (Rocky Hill, NJ), Promega (Madison, WI, USA), Qiagen (Hilden, Germany), R&D Systems (Minneapolis, MN, USA), Sigma Aldrich (St Louis, MO, USA), Stratech Scientific (Ely, UK), Wolf Laboratories (York, UK), ThermoFisher (Waltham, MA, USA), and Zoetis (Surrey, UK).

2.2 Animal Maintenance and Models

All *in vivo* work in this thesis was carried out in accordance with the Animal Scientific Procedures ACT of 1986 following regulations set by the UK Home Office under project licences 70/8814 (Prof. Kristian Bowles) and PP023671 (Dr Stuart Rushworth).

Animals were housed in the Disease Modelling Unit (DMU) at the University of East Anglia in a pathogen-free, containment level 3 facility. Breeding pairs were set up at 6-8 weeks and maintained for 6 months before separation. The offspring were weaned at 3 weeks post-birth. Mice of both genders were used at the age of 8-12 weeks for experimentation.

2.2.1 Wildtype C57BL/6 mice

C57BL/6 mice (Jackson Laboratory, Bar Harbour, ME, USA) are a widely used inbred mouse strain. In this thesis, C57BL/6 mice were used to generate bone marrow-derived macrophages (BMDM) as described in section 2.3.4.1 and to study the mtDNA content of peripheral blood in MM. This mouse strain has a functioning immune system, therefore, in experiments requiring the engraftment of murine MM (5TGM1) mice were pre-conditioned with a non-myeloablative dose of busulfan (25 mg/kg) for three consecutive days administered by intraperitoneal (i.p.) injection.

2.2.2 CBA mice

CBA mice were obtained from Charles River Laboratories (Massachusetts, United States). CBA mice are an inbred general-purpose mouse strain, and their mitochondrial DNA can be distinguished from C57BL/6 mtDNA by a single nucleotide polymorphism. These mice were used to assess mtDNA release from 5TGM1 cells. The mice were sacrificed, and the bone marrow was harvested and used to generate BMDM.

2.2.3 NSG mice

Nonobese diabetic (NOD) severe combined immunodeficient (SCID) gamma mice (NOD. Cg-Prkdcscid Il2rgtm1Wjl/SzJ) were obtained from Jackson Laboratory (Bar Harbour, ME, USA). This mouse strain is deficient in B and T cells due to a mutation in the DNA repair complex protein (Prkdc). Additionally, they lack mature natural killer cells due to the IL2rg^{null} mutation which inhibits multiple receptor cytokine signalling. This severe combined immunodeficiency permits the generation of a human xenograft mouse model after non-myeloablative busulfan (25 mg/kg) pre-conditioning for three consecutive days. These mice were used for the engraftment of human MM cell lines (U266 and MM1S) in order to determine the source of circulating mtDNA in peripheral blood serum, as well as to analyse levels of circulating mtDNA in peripheral blood and bone marrow serum in MM.

2.2.4 C57BL/KaLwRij mice

C57BL/KaLwRij were purchased from Jackson Laboratory (Bar Harbour, ME, USA). They are a spontaneously derived and inbred mouse strain that are predisposed to developing myeloma. Due to this predisposition, mice did not require pre-conditioning with busulfan prior to engraftment with murine 5TGM1 cells which recapitulates similar clinical features of human MM. This syngeneic mouse model was used to study the mtDNA content of peripheral blood serum in MM. Furthermore, C57BL/KaLwRij mice were used in receptor inhibition experiments using H-151 (STING inhibitor) and ODN 2088 (TLR-9 inhibitor). Additionally, this mouse model was used to study the effects of macrophage depletion (via clodronate liposomes) and STING inhibition (via H-151) on the homing of MM.

2.3 Animal Procedures

Animal handling and procedure training was carried out by Mr Richard Croft (IGEBEFB87) and Mrs Anja Croft (L8A2ACED). Procedures were conducted by me under UK Home Office personal licence number I96361629 with the help and supervision of Dr Jayna Mistry (I2777C6D5), Dr Charlotte Hellmich (IE10ADD51), and Dr Stuart Rushworth (ICD3874DB).

2.3.1 Intraperitoneal injections

Busulfan, H-151, ODN, clodronate liposomes, and D-luciferin were administered by intraperitoneal (i.p.) injections. Busulfan was administered at a dose of 25 mg/kg in a volume of 200 μl for all experiments. H-151 was administered at a dose of 750 nmol in a volume of 200 μl. ODN 1826 and ODN 2088 were administered at a dose of 10μg in 200 μl. 150 μl of control and clodronate liposomes were administered to mice. D-luciferin was administered at a dose of 150 mg/kg in a volume of 200 μl. Mice were restrained using a scruff technique and i.p. injections were carried out using a 26-gauge needle into the peritoneum.

2.3.2 Intravenous injections

Mice were placed in a 37°C heat chamber for 10 minutes to promote vasodilation of the lateral tail vein. The mice were then placed in a benchtop cone restraint and 200 μl of cells suspended in PBS were injected into the tail vein using a sterile 26-gauge needle. The mice were then placed into a new clean cage and monitored for a short recovery period before being returned to their home cage. For the human xenograft NSG model, human MM1S or human U266 cells ($2x10^5$) were administered to busulfan pre-treated NSG mice. For murine MM mouse models, 5TGM1 cells ($1x10^{5)}$ were administered to busulfan pre-treated C57/BL6 mice or C57BL/KaLwRij mice.

2.3.3 Blood sampling

Blood samples were collected from the tail vein of mice to examine peripheral blood serum mtDNA content. Mice were placed in a 37°C heat chamber for 10 minutes before being restrained in a benchtop holding cone. Blood samples were taken using a trimmed 26-gauge butterfly needle and a volume of up to 200 μl was collected in an EDTA-coated tube for further processing.

2.3.4 Live bioluminescence imaging

To assess the tumour burden and engraftment of live mice, bioluminescent imaging was carried out. Mice engrafted with 5TGM1 cells transduced with rLV.EF1.mCherry-mito9 lentivirus were injected with 150 mg/kg of D-luciferin intraperitoneally, this allows for light production as oxyluciferin is formed from the catalysation of luciferin by the luciferase in the modified MM cells. The mice were left for around 10 minutes at room temperature to allow for optimal detection of the luciferase signal. Mice were anaesthetised with isoflurane at a flow rate of 2-3% in an anaesthetic chamber. The mice were then transferred to the Bruker In-Vivo Xtreme (Bruker, Coventry, UK) machine. A pre-set of 1-minute exposure bioluminescence image, followed by an x-ray and a light image was used. Mice were then transferred to their home cage for recovery. The captured bioluminescent images and x-ray images were merged and edited using ImageJ software (Fiji) for visualisation and bioluminescence quantification was also carried out in ImageJ.

2.3.5 Schedule 1 Euthanasia

Mice were sacrificed humanely at the endpoint of each experiment if they were exhibiting any sign of illness or distress such as piloerection, overgrooming, hind-limb paralysis, weight loss, and hunching. Gradual CO_2 asphyxiation followed by neck dislocation for confirmation of death was the schedule 1 method of choice.

2.3.6 NSG xenograft MM model

NSG mice were pre-conditioned with 25 mg/kg busulfan for three days prior to i.v injection of $2x10^5$ human myeloma cell lines MM1S or U266. Peripheral blood samples were taken via tail vein bleed on days 7 and 14 and the mice were sacrificed on day 21. Serum was extracted from the blood samples and analysed for human and murine mtDNA presence by qPCR. The bone marrow was isolated, and myeloma engraftment was confirmed by the presence of human CD38+ cells via flow cytometry analysis.

2.3.7 Syngeneic 5TGM1 MM model

C57BL6 or C57BL/KaLwRij mice were engrafted with $1x10^6$ murine $5TGM1^{(GFP+\ Luci+)}$ cells (C57BL/6 mice were pre-conditioned with 25 mg/kg busulfan treatment. Peripheral blood samples were taken by tail vein bleed at varying intervals and serum was extracted for mtDNA content analysis via qPCR.

2.3.8 *In vivo* STING and TLR-9 receptor inhibition

C57BL/KaLwRij mice were engrafted with $1x10^6$ murine $5TGM1^{(GFP+\ Luci+)}$ cells. On days 20, 22, 24 and 26 post-injection, mice were intraperitoneally injected with 200 µl of H-151 (750 nM, Invivogen), ODN 2088 (10 µg), or vehicle (PBS with 0.1% Tween-80). Mice were imaged via live bioluminescent imaging (section 2.3.4) before and after inhibitor treatment. The animals were sacrificed at day 27 post-injection and the BM was isolated. The BM was analysed using flow cytometry for 5TGM1 engraftment (GFP^+) and BM macrophage cell populations to identify resident bone marrow macrophages (BMMΦ) (GR1-, CD115 lo/int, F4/80+) and MM-associated macrophages (MAMΦ) (Ly6G-, CD11b+). The MAMΦ were FACS purified into RNA lysis buffer via BD FACSMelody (BD Bioscience), and the RNA was extracted for qPCR analysis of the relative gene expression of IL-6, Gbp2, Ifit3, and Irf7.

2.3.9 *In vivo* macrophage depletion

C57BL/KaLwRij mice were engrafted with $1x10^6$ murine 5TGM1$^{(GFP+\ Luci+)}$ cells via i.v. injection. 13 days post-engraftment mice were intraperitoneally injected with 150 µl of either control or clodronate-loaded liposomes (Clophosome®-A, Stratech, UK). 24 hours later, the mice were sacrificed, and the bone marrow and peripheral blood were isolated for analysis via flow cytometry. To ensure bone marrow macrophage depletion, the population of BMMΦ (GR1-, CD115$^{LO/INT}$, F4/80+) was compared between treatment groups. Peripheral blood and bone marrow samples were also analysed for 5TGM1$^{(GFP+)}$ content to assess 5TGM1 cell homing.

2.3.10 *In vivo* STING inhibition migration assay

C57BL/KaLwRij mice were engrafted with 5TGM1$^{(GFP+\ Luci+)}$ cells and engrafted for 34 days. On day 34, peripheral blood samples were taken prior to treatment with H-151 (750 nmol) administered intraperitoneally, after 24 hours another peripheral blood sample was taken to be analysed by flow cytometry for 5TGM1$^{(GFP+)}$ content to measure 5TGM1 cell retention.

2.4 Cell Culture

All cells in this study were cultured and maintained at 37°C with 5% CO^2 humidity.

2.4.1 Primary human cell isolation

Primary multiple myeloma samples were obtained from patients at the Norfolk and Norwich University Hospital after informed consent and under the approval of the UK Health Research Authority and East of England Research Ethics Committee (IRAS project ID: 33753). Bone marrow aspirates were collected in tubes containing 15 ml DMEM supplemented with 100 units of Heparin. Cell isolation was performed via density-gradient centrifugation of bone marrow aspirates using Histopaque-1077 (Millipore Sigma).

Briefly, bone marrow aspirate was gently overlaid onto a layer of Histopaque-1077 in a 50 ml Falcon tube and centrifuged at 300 xg for 15 minutes without brakes or acceleration. Following centrifugation, the red blood cells are pelleted at the bottom of the tube and the Histopaque-1077 is in a separate layer on top. A 'buffy coat' layer containing mononuclear cells sits on top of the Histopaque layer and above that is an upper layer of plasma (Figure 2.1). The buffy coat layer was isolated using a Pasteur pipette and transferred into a fresh 50 ml Falcon tube and washed with 1X PBS by centrifugation at 2000 rpm for 5 minutes with the brakes on to pellet the cells. The supernatant PBS was removed, and the pellet was resuspended in DMEM supplemented with 10% FBS (foetal bovine serum) and 1% Penicillin/Streptomycin. The cell suspension was then transferred to a tissue culture T75 flask and incubated at 37°C with 5% CO_2 humidity.

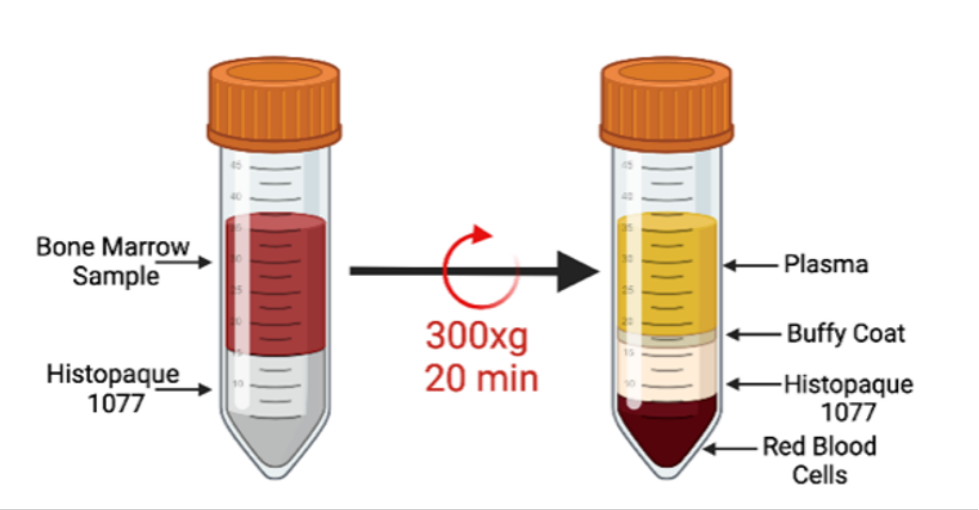

Figure 2.1. Density gradient centrifugation.

Bone marrow aspirate from myeloma patients was layered on top of Histopaque-1077 and centrifuged. The buffy coat contains the mononuclear cells of interest. (Created using Biorender.com).

2.4.2 Human MM cell lines

The human myeloma cell lines U266 and MM1S were cultured in RPMI-1640 medium supplemented with 10% FBS and 1% Penicillin/Streptomycin. For *in vivo* experiments, engraftment was determined by the detection of human CD38+ cells in the bone marrow via flow cytometry.

2.4.3 Primary mouse bone marrow isolation

The bone marrow was extracted from the tibia and femur of mice. The bones were cut in half and placed into a 0.5 ml Eppendorf tube with a hole in the bottom, which was then placed in a 1.5 ml Eppendorf to allow the bone marrow to be collected via short spin centrifugation for 6 seconds. The BM pellets from each mouse were pooled and washed in MACS buffer (1X PBS, 0.5% BSA, 2 mM EDTA, filtered) and then filtered through a 40 µm CellTrics filter (Sysmex).

2.4.3.1 Murine bone marrow-derived macrophages

Macrophages were derived from freshly isolated mouse BM. Briefly, 1-2 x10^7 bone marrow cells were plated onto 10 cm tissue culture dishes in RPMI-1640 (GIBCO, ThermoFisher Scientific) supplemented with 20% FBS and 1% Penicillin-Streptomycin and 20 ng/ml macrophage colony-stimulating factor (m-CSF) (Preptrotech). Fresh media was added on day 3. On days 6-7, cells were washed with PBS, before being removed by scraping in cold PBS. BMDMs were seeded in RPMI-1640 supplemented with 20% FBS and 1% Penicillin-Streptomycin. For longer survival, BMDMs were cultured in RPMI-1640 supplemented with 20% FBS and 1% Penicillin-Streptomycin and 10 ng/ml m-CSF. The generation of BMDMs was confirmed by identifying the characteristic morphology of macrophages via microscopy (EVOS™ M5000 Imaging System).

2.4.4 Murine 5TGM1 cell line

5TGM1 cells were cultured in an RPMI-1640 based medium supplemented with 20% FBS, 1% Penicillin-Streptomycin, 1% sodium pyruvate and 1% non-essential amino acids. To generate 5TGM1$^{(GFP+\ Luci+)}$ cells, 5TGM1 cells were seeded at a density of 5x10^4 in 500 µl of 5TGM1 media and dual-transduced with 0.5 µl of rLV.EF1.mCherry-Mito-9 and rLV.EF1.AcGFP-Mem9 lentivirus (Clontech), the mCherry tag fluoresces red whilst the plasma membrane green fluorescent protein (GFP) tag expresses a green fluorophore. After 24 hours 1 ml of 5TGM1 media was added and the cells were cultured for a further week to ensure that there was no residual lentivirus. Successful transduction was confirmed by the detection of mCherry and GFP fluorescence in 5TGM1 cells via fluorescence microscopy.

2.4.5 Serum extraction

Serum was extracted from (human and mouse) peripheral blood or bone marrow samples by centrifugation at 1,600 xg for 10 minutes, and the supernatant was further centrifuged at 16,000 xg for 5 minutes to remove cells and cellular debris. Mouse bone marrow serum was extracted by allowing $5x10^6$ isolated bone marrow cells to sediment and centrifuging the resulting supernatant at 1,400 rpm for 5 minutes to remove cells. Serum samples were stored at -20˚C until needed for further DNA extraction. Based on methods described by Perdas et al. 2010 [322].

2.4.6 Cell cryopreservation

Primary MM cells and cell lines were cryopreserved for long-term storage. Cells were pelleted at a density of $5x10^5$ cells/ml and resuspended in a freezing mix (10% dimethyl sulfoxide (DMSO) in FBS). Cells were then transferred to a cryotube and placed in a Mr. Frosty™ container which cools cells at an optimal rate of -1˚C/minute and preserves cell integrity. The cryotubes were preserved in a -80˚C freezer.

To thaw cells, culture medium was warmed to 37˚C, the cryotubes were removed from the -80 µl freezer and partially defrosted at 37˚C. The cells were transferred to a 15 ml Falcon tube and 10ml of pre-warmed medium was then added in a drop-wise manner to slowly dilute the DMSO. The cells were centrifuged at 1400 rpm for 5 minutes to completely remove the DMSO. The pellet was resuspended in fresh media and cultured accordingly.

2.5 Generation of mtDAMPs

The Mitochondrial Isolation Kit for Cultured Cells (PIERCE, Rockford, IL) was used to isolate mitochondrial pellets from 200 mg of healthy mouse liver tissue using the reagent-based method. Briefly, liver tissue was washed twice with PBS on ice and cut up into small pieces using a scalpel to obtain a homogenous suspension. The tissue was centrifuged at 1000 xg for 3 minutes before the pellet was resuspended in 800 µl of BSA/Reagent A solution. Following vortexing, 10 µl of Mitochondrial Isolation Reagent B was added and the suspension was incubated on ice for 5 minutes vortexing at maximum speed every minute. Next, 800 µl of Mitochondrial Isolation Reagent C was added to the tube and centrifuged at 700 xg for 10 minutes. The supernatant was transferred to a clean tube and centrifuged at 12,000 xg for 15 minutes. 500 µl of wash buffer was added and centrifuged at 12,000 xg for 5 minutes. The mitochondrial pellet was maintained on ice for downstream processing.

The isolated mitochondrial pellets were resuspended in 1 ml of HBSS and a protease inhibitor cocktail (1:100) was added to the suspension. The mitochondria were disrupted by sonication on ice (10 times, 30 seconds each with 30-second intervals in between) at 100% amplitude to simulate tissue injury. The mitochondrial suspensions were centrifuged at 12,000 rpm for 10 minutes at 4°C followed by centrifugation at 15,000 xg at 4°C for a further 10 minutes (Figure 2.3). mtDAMPs suspensions were stored at -20˚C for further experiments. Protein concentration was determined using the Nanodrop 2000.

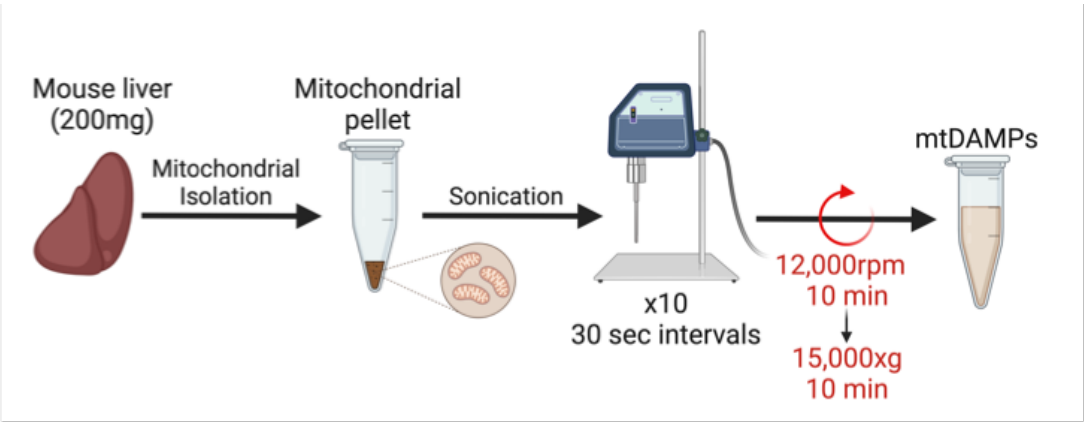

Figure 2.2. The generation of mtDAMPs

Schematic showing the process of isolating mitochondria from mouse liver and obtaining mtDAMPs suspension by sonication and centrifugation. (Created using Biorender.com).

2.6 Cell culture assays

2.6.1 Cell counting

To determine cell viability and cell numbers for experiments the Trypan Blue exclusion method was used. Non-viable cells do not have an intact cell membrane therefore they take up the Trypan blue dye whilst viable cells do not as their cell membranes are intact. 10 µl of cell suspension was diluted in a 1:1 ratio with Trypan blue. 10 µl of this mixture was loaded onto a Neubauer haemocytometer. All viable cells were counted in each of the four outer quadrants and the total cell count per ml was calculated (Figure 2.2).

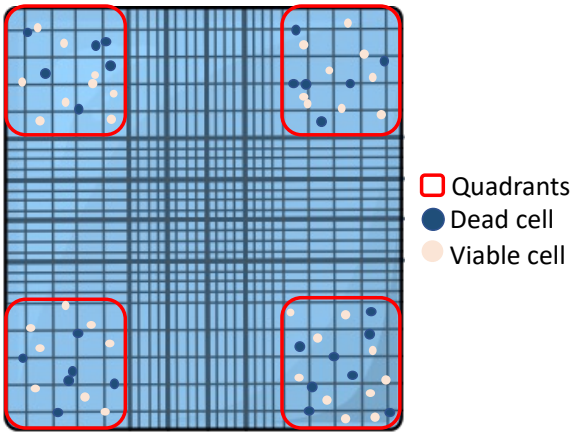

$$\text{Cell number (cells/ml)} = \left(\frac{\text{Viable cell number}}{\text{Number of quadrants counted}} \right) \times \text{Dilution factor} \times 10^4$$

Figure 2.3. Cell counting via Trypan blue exclusion.

Haemocytometer layout shows outer quadrants to be counted, viable cells (white) and dead cells (blue). The calculation for cell number per ml is shown.

For animal experiments, cell numbers were counted automatically using the Cellometer Auto T4 Brightfield Viability Cell Counter (Nexcelom Bioscience, Lawrence, MA, USA). Cells isolated from BM were diluted 1:10 in MACS buffer and further diluted 1:1 with Trypan blue, 20 µl of this mixture was loaded onto a counting chamber (Nexcelom Bioscience, Lawrence, MA, USA). The cell concentration was calculated taking into account the 20x dilution factor.

2.6.2 BMDM stimulation and STING inhibition

BMDMs were seeded at a density of $2x10^5$ in 500µl of RPMI-1640 containing 10% FBS and 1% Penicillin-Streptomycin in a 24-well plate. Cells were treated for 6 hours with ODN 1826 (10 µg), which acted as a molecular mimic for mtDNA, or mtDAMPs suspension (10 µg). BMDM RNA was extracted and analysed for cytokine gene expression via qPCR. In experiments where STING was inhibited, BMDMs were pre-treated for 2 hours with STING inhibitor H-151 (10 µM) prior to the administration of other treatments.

2.6.3 5TGM1 conditioned medium on BMDM

In order to assess the effects of secreted factors from MM cells on BMDMs, conditioned media from 5TGM1 cells was centrifuged at 12,000 xg for 10 minutes to remove large and medium extracellular vesicles (EVs), and the supernatant was then filtered through a 100 kDa Amicon Ultra-15 centrifugal filter (Merck, Burlington, MA, USA) at 4000 xg for 10 minutes. The filter membrane has a molecular weight cut-off of 100,000 meaning that molecules with a molecular weight above this such as small extracellular vesicles are retained by the filter in the concentrate. BMDM cells were cultured for 24 hours in the ultrafiltrate, after which the BMDM RNA was extracted, and cytokine gene expression was analysed via qPCR.

2.6.4 5TGM1 *in vitro* migration assay

To examine the effects of mtDAMPs stimulation and STING inhibition on the migratory capacity of 5TGM1 cells a migration assay was conducted. Briefly, BMDMs were treated with either mtDAMPs (10 µg) or H-151 (10 µM) for 24 hours. The conditioned media was retrieved by centrifugation at 5000 rpm for 10 minutes to pellet cells and cellular debris. 600 µl of the conditioned media was used as a chemotactic medium in the bottom chamber of an 8µm Transwell (Costar, Fisher Scientific). 5TGM1$^{(GFP+\ Luci+)}$ cells were seeded in the upper chamber at a density of $1x10^5$ in 100 µl. 5TGM1 migration towards conditioned medium from untreated BMDMs was used as a control. The cells were left to migrate and the number of 5TGM1$^{(GFP+)}$ cells in the bottom chamber was counted at 4 and 24 hours via fluorescent microscopy, counting an average of four distinct areas of each well.

2.7 Flow cytometry and cell sorting

Flow cytometry was used in this study to identify cell populations, determine engraftment levels and sort specific cell populations for RNA analysis. These processes relied on the staining of surface receptors on cells with antibodies that are conjugated with a detectable fluorophore. Different flow cytometers were used depending on the function, the number of lasers and thus the number of fluorophores that can be detected, and also access and availability due to Covid-19 restrictions at the time.

The antibody panels used in this study are shown below (Table 2.2). For each antibody panel, a compensation was set up using OneComp eBeads™ Compensation Beads (ThermoFisher, Waltham, MA, USA) on the relevant flow cytometer to measure fluorophore emission crossover. Furthermore, fluorescence-minus-one controls were run for each panel to optimally identify positively and negatively stained cell populations to ensure optimal gating strategies were used. All antibodies were purchased from Miltenyi Biotech (Bergisch Gladbach, Germany), or BioLegend (San Diego, CA, USA).
Data was downloaded as flow cytometry standard (FCS) files and analysed using FlowJo version 10.8.1 software (FlowJo, LLC, Ashland, OR, USA).

Table 2.2. Antibody panels used for flow cytometry analysis.

Biolegend / Miltenyi	Fluorophore						
Antibody Panel	**FITC**	**PE-Cy5**	**PE-Cy7**	**APC-Cy7**	**APC**	**BV421**	**PE**
BMMΦ Flow	5TGM1-GFP	GR1	F4/80	CD115	-	CD86	CD206
BMMΦ Sort	5TGM1-GFP	GR1	F4/80	CD115	-	-	-
MAMΦ Flow	5TGM1-GFP	Ly6G	-	-	CD11b	CD86	CD206
MAMΦ Sort	5TGM1-GFP	Ly6G	-	-	CD11b	-	-
NSG Engraftment	-	-	-	-	hCD38	-	-

2.7.1 Sample preparation for flow cytometry

For each antibody panel, $5x10^6$ isolated BM cells were aliquoted in 200 µl of MACS buffer and incubated in a master mix of antibody cocktail for at least 20 minutes in the dark at 4˚C. The master mix contained 1 µl of each antibody per sample.

2.7.2 Flow cytometers

2.7.2.1 BD FACSCanto II

Located in the Pathology Laboratory of the Norfolk and Norwich University Hospital and maintained by Dr Allyson Tyler, the FACSCanto II (BD, Franklin Lakes, NJ, USA) holds three lasers, 488, 633 and 405 nm and can detect eight fluorophores (FITC, PE, PE-Cy5, PE-Cy7, APC, APC-Cy7, BV421, and BV510). This flow cytometer was used in the majority of flow cytometry experiments in this study for the detection of engraftment levels and differences in cell populations.

2.7.2.2 BD FACSymphony A1

Located in the Bob Champion Research and Education Building at the University of East Anglia, the BD FACSymphony A1 has four lasers (405, 488, 561, and 637 nm) and can detect up to 16 colours at a time. This flow cytometer was available towards the end of this study and was used to analyse *in vivo* migration experiments.

2.7.2.3 Sony SH800 Cell Sorter

Located in the Quadram Institute on the Norwich Research Park, this cell flow cytometer has four lasers (405, 488, 561, and 637 nm) and can detect six colours at a time. It was used to sort GFP and mCherry dual-positive 5TGM1 cells into culture medium to be maintained by cell culture for further experiments. This sorting was kindly carried out by Dr Stuart Rushworth.

2.7.2.4 BD FACSMelody

The FACSMelody is located in the Earlham Institute on the Norwich Research Park. It has the same capabilities as the FACSCanto II with the additional capacity to sort cells via fluorescence-activated cell sorting (FACS). This flow cytometer was used to sort resident bone marrow macrophages (BMMΦ) (GR1-, CD115 lo/int, F4/80+) and MM-associated macrophages (MAMΦ) (Ly6G-, CD11b+), BM samples were sorted into lysis buffer for RNA analysis. This was kindly carried out by Dr Stuart Rushworth and Dr Edyta Wojtowicz.

2.8 Molecular biology

2.8.1 RNA extraction

RNA extraction was carried out using the Reliaprep RNA Cell Miniprep System (Promega, WA, USA) following the manufacturer's instructions. For BMDM experiments the media was removed from the wells and the cells were washed twice with PBS and then manually lysed by the addition of 500 µl of BL+TG (1-Thioglycerol) buffer, pipetting the solution in the wells up and down 10 times to detach the cells from the well surface and form a cell lysate. For analysis of FACS purified cells, cells were sorted directly into BL+TG lysis buffer. The lysate was transferred to a microcentrifuge tube and 170 µl of absolute Isopropanol was added and vortexed for 5 seconds. The lysate was transferred to a Reliaprep minicolumn in a collection tube and centrifuged at 13,000 xg for 30 seconds. The flow-through was discarded and the column was washed with 500 µl of RNA Wash Solution and centrifuged at 13,000 xg for 30 seconds. 200 µl of Column Wash Solution was then added and centrifuged at 13,000 xg for 15 seconds. The column was then washed with 500 µl of RNA Wash Solution and centrifuged at 13,000 xg for 30 seconds, followed by a second wash with 300 µl of RNA Wash Solution centrifuged at 13,000 xg for 2 minutes. The column was then centrifuged again at 13,000 xg for 2 minutes to dry the column. The minicolumn was transferred to a 1.5 ml elution tube and 20 µl of nuclease-free water was added and centrifuged at 13,000 xg for 1 minute to elute the RNA. Isolated RNA was stored at -20˚C.

2.8.2 DNA extraction

To determine the levels of mitochondrial and genomic DNA in mouse and human serum samples and cell culture experiments, DNA was isolated using the GenElute Mammalian Genomic DNA Miniprep Kit (Sigma Aldrich, St Louis, MO, USA) following the manufacturer's instructions. The samples were first lysed via the addition of 20 µl of Proteinase K to up to 200 µl of sample, followed by 200 µl of Lysis solution C. The lysate was then incubated at 70°C for 10 minutes to allow for efficient lysis. 200µl of absolute ethanol was added to the lysate post-incubation. Prior to loading, the binding column was pre-treated with 500 µl column preparation solution to maximise binding and DNA yield. The lysate was loaded onto the column and centrifuged at 6500 xg for 1 minute. The flow through was discarded and 500 µl of Wash Solution was loaded onto the column and centrifuged at 6500 xg for 1 minute. The column was washed a second time with 500 µl of Wash Solution and centrifuged at 16,000 xg for 3 minutes. The flow through was discarded and the column was centrifuged again at 16,000 xg for 1 minute to dry. To elute the DNA, 50 µl of Elution Solution was added to the column and centrifuged at 6500 xg for 1 minute. The DNA was stored at -20°C for further analysis.

2.8.3 Quantification of RNA and DNA

Extracted RNA and DNA samples were quantified using the NanoDrop 2000 spectrophotometer (ThermoFisher, Waltham, MA, USA). The NanoDrop was first cleaned, and a blank sample was run using 1 µl of elution buffer (nuclease-free water or Elution Solution) before each use. 1 µl of the sample was loaded onto the NanoDrop and RNA/DNA concentration (ng/µl) was determined. The purity of the sample was determined using the A260/230 ratio, a ratio of between 1.7 and 2.3 was deemed sufficiently pure.

2.8.4 cDNA synthesis

To analyse the gene expression of BMDMs and FACS purified macrophages, extracted RNA was processed into cDNA using two reverse transcription methods. The first method utilised the qPCRBIO cDNA Synthesis Kit (PCR Biosystems) following the manufacturer's instructions. Briefly, a 10 µl reaction was made up comprising of 2 µl of 5x cDNA synthesis mix, 0.5 µl of 20x RTase, 5.5 µl of RNase-free water, and 2µl of RNA sample. Using the Bio-Rad T100 Thermal Cycler (Bio-rad, Watford, UK), PCR reactions were run on a pre-defined program of an initial 42°C incubation for 30 minutes, followed by a 10-minute incubation at 85°C to denature RTase. The cDNA samples were held at 4°C until removed and stored at -20°C until needed.

Alternatively, the PCRBIO 1-step Go RT-PCR Kit (PCR Biosystems, London, UK) was used as this method does not require a separate cDNA synthesis step and RNA samples are prepared directly for qPCR analysis using an RTase-containing master mix.

2.8.5 Real-Time quantitative PCR

Real-Time quantitative PCR (qPCR) was performed using the Roche Lightcycler 480 (Roche, Basel, Switzerland) in 384-well Roche Lightcycler reaction plates. qPCR was utilised to examine gene expression using SYBR-Green technology or analyse mtDNA content using Taqman-based technology. The details of the primers used are provided in Table 2.3.

Table 2.3. Primers used for qPCR analysis

QuantiTect SYBR-Green Primers (Qiagen)		
Gene	**Primer Assay Name**	**GeneGlobe ID**
GAPDH	Mm_Gapdh_3_SG	QT01658692
IL-6	Mm_Il6_1_SG	QT00098875
GBP2	Mm_Gbp2_1_SG	QT00106050
IFIT3	Mm_Ifit3_1_SG	QT00292159
IRF7	Mm_Irf7_1_SG	QT00245266
KiCqStart® SYBR-Green Primers (Sigma-Aldrich)		
Gene	**Gene ID**	**RefSeq ID**
CCL5	20304	NM_013653
CXCL2	20310	NM_009140
CXCL10	15945	NM_021274
TaqMan® Primers (ThermoFisher)		
Gene	**Assay name**	**Assay specifics**
Human Tert	TaqMan® copy number reference assay human	4403316
Human ND1	Hs02596873_S1	4331182
Mouse Tert	TaqMan® copy number reference assay mouse	4458368
Mouse ND1	Mm04225274_S1	4331182
COX3_9348snp	Custom TaqMan® COX3 assay	ANNKVUR

2.8.5.1 Gene expression

To analyse the gene expression profiles of FACS purified macrophages and BMDMs from experiments, SYBR-Green technology (PCR Biosystems, London, UK) was used. Where synthesised cDNA was used, a master mix containing 0.5 µl of primer, 5µl of SYBR-Green mix, and 2.5 µl of nuclease-free was made up and 6 µl of this master mix was plated into a 384-well Roche Lightcycler reaction plate before 2 µl of diluted cDNA was added for a total 10 µl reaction volume. For the 1-step Go qPCR method, a master mix of 0.1 µl of RTase Go 1-step, 2.5 µl of SYBR-Green mix, and 0.4 µl of PCR primer was pipetted directly into a 384-well plate and 2 µl of RNA sample was added.

Samples were plated in quadruplicate. The plates were sealed and centrifuged at 1000 rpm for 1 minute to ensure reactions were thoroughly mixed. Plates were then placed in the Roche Lightcycler 480 (Roche, Basel, Switzerland) and qPCR reactions were run using pre-programmed cycles as described in Table 2.4.

Table 2.4. qPCR SYBR-Green Lightcycler programs.

cDNA qPCR			
Process	**Cycles**	**Temperature**	**Time**
Pre-amplification	1	95°C	2 mins
Amplification	45	95°C 60°C 72°C	15 secs 10 secs 10 secs
Melt curve	1	95°C 65°C 97°C	5 secs 1 min Continuous
Cooling	1	40°C	30 secs
1-step Go RT-PCR			
Process	**Cycles**	**Temperature**	**Time**
Reverse transcription	1	45°C	10 mins
Polymerase activation	1	95°C	2 mins
Amplification	40	95°C 60°C 72°C	10 secs 10 secs 30 secs
Melt curve	1	95°C 65°C 97°C	5 secs 1 min Continuous
Cooling	1	40°C	30 secs

The raw output generated by the Lightcycler is known as the cycle threshold (Ct) value. Genes of interest were normalised to the housekeeping gene Glyceraldehyde 3-phosphate dehydrogenase (GAPDH) which is present in every cell and its expression is unaffected by genetic alterations or cellular treatments. To quantify gene expression, the Ct value of the housekeeping gene was subtracted from the Ct value of the gene of interest. This value was termed the delta (Δ) Ct. Next, the ΔCt value of the test condition was subtracted from the appropriate control condition ΔCt value, in order to obtain the ΔΔCt value. The fold change in expression was then determined relative to untreated samples by calculating $2^{-\Delta\Delta Ct}$.

2.8.5.2 Taqman® based mtDNA analysis

For the detection and quantification of mitochondrial and genomic DNA in isolated serum samples and cell culture experiments, DNA was extracted as described in 2.8.2. Pre-designed Taqman probes (ThermoFisher) encompassing murine COX 3 mtDNA, murine ND1 mtDNA, human ND1 mtDNA and human and murine Tert (genomic) DNA were used in this assay. This assay works as probes contain 2'- chloro-7'phenyl-1,4-dichloro-6-carboxyfluorescein (VIC) and/or 6- carboxyfluorescein (FAM) fluorophores and have a TAMRA® quencher bound to the gene of interest. As the DNA is amplified, the probe is cleaved which releases the fluorophore from the quencher and allows for the detection of a fluorescent signal. In experiments where the probes were on the same fluorophore, the TaqMan® assay was run in simplex reactions, and where the probes were on different fluorophores the TaqMan® assay was run in a duplex reaction in quadruplicates. The qPCR was run with a pre-programmed setting (Table 2.5).

Table 2.5. TaqMan® assay Lightcycler program.

TaqMan® assay			
Process	**Cycles**	**Temperature**	**Time**
Pre-amplification	1	60°C 95°C	30 secs 5 mins
Amplification	50	95°C 60°C	15 secs 1 min
Cooling	1	40°C	30 secs

2.8.5.3 Human and murine mtDNA analysis

To examine the levels of circulating mtDNA in the serum of human and murine samples, human and murine Tert and ND1 probes were used in a duplex reaction as the Tert probe is VIC and the ND1 probe is on FAM. The duplex mastermix contained: 0.25 µl of each primer was added to 2.5 µl of TaqPath ProAmp enzyme (ThermoFisher, Waltham, MA, USA), and 1 µl of nuclease-free water. 4 µl of this master mix and 1 µl of extracted DNA was plated into a 384-well plate. The plate was sealed and centrifuged for 1 minute at 1000 rpm and then run on a pre-defined program in the Roche Lightcycler 480 (Roche, Basel, Switzerland). The fold change in mtDNA or gDNA expression was quantified from the qPCR-generated Ct values. Briefly, the ΔΔCt value of each sample was determined by subtracting the average Ct value of control (healthy) samples from the test (myeloma) samples. The fold change was then determined by calculating $2^{-\Delta\Delta Ct}$.

2.8.5.4 Murine mtDNA SNP detection

To analyse the effects of mtDAMPs-mediated BMDM activation on the release of mtDNA from 5TGM1 cells the mouse mtDNA Taqman assay was used. Briefly, BMDMs cultured from CBA mice were treated with mtDAMPs (10 µg) or untreated for 24 hours. The media was removed and centrifuged at 5000 rpm for 10 minutes to pellet cells and cellular debris. $5x10^4$ 5TGM1 cells were then cultured in this cell-free medium for 24 hours. The media was removed and centrifuged gently at 1500 rpm for 5 minutes to pellet cells whilst ensuring the cells are not damaged. The culture medium supernatant was then subjected to DNA extraction as described in section 2.8.2. The COX3 mtDNA probe contains two sequence-specific fluorophores VIC and FAM, that can be used to distinguish between single nucleotide polymorphisms in the mtDNA of C57/BL6 mice and CBA mice. In cells from a C57BL/6 mouse strain background, such as 5TGM1 cells derived from C57BL/KaLwRij mice, COX3 is detected on VIC, whilst CBA-derived COX3 is detected on FAM.

This means that in the experiment outlined above, any COX3 detected on VIC originated from the 5TGM1 cells and not residual mtDNA released from the CBA-derived BMDMs. Fold change in mtDNA expression was quantified using the qPCR-generated Ct values using the ΔΔCt method described above and normalised to control 5TGM1 cell COX3 SNP expression.

2.8.6 Cytokine array

For the analysis of the effect of mtDAMPs on the BMDM gene expression profile, the Proteome Profiler Mouse Cytokine Array Panel A (R&D Systems) was used following the manufacturer's instructions. This enabled the analysis of the relative expression levels of 40 cytokines. The assay employs selected capture and control antibodies that have been spotted in duplicate on nitrocellulose membranes. BMDMs were plated at a density of 1.5 x 10^6 in a 6-well plate in RPMI-1640 supplemented with 10% FBS and 1% Penicillin-Streptomycin. mtDAMPs (10 µg) were added to the BMDMs for 24 hours. The media samples were aspirated and cleared of cells and cellular debris by centrifugation at 10,000 rpm for 10 minutes. The samples were prepped for cytokine array by adding 1 ml of sample to 0.5ml of Array Buffer 4 followed by the addition of 15 µl of reconstituted Mouse Cytokine Array Panel A Detection Antibody Cocktail. The samples were then incubated for 1 hour. Array membranes were blocked with 2 ml of Array Buffer 6 and incubated at room temperature for 1 hour on a rocking platform. After blocking and incubating, the prepared samples were applied onto each membrane and incubated overnight at 4℃ on a rocking platform. The membranes were then washed in individual containers with 20 ml 1X Wash Buffer for 10 minutes on a rocking platform, this was repeated for a total of 3 washes. The membranes were then placed in a 4-well multi-dish containing 2 ml of Streptavidin-HRP diluted 1:2000 in Array Buffer 6. The membranes were incubated at room temperature on a rocking platform for 30 minutes.

The membranes were washed once as previously described and then gently blotted on paper towels to remove excess Wash Buffer. For detection, membranes were placed on a plastic sheet protector and covered evenly with 1 ml of Chemi Reagent Mix ensuring no air bubbles and then incubated for 1 minute at room temperature. The membranes were imaged for chemiluminescence using the G: BOX Chemi XRQ (Syngene) with autoexposure (3 minutes). The mean pixel density of the blots was quantified against the reference spots using ImageJ (Fiji) software and normalised using background values. Heatmaps were generated using GraphPad Prism software version 9.4.1 (GraphPad Software, San Diego, CA, USA).

2.9 Statistical analysis

All data produced in this study were analysed using FlowJo software version 10.8.1 (FlowJo, LLC, Ashland, OR, USA), GraphPad Prism software version 9.4.1 (GraphPad Software, San Diego, CA, USA) and Microsoft Excel (Albuquerque, NM, USA). Due to variability, particularly when carrying out *in vivo* work, a statistical comparison was performed without an assumption of normal distribution. For statistical comparison between two groups, the Mann-Whitney test was used. For comparison of more than two groups, One-way ANOVA followed by Tukey's multiple comparisons test or Kruskal-Wallis statistical test followed by Dunn's multiple comparisons or Two-way ANOVA followed by Sidak multiple comparisons test was performed. Statistical analysis between matched samples was performed using the Wilcoxon matched-pairs signed rank test. Differences among groups were considered significant when the probability value, p, was less than 0.05 (*$p < 0.05$, **$p < 0.01$, ***$p < 0.001$, ****$p < 0.0001$, ns = not significant). Results represent the mean $\pm$ standard deviation of 3 or more independent samples. GraphPad Prism software version 9.4.1 (GraphPad Software, San Diego, CA, USA) was used to plot graphs. Sample size (n) represents the number of biological replicates. No statistical methods were used to pre-determine the sample size.

3 Circulating myeloma-derived cell-free mtDNA is elevated in the multiple myeloma bone marrow microenvironment

3.1 Introduction

To understand the role of mtDAMPs within the MM BM microenvironment, I chose to focus on mtDNA as a surrogate marker and indicator of mtDAMPs presence. In the last decade, cell-free mtDNA has emerged as a mtDAMP that has been proposed as a useful prognostic and diagnostic biomarker in a range of cancers [313]. Due to its short length and high copy number in comparison to nuclear DNA, it is easily detected by qPCR in the liquid serum and plasma compartments of peripheral blood. Therefore, only a simple blood sample would be required for clinical testing. This offers a welcome opportunity for a reduction in invasive methods such as tissue biopsy currently used for the purpose of diagnosing and monitoring cancer patients.

Whilst many observations have been made regarding circulating cell-free mtDNA levels in many cancer states [314, 315, 317, 318], most studies were carried out in solid tumour cancers, and none have done so in liquid blood malignancies. A study by Ruiz-Heredia et al. reported that mtDNA copy number is increased in the preceding asymptomatic disease states monoclonal gammopathy of undetermined significance (MGUS) and smouldering myeloma (SMM), as well as in MM in correlation with disease progression [323]. This suggests that mtDNA content is implicated in MM pathogenesis. However, these studies have been purely observational. Furthermore, it is yet unknown where this mtDNA originates from.

In this chapter of my thesis, using human MM samples and *in vivo* models of MM, I investigated the association between MM and the presence of mtDNA as a potential biomarker of disease. I also aimed to determine the origin of the cell-free mtDNA.

3.2 Cell-free mtDNA is elevated in the serum of MM patients

Firstly, to ascertain whether we could detect an association between mtDNA and multiple myeloma in a clinical setting, peripheral blood (PB) and matched bone marrow (BM) samples were collected from newly diagnosed MM patients attending clinic appointments at the Norfolk and Norwich University Hospital. Peripheral blood samples were also collected from hemochromatosis patients undergoing routine venesection, patients with no other underlying conditions were selected as a healthy control group. Cell-free serum was extracted from these patient samples via a series of centrifugation steps as shown in Figure 3.1 and described in 2.4.5.

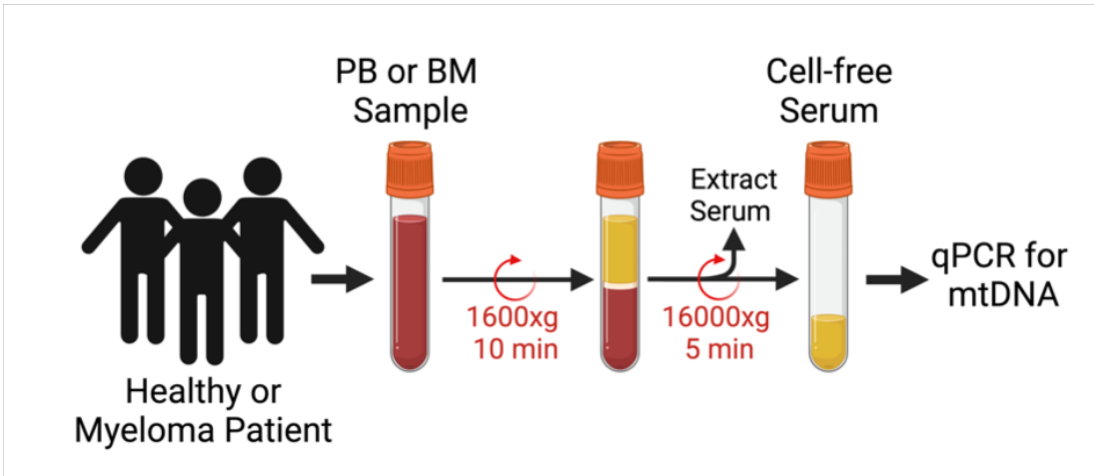

Figure 3.1. Schematic of the serum extraction process.

Patient peripheral blood (PB) or bone marrow (BM) aspirates were subjected to centrifugation to extract serum which was further centrifuged to obtain cell-free serum. Serum DNA was extracted via DNA extraction for downstream mtDNA qPCR analysis. (Created using Biorender.com).

Total DNA was extracted from the serum samples and qPCR was used to detect and quantify genomic (gDNA) and mitochondrial (mtDNA) DNA content. There was a significant increase (p = 0.001) in the amount of mtDNA in the serum of MM patients compared to healthy controls (Figure 3.2A), whilst there was no significant difference (p = 0.9385) in gDNA between the two groups (Figure 3.2B). Notably, there is a high amount of variability observed in the amounts of mtDNA and gDNA in the myeloma samples.

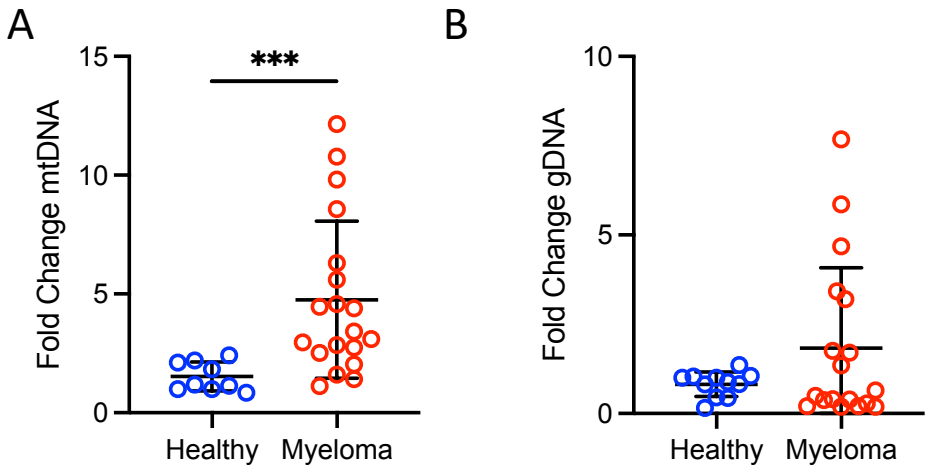

Figure 3.2. Cell-free mtDNA is elevated in MM patient PB serum.

*DNA was extracted from patient peripheral blood (PB) serum and analysed via TaqMan qPCR to assess mitochondrial and genomic DNA (mtDNA and gDNA) content. (A) Fold change in serum mtDNA in healthy (n=9) vs myeloma patients (n=21). (B) Fold change in serum gDNA in healthy (n=11) vs myeloma (n=20) patients. Fold change was calculated based on the ΔΔCt value of the Ct value of control (healthy) samples subtracted from the test (myeloma) samples. Data indicate mean ± SD. Statistics are presented as Mann-Whitney U test. ***p < 0.001.*

As MM is a malignancy that resides in the BM and after having observed this elevated level of cell-free mtDNA circulating in the peripheral blood, we wanted to investigate whether there would be differences in the amount of circulating mtDNA in the peripheral blood serum compared to the bone marrow by comparing the serum from both regions in matched patient samples. Figure 3.3 shows that there is significantly more (p= 0.0039) circulating mtDNA in the BM serum. This suggests that circulating mtDNA first accumulates in the BM before being released into the peripheral blood circulation. Furthermore, it may suggest that the source of this circulating mtDNA is located in the BM.

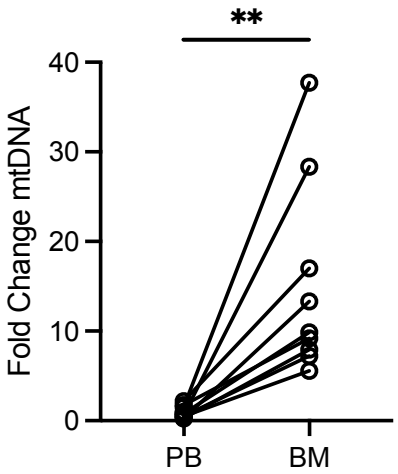

Figure 3.3. Cell-free mtDNA is elevated in MM patient BM serum.

*DNA was extracted from matched MM patient peripheral blood (PB) and bone marrow (BM) serum and analysed via TaqMan qPCR to assess the fold change in mtDNA content of PB vs BM (n=11). Fold change was calculated based on the ΔΔCt value of the Ct value of PB samples subtracted from the BM samples. Data indicate mean ± SD. Statistics are presented as Wilcoxon matched-pairs signed rank test. **p < 0.01.*

3.3 MM cell culture medium contains increased cell-free mtDNA

To further assess the association between myeloma and increased cell-free mtDNA we analysed cell-free culture media from control HSC cells (human CD34+ cells), primary myeloma cells and immortalised human myeloma cell lines (Figure 3.4). The fold change in mtDNA was analysed via qPCR, and mtDNA levels were significantly elevated in primary MM cell culture medium (p = 0.0312), and also elevated in immortalised cell line culture medium (Figure 3.5).

This indicates that myeloma cells themselves could be the cell of origin for this extracellular mtDNA that is released. This interesting finding warranted further investigation.

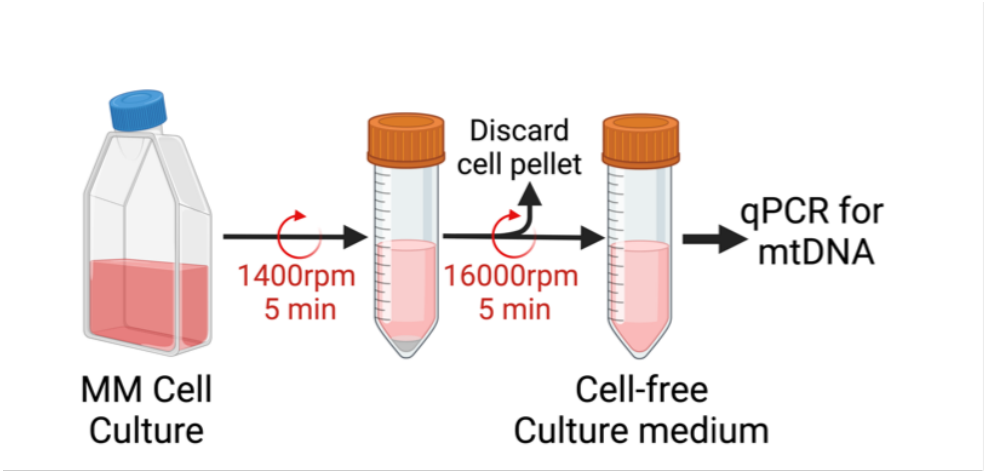

Figure 3.4. Schematic of the cell-free media extraction process.

MM cells in culture were subjected to centrifugation to pellet cells, the supernatant underwent further centrifugation to obtain debris and cell-free culture medium. DNA was extracted from this media and further analysed via TaqMan qPCR for mtDNA. (Created using Biorender.com).

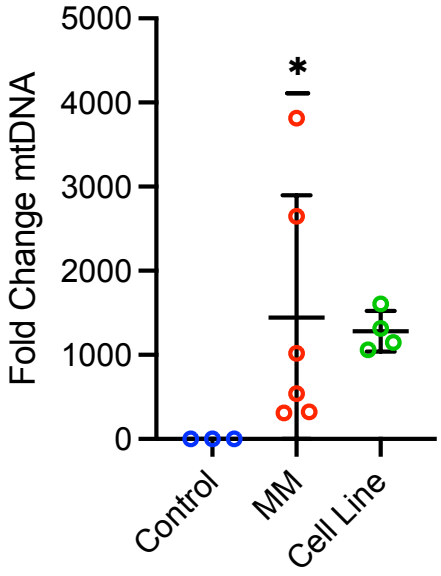

Figure 3.5. Cell-free mtDNA is elevated in MM patient PB serum.

*DNA was extracted from cell-free media extracted from cells in culture and analysed via TaqMan qPCR. Fold change in mtDNA in the media of control human CD34+ cells (n=3), MM patient-derived cells (n=6) and immortalised MM cell lines (n=4). Fold change was calculated based on the ΔΔCt value of the Ct value of control samples subtracted from the test (MM and cell line) samples. Data indicate mean ± SD. Statistics presented as Wilcoxon signed rank test. *p < 0.05.*

3.4 Cell-free mtDNA is elevated in mouse models of MM

In order to confirm the findings of elevated mtDNA *in vitro* and in human samples, we deployed two mouse models of myeloma. In the first model, C57BL/6 mice were pre-treated with 25mg/kg of busulfan via intraperitoneal (i.p) injections for three consecutive days prior to intravenous (i.v) injection of $1x10^6$ murine $5TGM1^{(GFP+\ Luci+)}$ cells. Peripheral blood samples were taken at 11 days post-engraftment (Figure 3.6A). After serum isolation, DNA was extracted and analysed for mtDNA content via qPCR, in the 5TGM1 engrafted group there was a significant increase ($p = 0.0411$) in mtDNA in the PB serum (Figure 3.6B).

To further consolidate this finding, we used the established syngeneic 5TGM1-C57BL/KaLwRij mouse model. The inbred C57BL/KaLwRij (KaL) mouse strain is predisposed to develop a condition called benign idiopathic paraproteinemia (BIP) which is clinically similar to MGUS in humans and develops into multiple myeloma with age [324]. The 5TGM1 cell line is a propagated sub-clone derived from isolated primary 5TMM cells from elderly C57BL/KaLwRij mice that had spontaneously developed myeloma, these cells are highly tumorigenic when engrafted into syngeneic mice [325].

C57BL/KaLwRij mice were engrafted with $1x10^6$ murine $5TGM1^{(GFP+\ Luci+)}$ cells, after 21 days the mice were sacrificed, and peripheral blood samples were taken (Figure 3.7A). The serum was isolated from the blood samples and DNA was extracted for mtDNA analysis via qPCR. Again, mtDNA was found to be significantly increased ($p = 0.0357$) in the serum of engrafted mice compared to control non-engrafted mice (Figure 3.7B).

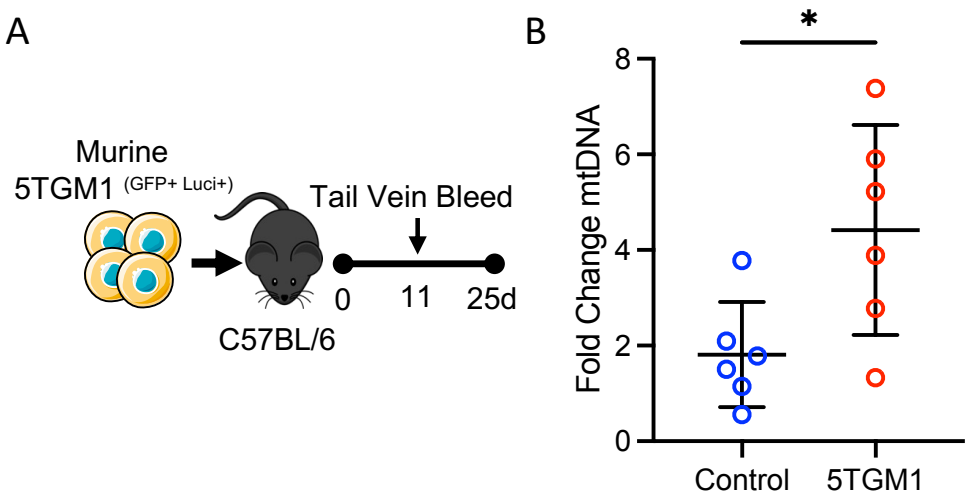

Figure 3.6. Serum mtDNA is elevated in the C57/BL6 MM mouse model.

*(A) Schematic of experimental design. Murine 5TGM1$^{(GFP+\ Luci+)}$ cells (1x10^6) were injected into busulfan (25mg/kg) pre-treated C57BL/6 mice, on day 11 peripheral blood samples were taken via I.V. tail vein bleed and analysed via qPCR. Mice were sacrificed at 25 days. (B) Fold-change in serum mtDNA at day 11 of control non-engrafted C57BL/6 mice and 5TGM1 engrafted C57BL/6 mice. Fold change was calculated based on the ΔΔCt value of the Ct value of control samples subtracted from the 5TGM1 samples. Data indicate mean ± SD. Statistics presented as Mann-Whitney U test. *p < 0.05.*

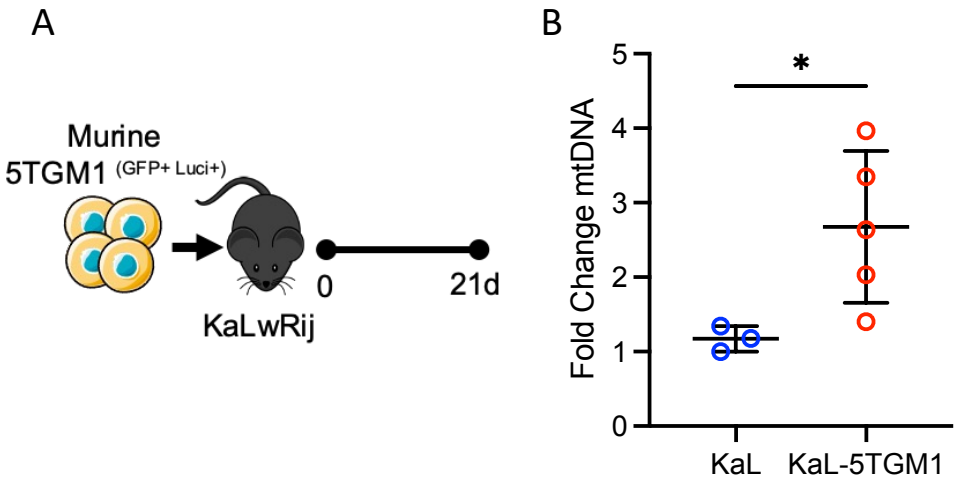

Figure 3.7. Serum mtDNA is elevated in the C57BL/KaLwRij MM model.

*(A) Schematic of experimental design. Murine 5TGM1$^{(GFP+\ Luci+)}$ cells (1x10^6) were injected into C57BL/KaLwRij mice, mice were sacrificed at 21 days and peripheral blood serum samples were extracted and analysed via qPCR. (B) Fold-change in serum mtDNA at day 21 of non-engrafted (KaL) and engrafted (KaL-5TGM1) mice. Fold change was calculated based on the ΔΔCt value of the Ct value of control (KaL) samples subtracted from the KaL-5TGM1 samples. Data indicate mean ± SD. Statistics presented as Mann-Whitney U test. *p < 0.05.*

3.5 Circulating cell-free mtDNA in the peripheral blood and bone marrow serum is derived from MM cells

I next aimed to establish the origin of the cell-free mtDNA we observed to be circulating in the serum of myeloma samples. To do so, a humanised mouse model of MM was established using the nonobese diabetic (NOD) severe combined immunodeficiency (SCID) Il2rg knockout NOD.Cg. PrkdscidIL2rg^{tm1Wji}/SzJ (NSG) mouse strain. The immunocompromised NSG mice were pre-treated with 25mg/kg busulfan for three days prior to i.v injection of 2x10^5 human myeloma cell lines MM1S or U266. Blood samples were taken via tail vein bleed on days 7 and 14 and the mice were sacrificed on day 21 (Figure 3.8A). The BM was extracted, and myeloma engraftment was confirmed by the presence of human CD38+ cells via flow cytometry analysis (Figure 3.8B). Figure 3.8C shows that only the MM1S treatment group successfully engrafted, therefore, the NSG-U266 model was not used in any further experiments.

Serum was extracted from the peripheral blood samples, and DNA was extracted for qPCR analysis of murine and human mtDNA (Figure 3.9A). The mean of the fold change in mtDNA calculated at day 7 was used as a reference value to assess fold change in mtDNA over the 21-day engraftment period (Figure 3.9B). No change in murine mtDNA was observed in either treatment group over the 21 days. However, human mtDNA was detected in the MM1S engrafted group on day 14 (p = 0.0357) and was observed to be further elevated on day 21 (p = 0.0159). Together these data suggest that the humanised NSG-MM1S model is functional and crucially demonstrates that MM cells are the source of cell-free mtDNA in circulation.

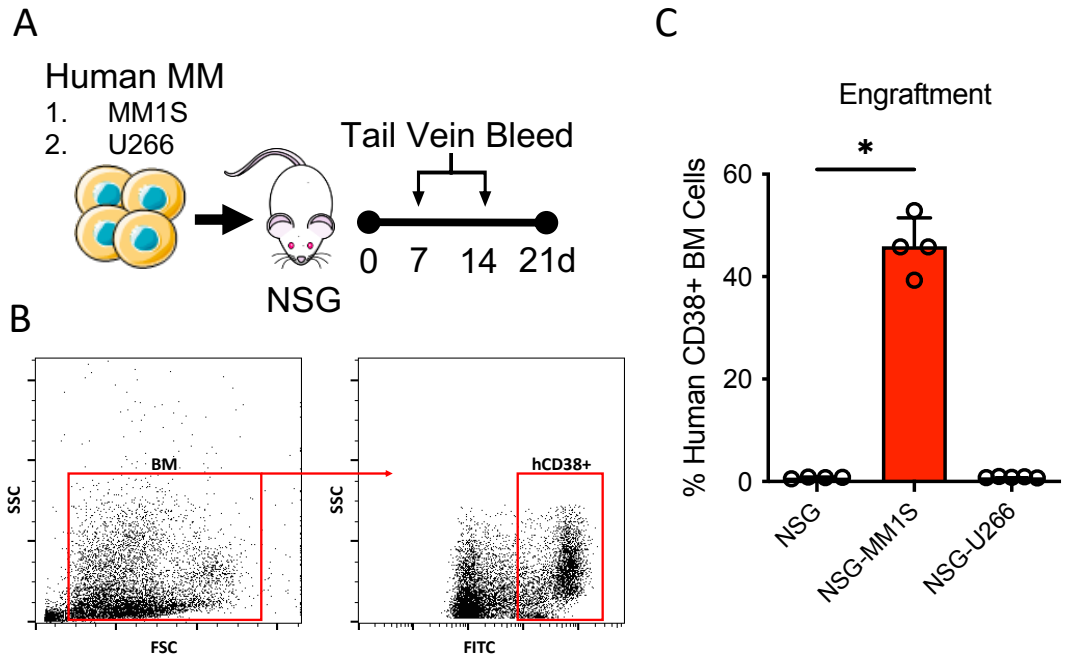

Figure 3.8. Generating a humanised mouse model of MM.

*(A) Schematic of experimental design. Human MM1S and U266 cells (2x10^5) were injected I.V into busulfan (25mg/kg) pre-treated NSG mice. Peripheral blood samples were taken via I.V tail vein bleed at 7- and 14-days post-engraftment. The animals were sacrificed on day 21 and bone marrow was extracted. (B) Flow cytometry gating of mouse bone marrow with human CD38 engraftment via FITC. (C) Percentage of hCD38+ cells in the bone marrow of control NSG mice (n=4), NSG-MM1S mice (n=4), and NSG-U266 mice (n=5). Data indicate mean ± SD. Statistics presented as Kruskal-Wallis test to analyse overall statistical differences (p=0.067), followed by Dunn's post-hoc multiple comparisons test for pair-wise comparisons of control vs NSG-MM1S (p=0.0246) and NSG-U266 (p=0.99). *p < 0.05.*

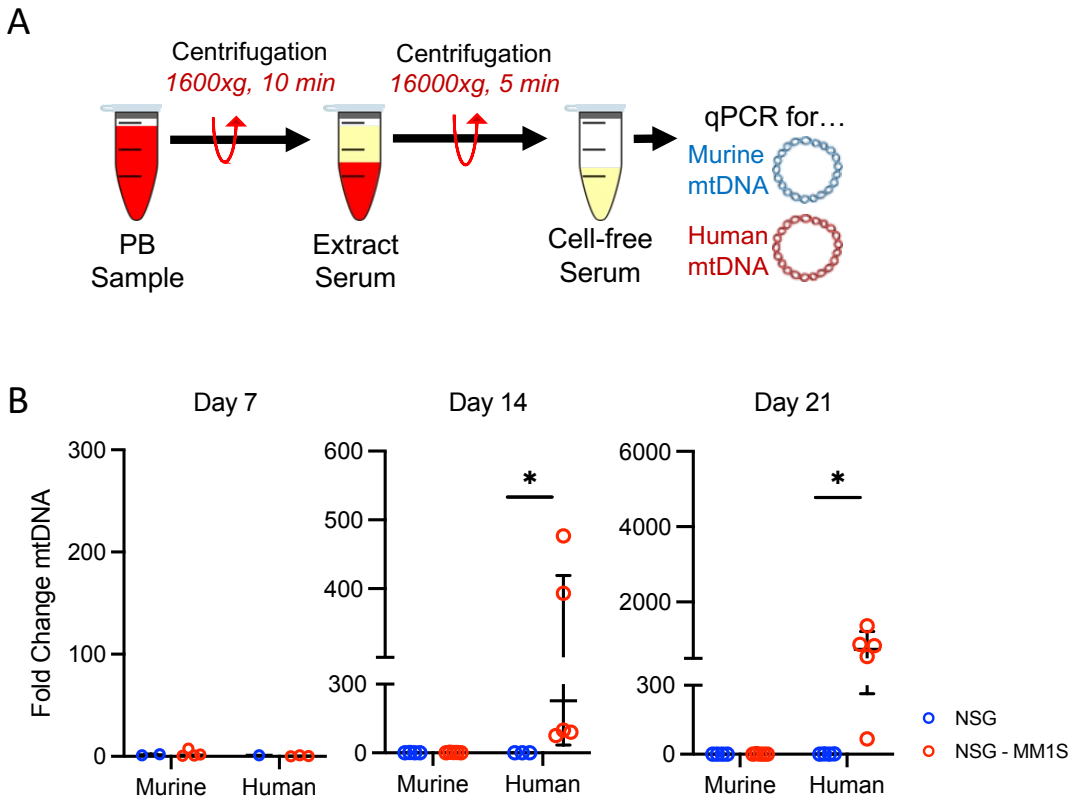

Figure 3.9. Cell-free serum mtDNA is derived from MM cells.

*(A) Schematic of experimental design. Cell-free serum was extracted from peripheral blood via centrifugation, and DNA was extracted and analysed via qPCR for the presence of murine and human mtDNA. (B) Fold change in murine vs human mtDNA at days 7, 14, and 21 post-engraftment. Control NSG mice (n=4) and NSG-MM1S mice (n=4). Data indicate mean ± SD. Statistics presented as Mann-Whitney U test. *p < 0.05.*

Finally, to recapitulate the observation of cell-free mtDNA being more abundant in the bone marrow serum of MM patients (Figure 3.3), the humanised NSG-MM1S mouse model was utilised again. 21 days post-engraftment, PB and BM serum samples were collected and analysed for human and mouse mtDNA content via qPCR (Figure 3.10A).

Whilst the levels of murine mtDNA were not significantly changed in both engrafted and control groups in peripheral blood (p = 0.9453), there was a statistical difference found in the bone marrow (p = 0.0273). The levels of human mtDNA were significantly elevated in the MM1S engrafted mice in both the peripheral blood (p = 0.0078) and the bone marrow (p = 0.0156), with a greater fold change in mtDNA observed in the bone marrow (Figure 3.10B). This is consistent with our findings in human patient myeloma bone marrow serum samples (Figure 3.3).

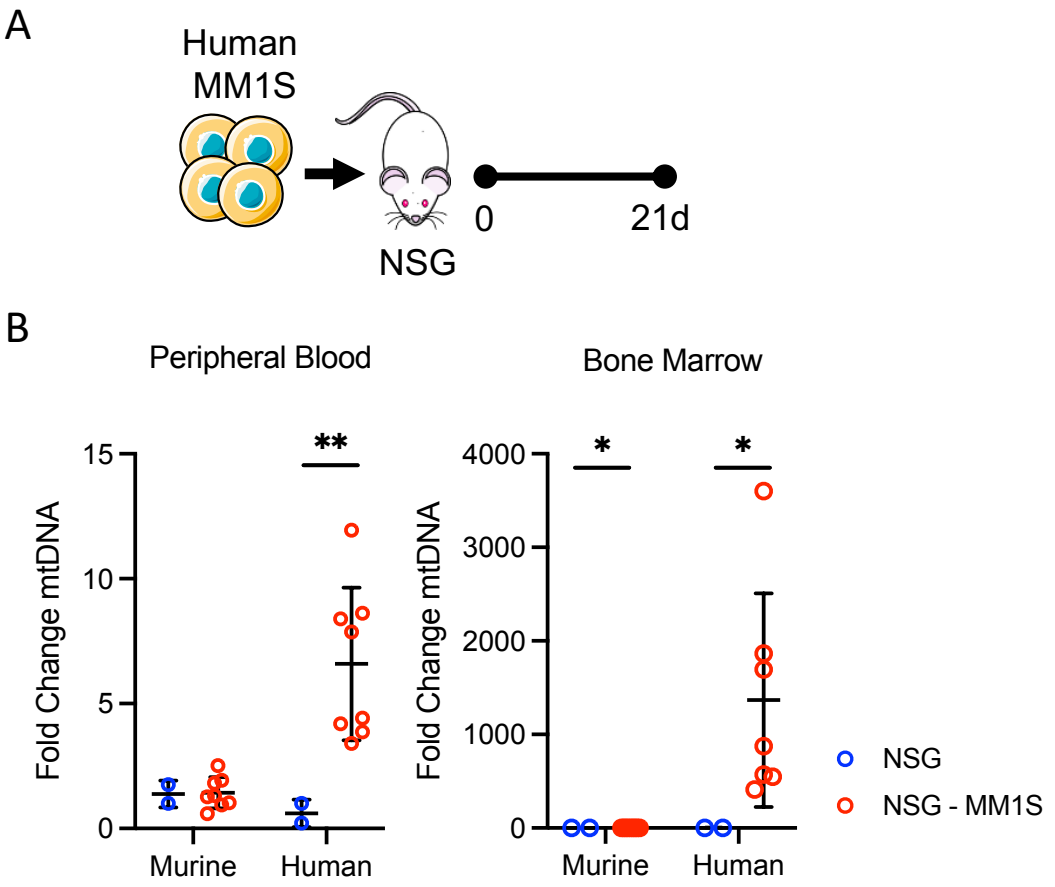

Figure 3.10. MM-derived cell-free mtDNA is more abundant in BM serum.

*(A) Schematic of experimental design. Human MM1S cells (2x10^5) were injected into busulfan (25 mg/kg) pre-treated NSG mice, and peripheral blood and bone marrow samples were taken at the endpoint of 21 days. Cell-free serum was extracted from peripheral blood and bone marrow, and DNA was extracted and analysed via qPCR. (B) Fold change in murine and human mitochondrial DNA in the peripheral blood vs bone marrow serum. Fold change was calculated based on the ΔΔCt value of the Ct value of control (NSG) samples subtracted from the NSG-MM1S samples. Control NSG mice (n=2) and NSG-MM1S mice (n=9). Data indicate mean ± SD. Statistics presented as Wilcoxon signed rank test. *p < 0.05, **p < 0.01.*

3.6 Summary

In this first chapter, I investigated the association between multiple myeloma and circulating cell-free mtDNA. I have shown that we can detect elevated levels of mtDNA in MM patients' peripheral blood serum and this mtDNA is more notably elevated in the bone marrow serum. Moreover, this finding of elevated PB serum mtDNA was observed *in vitro* using primary MM cell cultures and MM cell lines, as well as *in vivo* using two syngeneic mouse models of MM. Notably, using a humanised xenograft NSG mouse model of MM, I have demonstrated that circulating cell-free mtDNA in the PB and BM serum is derived from MM cells and its release is correlated with disease progression. Taken together, the data presented here indicate that serum circulating mtDNA is elevated in MM and that MM cells are the source of mtDNA, responsible for releasing it into the surrounding BM tumour microenvironment where it accumulates and disperses into the peripheral blood circulation.

4 STING activation in bone marrow macrophages is mediated by mtDAMPs signalling and promotes multiple myeloma progression

4.1 Introduction

In the previous chapter, I have shown that mitochondrial DNA is elevated in the MM microenvironment adding to the existing literature that recognises mtDNA as a biomarker that is elevated in and associated with a plethora of cancers. Furthermore, I identified that myeloma cells are responsible for this increase as a source of circulating mtDNA. However, despite mtDNA being implicated in the pathogenesis of a vast range of human diseases, there is still very little scientific understanding of the functional purpose and mechanism by which mtDNA, and mtDAMPs as a whole category act.

As discussed in sections 1.7.1 and 1.7.5, there are two major DNA sensing pathways, toll-like receptor 9 (TLR-9) and cyclic GMP-AMP synthase (cGAS)-stimulator of interferon genes (STING), which mediate the activation of the innate immune response and subsequent type I interferon and pro-inflammatory cytokine production [326, 327]. Furthermore, MM is heavily reliant on cellular interactions between cells of the BM microenvironment [159]. As such, macrophages have been identified as cells that are vital to the tumour microenvironment in MM, mediating processes such as tumour cell growth, drug resistance, and angiogenesis which contribute to the initiation and progression of MM disease [328]. Moore *et al. (2022)* found that mtDNA induced STING signalling in bone marrow macrophages, and phenotypically this kerbed acute myeloid leukaemia (AML) progression via increased LC3-associated phagocytosis [321]. Thus, highlighting a potential means of mtDAMPs signalling that is yet to be investigated in MM.

In this chapter, I investigate the role of BM macrophages in the recognition and response of mtDAMPs and explore key mtDAMPs receptor signalling pathways to ascertain the mechanism by which MM progression is mediated.

4.2 Macrophage gene expression is altered in MM

Firstly, to investigate the effects of MM on bone marrow macrophages flow cytometry was used to identify discrete cell populations and their polarity. To do so, C57BL/KaLwRij mice were injected with 5TGM1$^{(GFP+\ Luci+)}$ cells (1x10^6), after 28 days of engraftment the mice were sacrificed, and the bone marrow was isolated and stained with antibody panels for flow cytometry analysis (Figure 4.1A). Resident bone marrow macrophages (BMMΦ) were identified as GR1-, CD115$^{LOW/INT}$, F4/80+ and myeloma-associated macrophages (MAMΦ) were identified as Ly6G-, CD11b+. All gating was determined using fluorescence-minus-one controls and the gating strategy used to analyse the cell populations of interest is shown in Figure 4.1B. Antibodies for the M1 macrophage marker (CD86) and the M2 macrophage marker (CD206) were used to examine the effects of polarity in the two macrophage populations.

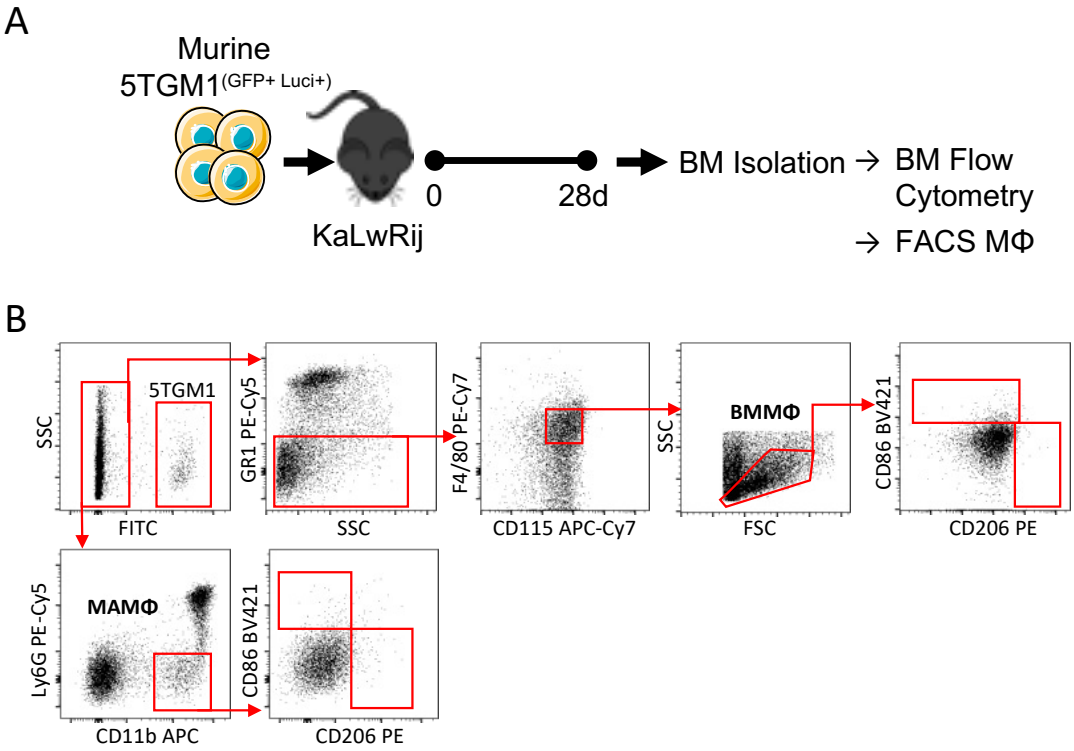

Figure 4.1. Flow cytometry gating strategy for the identification of macrophage populations.

(A) Schematic of experimental design. Murine 5TGM1$^{(GFP+\ Luci+)}$ cells (1x10^6) were injected into C57BL/KaLwRij mice, mice were sacrificed at 28 days, BM was isolated for flow cytometry analysis and macrophages were sorted via FACS. (B) BM cells were analysed for GR1, F4/80, CD115, LY6G, CD11b, CD86, and CD206 expression and used to identify resident bone marrow macrophages (BMMΦ) (GR1-, CD115 lo/int, F4/80+) and MM-associated macrophages (MAMΦ) (Ly6G-, CD11b+). The gating strategy is shown.

BMMΦ and MAMΦ cell populations were reported as cell counts calculated from the total isolated BM cell count. Interestingly, there appeared to be a reduction in the number of BMMΦ (p = 0.0173) in 5TGM1 engrafted mice and a reduction in both M1 (p = 0.0317) and M2 (p = 0.0303) polarised BMMΦ (Figure 4.2A). Furthermore, there was no statistically significant change in the numbers of MAMΦ or their M1 and M2 polarisation in engrafted mice compared to non-engrafted mice, though it is worth mentioning that the cell counts in the engrafted group were lower than the controls much like the pattern observed with the BMMΦ population (Figure 4.2.B).

Whilst these results appear contrary to the literature that suggests that the number of tumour-associated macrophages which are polarised to an M2 phenotype is increased in MM [329, 330], we recognise that other intracellular biochemical changes not capable of being captured by flow cytometry could be occurring.

Such changes of interest include the gene expression profile as it is understood that macrophages are highly plastic cells that are involved in innate immunity and secrete various pro-inflammatory cytokines in response to external stimuli.

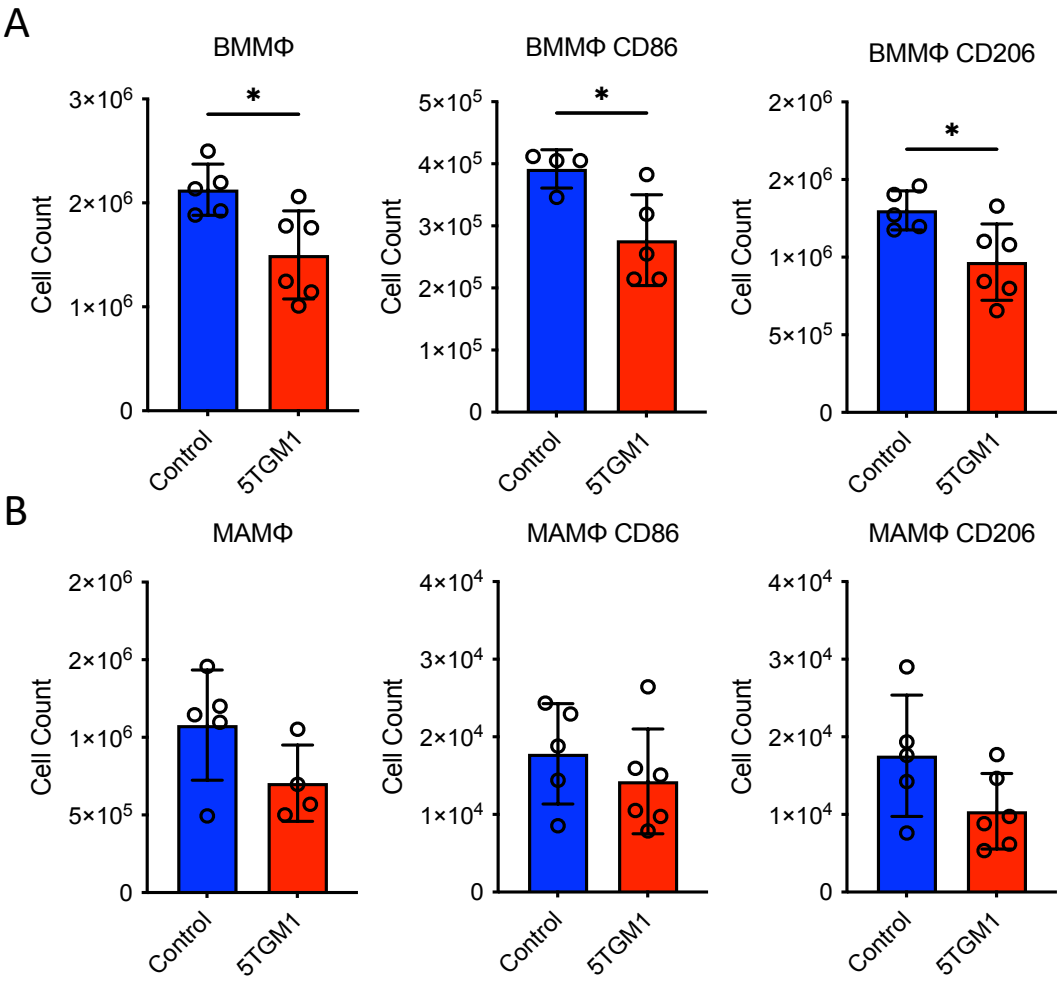

Figure 4.2. 5TGM1 engraftment does not alter MM associated macrophage population.

*(A) Cell numbers of resident bone marrow macrophages (BMMΦ) cell numbers and CD86+ and CD206+ macrophages within that population. (B) Cell numbers of MM-associated macrophages (MAMΦ) and CD86+ and CD206+ macrophages within that population. Comparing control (n=5) and 5TGM1 engrafted animals (n=6). Data indicate mean ± SD. Statistics are presented as Mann-Whitney U test. *p < 0.05.*

The cGAS-STING receptor is a mediator of the pro-inflammatory and type I interferon response [260, 263] and so, to investigate such changes in the context of myeloma, MAMΦ cells were isolated from the BM via FACS purification and RNA was extracted for gene expression analysis by RT-qPCR for STING-related genes (section 2.8.5.1), *Gbp2, Ifit3,* and *Irf7* [265, 331] as well as the key pro-inflammatory cytokine gene *IL-6* [332].

Gene expression of *IL-6* (p = 0.0159), *Gbp2* (p = 0.0303), *Ifit3* (p = 0.0159), and *Irf7*(p = 0.0159) was significantly increased in MAMΦ cells from 5TGM1 engrafted mice when compared to controls (Figure 4.3), suggesting increased activation of the STING signalling pathway.

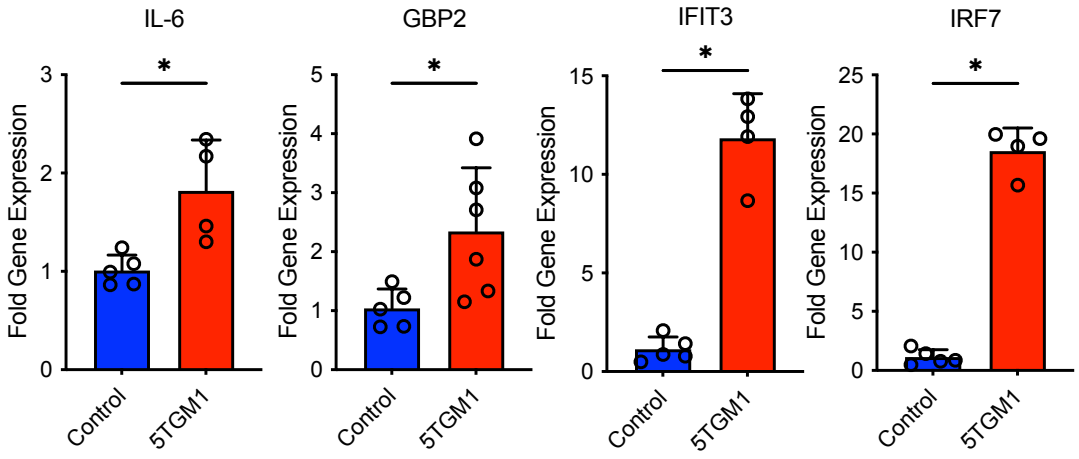

Figure 4.3. 5TGM1 engraftment causes an up-regulation of STING-associated gene expression.

*MM-associated macrophages (MAMΦ) were isolated from BM via FACS purification. the RNA was extracted and analysed via qPCR. Relative gene expression between control (n=5) and 5TGM1 engrafted animals (n=6). Fold change was calculated based on the ΔΔCt value obtained from the ΔCt value calculated from the Ct value of the housekeeping gene (GAPDH) subtracted from the Ct value of the gene of interest. Data indicate mean ± SD. Statistics are presented as Mann-Whitney U test. *p < 0.05.*

4.3 STING activation in bone marrow-derived macrophages is mediated by mtDAMPs

Next, we wanted to determine whether the STING activation we observed was a direct consequence of factors secreted by MM cells. The first step in this process was to culture bone marrow-derived macrophages (BMDM) in 5TGM1 conditioned media for 24 hours, this media had undergone centrifugation to remove cells and large extracellular vesicles (EVs), small EVs and any remaining large proteins were removed by a further ultra-centrifugal filtration step (Figure 4.4A). The RNA was then extracted from the BMDMs and analysed for STING gene expression via qPCR. Figure 4.4B shows increased *Gbp2, Ifit3,* and *Irf7* gene expression in BMDMs cultured in filtered 5TGM1 conditioned media, with *Gbp2* (p = 0.0286) and *Irf7* (p = 0.0286) being statistically significant. Whilst there was no significant change (p = 0.0571) detected in *IL-6* gene expression.

This data suggests that myeloma cells do release small cell-free molecules that are capable of triggering STING activation in macrophages. Therefore, there is an implication that mtDAMPs fit this description and could be the potential facilitator of this response.

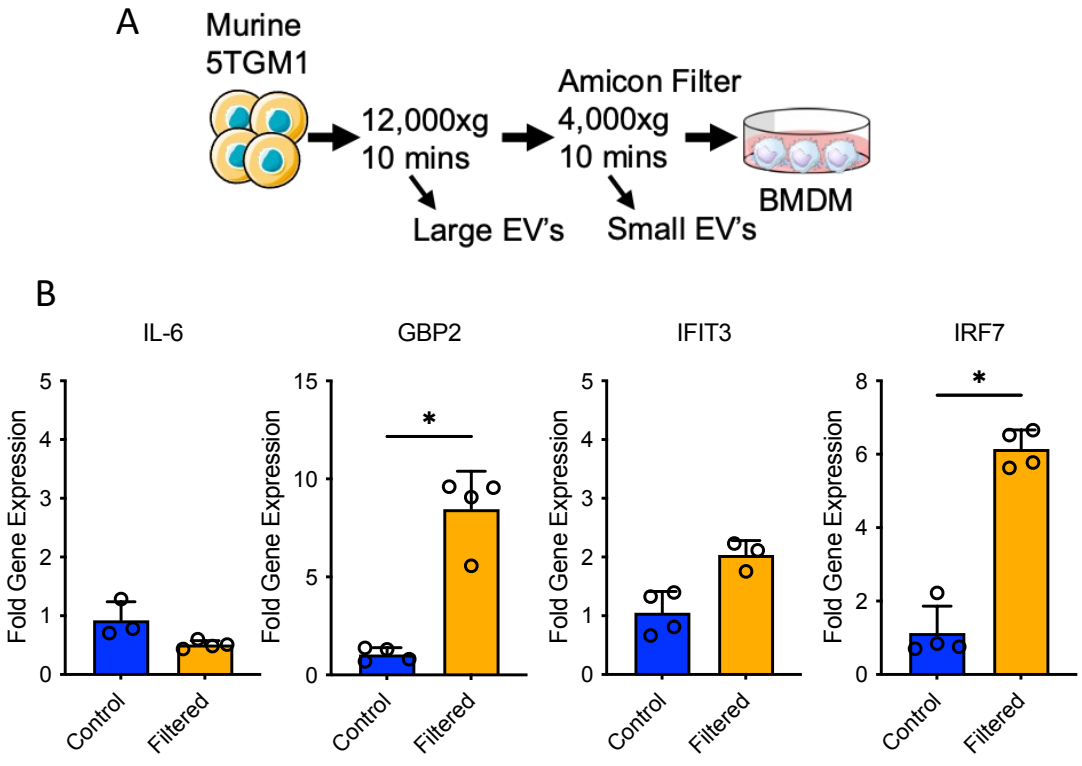

Figure 4.4. Cell-free 5TGM1 conditioned media stimulates STING activation in bone marrow-derived macrophages.

*(A) Cell-free media from 5TGM1 cells in culture was obtained via centrifugation and ultra-filtration via an Amicon filter to remove cells, large extracellular vesicles (Evs), and small EVs. Bone marrow-derived macrophages (BMDMs) were treated with this media for 24 hours after which, RNA was extracted, and gene expression analysed via qPCR. (B) Relative gene expression of IL-6, Gbp2, Ifit3, and Irf7 in control untreated BMDMs and filtered conditioned media treated BMDMs. n=4. Fold change was calculated based on the ΔΔCt value obtained from the ΔCt value calculated from the Ct value of the housekeeping gene (GAPDH) subtracted from the Ct value of the gene of interest. Data indicate mean ± SD. Statistics are presented as Mann-Whitney U test. *p < 0.05.*

As established in chapter 3, circulating mtDNA is upregulated in the MM microenvironment, hence we wanted to determine whether STING activation was specific to mtDNA or a more generalised broad response to mtDAMPs.

In order to do so, BMDMs were treated with unmethylated cytosine-guanine dinucleotide (CpG) containing oligodeoxynucleotide (ODN) or mtDAMPs isolated from mouse liver (as described in 2.4.3.1) for 6 hours after which the RNA was extracted from the cells and analysed via qPCR (Figure 4.5A). CpG ODNs are synthetic oligonucleotides that are TLR9 agonists and, due to the presence of unmethylated CpG motifs, act as a molecular mimic for mtDNA [333].

In the CpG-treated BMDMs, the pattern of STING-related gene expression was not the same as that observed *in vivo* in MAMΦ isolated from 5TGM1 engrafted mice (Figure 4.3). Gene expression of *IL-6* (p = 0.0286) and *Irf7* (p = 0.0286) was significantly up-regulated, whilst *Gbp2* (p = 0.1143) and *Ifit3* (p = 0.1143) were not (Figure 4.5B). In mtDAMPs treated BMDMs on the other hand (Figure 4.5B), gene expression of all genes was significantly increased (p = 0.0286). This resembles the gene expression profile observed in isolated MAMΦ cells from 5TGM1 engrafted mice (Figure 4.3).

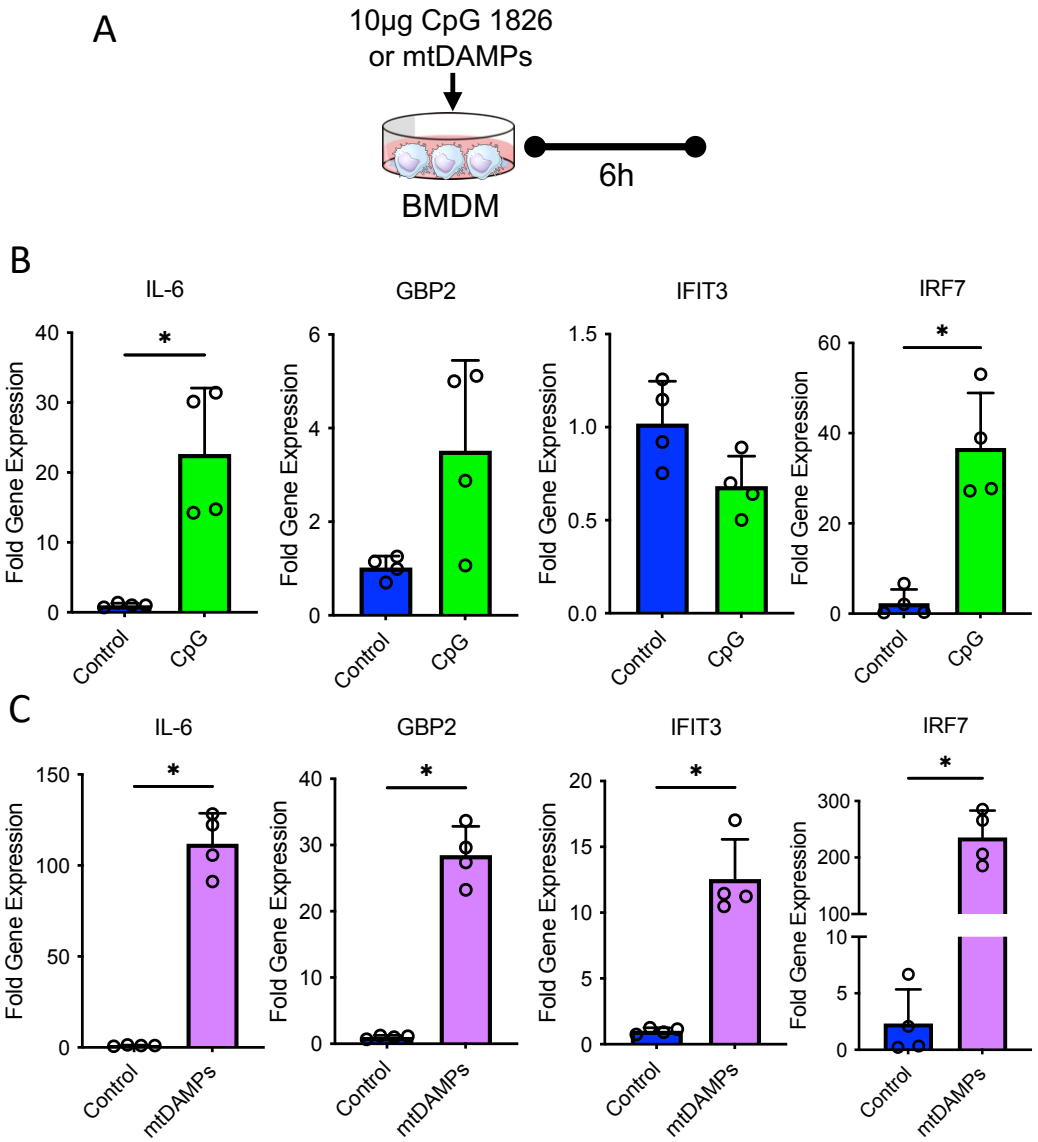

Figure 4.5. mtDAMPs, but not CpG, induces STING-associated gene expression in bone marrow-derived macrophages.

*(A) Schematic of experimental design. Bone marrow-derived macrophages (BMDM) were treated with either CpG ODN 1826 or mtDAMPs (10µg) for 6 hours. RNA was extracted and gene expression was analysed via qPCR. (B) Relative gene expression of IL-6, Gbp2, Ifit3, and Irf7 in control untreated BMDMs and CpG 1826 treated BMDMs. (C) Relative gene expression of IL-6, Gbp2, Ifit3, and Irf7 in control untreated BMDMs and mtDAMPs treated BMDMs. n=4. Fold change was calculated based on the ΔΔCt value obtained from the ΔCt value calculated from the Ct value of the housekeeping gene (GAPDH) subtracted from the Ct value of the gene of interest. Data indicate mean ± SD. Statistics are presented as Mann-Whitney U test. *p < 0.05.*

To discern whether this gene expression profile was mediated through the cGAS-STING signalling pathway, we used H-151, a covalent small-molecule inhibitor of the receptor STING identified by Haag et al. [334]. BMDMs were pre-treated with H-151 or vehicle for 2 hours before a 6-hour treatment with either CpG or mtDAMPs (Figure 4.6A), the RNA was extracted from the BMDMs, and the fold change in gene expression was analysed via qPCR as described in section 2.8.5.1.

We found that STING inhibition with H-151 led to a reduction in the expression of STING-related genes compared to non-STING inhibited controls (Figure 4.6B). In the non-inhibited control group gene expression of *IL-6*, *Gbp2, Ifit3*, and *Irf7* was significantly up-regulated ($p < 0.0001$) upon mtDAMPs stimulation in comparison to untreated BMDMs. However, when STING signalling was inhibited with H-151 this gene expression profile was attenuated with only *Gbp2* ($p = 0.0273$) and *Ifit3* ($p = 0.0041$) gene expression being significantly upregulated but to a lesser degree than observed in the non-inhibited group. Upon CpG stimulation only *IL-6* ($p < 0.0001$) gene expression was found to be significantly upregulated, this upregulation was also attenuated by the inhibition of STING via H-151 (Figure 4.6B).

Collectively, this data suggests that myeloma-derived mtDAMPs activate bone marrow macrophages via the STING signalling pathway.

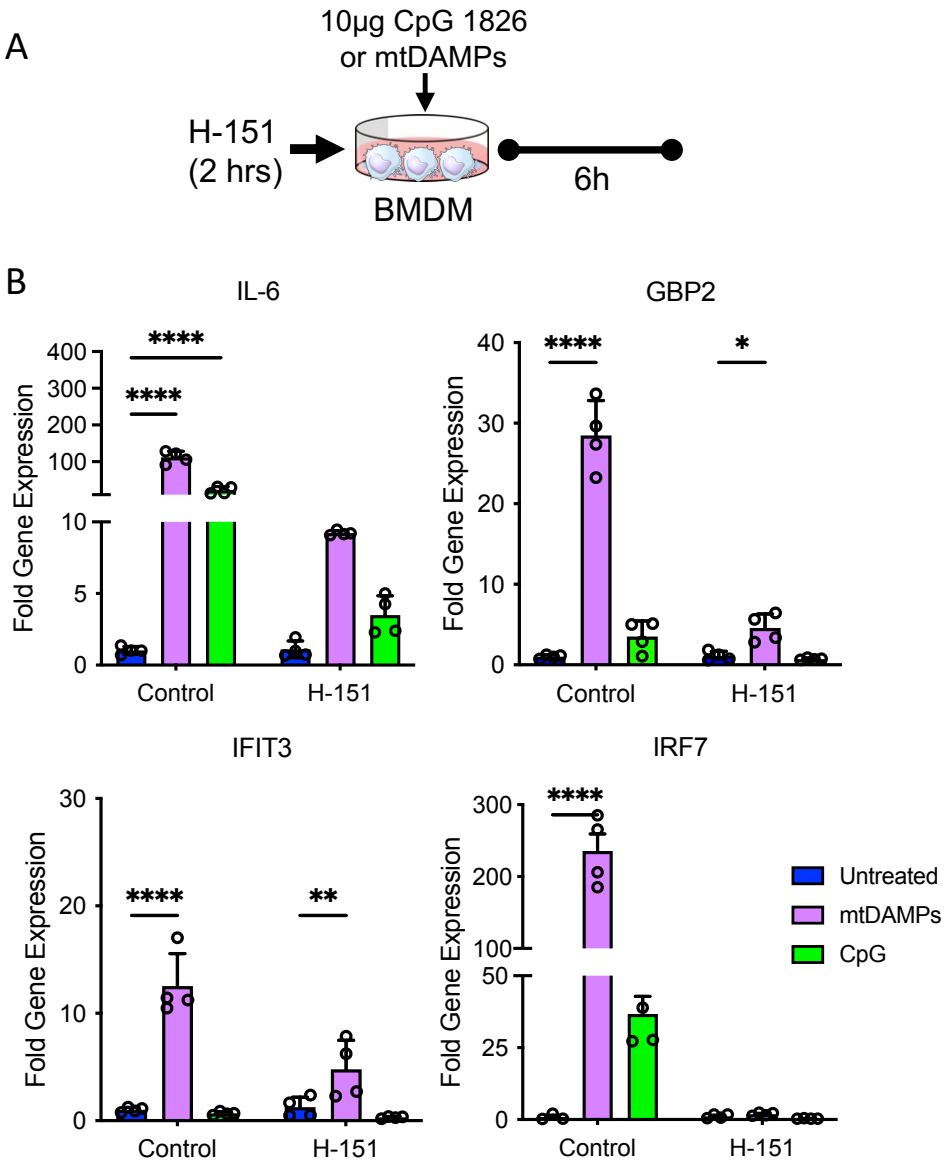

Figure 4.6. STING inhibition attenuates STING-associated gene expression in bone marrow-derived macrophages.

*(A) Schematic of experimental design. Bone marrow-derived macrophages (BMDM) were pre-treated with STING inhibitor H-151 (10 µM) for 2 hours before treatment with either CpG ODN 1826 or mtDAMPs (10 µg) for 6 hours. RNA was extracted and gene expression was analysed via qPCR. (B) Relative gene expression of IL-6, Gbp2, Ifit3, and Irf7 in untreated BMDMs, CpG 1826 treated, and mtDAMPs treated BMDMs without H-151 (control) and with H-151 STING inhibition. n=4. Data indicate mean ± SD. Statistics are presented as two-way ANOVA with Sidak post-hoc multiple comparisons test. *p < 0.05; **p < 0.01; ***p < 0.001; ***p < 0.0001.*

4.4 MM progression is attenuated by STING inhibition *in vivo*

In the previous section, I presented evidence that mtDAMPs mediated macrophage activation is facilitated by STING signalling, and that treatment with STING inhibitor H-151 diminished this activation and led to a reduction in gene expression of STING-related genes and pro-inflammatory cytokine IL-6 (Figure 4.6B), which are also upregulated in MM-associated macrophages *in vivo* (Figure 4.3).

Therefore, to substantiate the role of STING signalling in MM we wanted to determine the effects of STING inhibition on MM in an *in vivo* setting. Furthermore, TLR-9 inhibition was also investigated as another potential DNA sensing receptor pathway that could be implicated in the mtDAMPs-driven response, using the antagonist ODN 2088 [203].

To do so, the C57BL/KaLwRij-5TGM1 model of myeloma was used. Mice were engrafted with 5TGM1$^{(GFP+\ Luci+)}$ cells. At 20 days post-engraftment, mice were injected with either H-151 (750 nmol), ODN 2088 (10 µg), or vehicle control every other day for a total of 4 doses. The mice were sacrificed on day 27 and the bone marrow was harvested for flow cytometry analysis and macrophage isolation via FACS purification (Figure 4.7).

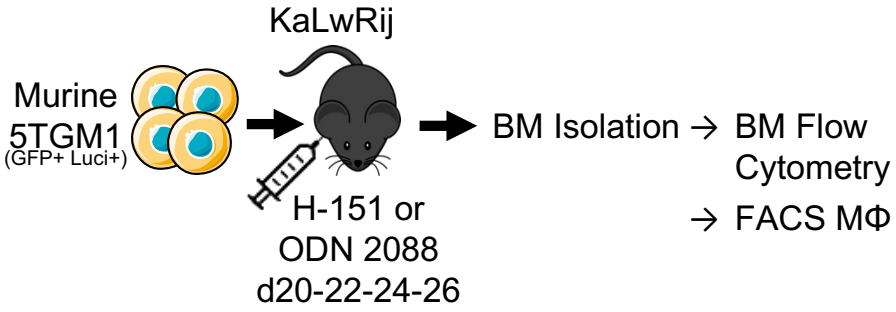

Figure 4.7. Inhibition of STING / TLR-9 signalling in vivo.

Schematic of experimental design. Murine 5TGM1$^{(GFP+\ Luci+)}$ cells (1x10^{6}) were injected into C57BL/KaLwRij mice. On days 20, 22, 24, and 26 post-engraftment mice were injected intraperitoneally (i.p.) with either, 200 µl H-151 (750 nmol), ODN 2088 (10 µg), or vehicle. Mice were sacrificed at 27 days; BM was harvested for flow cytometry analysis and macrophage FACS purification.

Myeloma engraftment in the bone marrow of each animal was determined by the identification of GFP+ 5TGM1 cells via flow cytometry (Figure 4.8). Both ODN 2088 and H-151 treatments resulted in a reduction in 5TGM1 engraftment compared to untreated mice with an overall Kruskal-Wallis *p*-value of 0.0102. The Dunn's post hoc multiple comparisons test revealed a statistically significant engraftment reduction in the 5TGM1+ODN 2088 group (p = 0.0146) with a marginally significant reduction (p = 0.0525) in the 5TGM1+H-151 group.

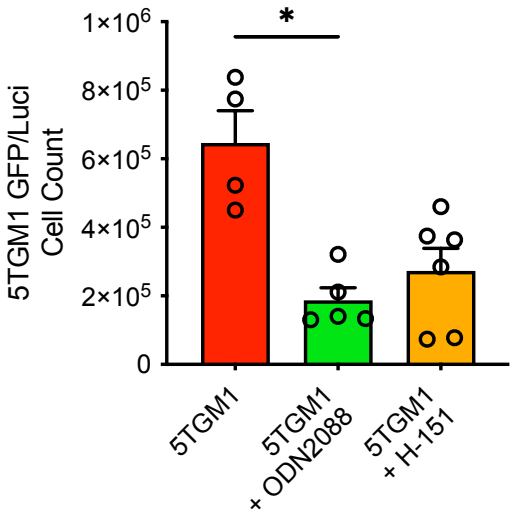

Figure 4.8. Bone marrow engraftment is reduced with receptor inhibition.

*Bone marrow was harvested and analysed for 5TGM1$^{(GFP+\ Luci+)}$ cell engraftment via flow cytometry. n=6 in each treatment group. Data indicate mean ± SD. Statistics presented as Kruskal-Wallis test with Dunn's post-hoc multiple comparisons test. *p < 0.05.*

Due to the 5TGM1 cells containing a luciferase (luci+) reporter, tumour burden could be detected using live *in vivo* bioluminescence imaging. *In vivo* images of each group were taken on days 19 and 27 post-engraftment, representing before and after inhibitor treatment (Figure 4.9A). The bioluminescence was quantified (Figure 4.9B) and revealed that tumour burden increased significantly in the control 5TGM1 and ODN 2088 groups (p = 0.0312) but not in the H-151 treatment group (p = 0.1562). This suggests that STING inhibition hampers the progression of MM.

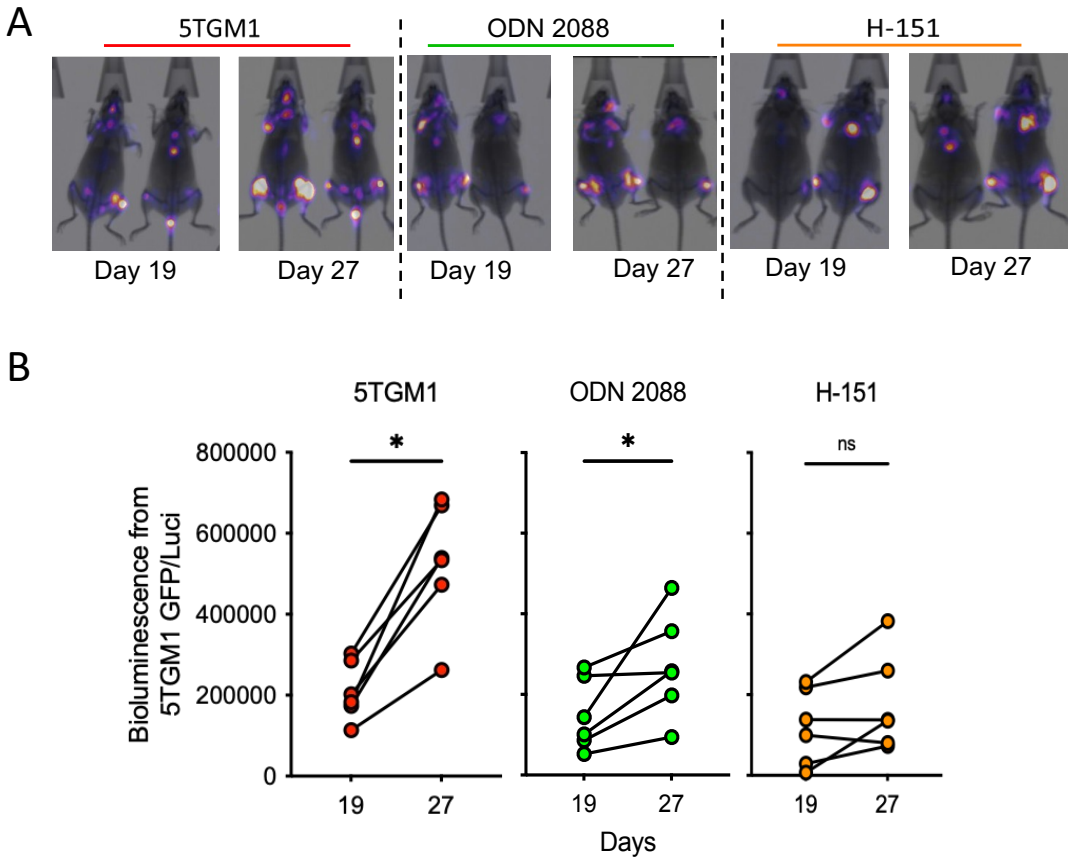

Figure 4.9. STING inhibition reduces MM tumour burden.

*(A) Representative live in vivo images of mice engrafted with 5TGM1$^{(GFP+\ Luci+)}$ on days 19 and 27, representing before and after ODN 2088 (10 µg) or H-151 (750 nmol) treatment. (B) Bioluminescence, before and after treatment, was quantified using ImageJ. n=6 in each group. Data indicate mean ± SD. Statistics presented as Wilcoxon matched-pairs signed rank test. *p < 0.05.*

Next, we wanted to examine the gene expression profile of MAMΦ to determine whether receptor inhibition had any effect on STING-related gene expression. MAMΦ cells were purified by FACS from the bone marrow and analysed for STING-related gene expression via qPCR as described in section 2.8.5.1. We found that, with the exception of *IL-6* ($p = 0.0014$), STING-related gene expression was not attenuated by ODN 2088. Whereas, whilst not found to be statistically significant, there was a trend toward increased gene expression of *Gbp2* ($p = 0.3733$), *Ifit3* ($p = 0.1088$), and *Irf7* ($p = 0.2617$) upon ODN 2088 treatment (Figure 4.10A). However, there was a trend towards attenuated gene expression of *IL-6* ($p = 0.0005$), *Gbp2* ($p = 0.0643$), *Ifit3* ($p = 0.2037$), and *Irf7* ($p = 0.1463$) observed with H-151 treatment (Figure 4.10B). This data further corroborates the involvement of the STING signalling pathway in the mtDAMPs-mediated pro-inflammatory cytokine response that drives MM progression.

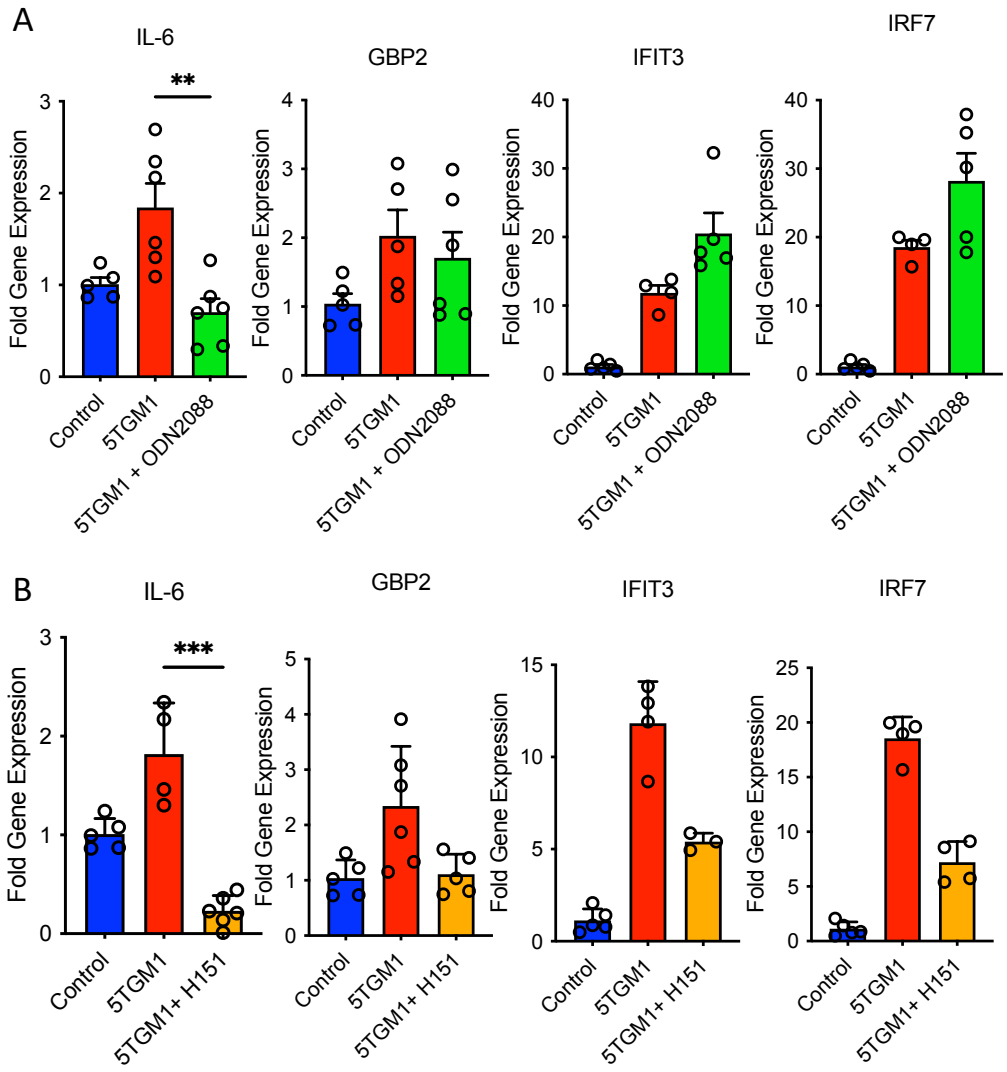

Figure 4.10. TLR-9 inhibition does not attenuate STING-associated gene expression, whilst STING inhibition does.

*MM-associated macrophages (MAMΦ) were FACS purified, the RNA was extracted and analysed via qPCR. (A) Relative gene expression of IL-6, Gbp2, Ifit3, and Irf7 in control, 5TGM1, and ODN 2088 (10 µg) treatment groups. (B) Relative gene expression of IL-6, Gbp2, Ifit3, and Irf7 in control, 5TGM1, and H-151 (750 nmol) treatment groups. n=6 in each treatment group. Fold change was calculated based on the ΔΔCt value obtained from the ΔCt value calculated from the Ct value of the housekeeping gene (GAPDH) subtracted from the Ct value of the gene of interest. Data indicate mean ± SD. Statistics presented as Kruskal-Wallis test with Dunn's post-hoc multiple comparisons test between the mean ranks of the treatment groups (ODN 2008 and H-151) and the 5TGM1 group. **p < 0.01; ***p < 0.001.*

4.5 Activated macrophages induce mtDNA release from 5TGM1 cells

As we show that macrophages are activated by mtDAMPs specifically via STING signalling, we wanted to investigate whether macrophage activation was related to the mtDNA release observed from MM cells. In order to do so, I used an established *in vitro* method designed to take advantage of the single nucleotide polymorphism (SNP) differences in the mtDNA of different mouse strains.

Yu et al. reported that there was a single nucleotide polymorphism (SNP) in the cytochrome c oxidase subunit 3 (COX3) region of mtDNA at the 9348th nucleotide position, where C57BL/6 mice had guanine (G) in that position, this was replaced by adenine (A) in BalbC mice [335]. Therefore, primers were designed to target the SNP in the COX3 region (Figure 4.11).

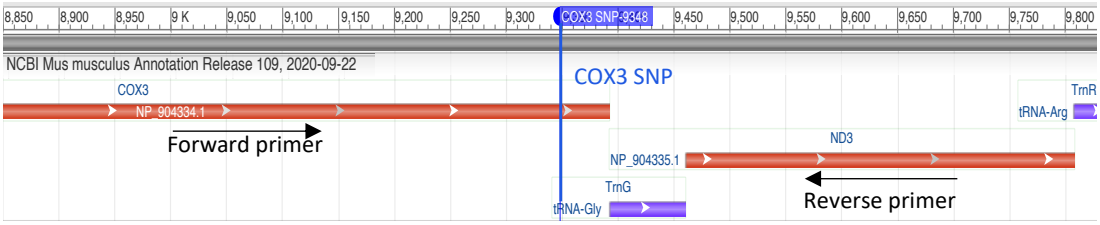

Figure 4.11. The genomic region of mitochondrial DNA and primer targets.

The genomic region of mitochondrial cytochrome c oxidase subunit 3 (mt-COX3), the position of the single nucleotide polymorphism SNP (9348), and primer targets.

A TaqMan SNP PCR assay using probes on different fluorophores was used to distinguish the differences in COX3 mtDNA, originally designed to distinguish between C57BL/6 and NSG mouse strains [336]. However, we found that the NSG SNP also targeted the same SNP in CBA mice. In the COX3 region of mtDNA, C57BL/6 mice have a guanine (G) nucleotide which is replaced by adenine (A) in CBA mice (Table 4.1).

Table 4.1. mtDNA SNP differences between C57BL/6 mice and CBA mice.

Protein	Nucleotide position	Nucleic Acid Change	C57BL/6	NSG or CBA
mt-COX3	9348	G/A	G	A

PCR analysis showed that 5TGM1 cell mtDNA, which has a C57BL/6 strain background showed positive fluorescence on VIC (Figure 4.12A) and negative fluorescence on FAM (Figure 4.12B).

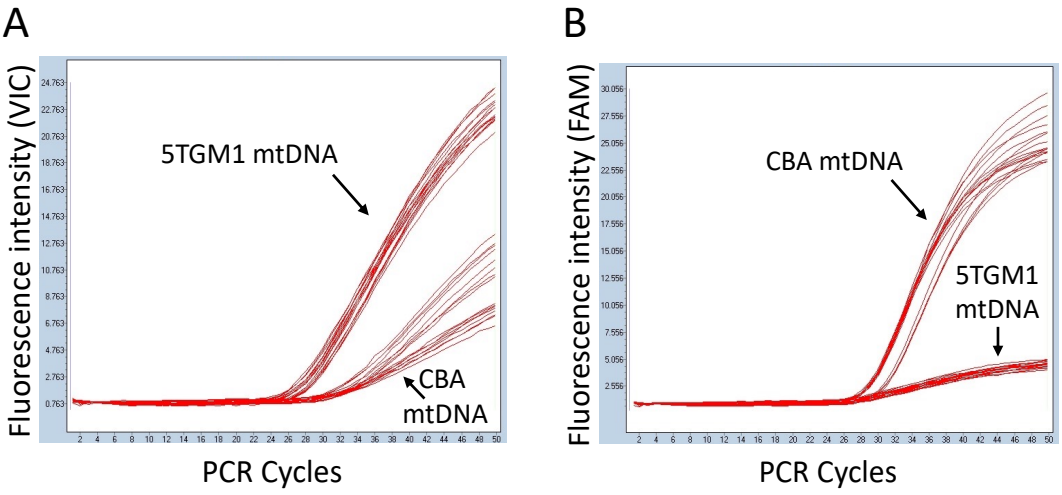

Figure 4.12. TaqMan qPCR analysis of 5TGM1 and CBA mt-COX3 SNP.

(A) PCR amplification curve plot shows positive fluorescence on VIC for 5TGM1 COX3 mtDNA but negative for CBA mtDNA. (B) PCR amplification curve plot shows positive fluorescence on VIC for CBA COX3 mtDNA but negative for 5TGM1 mtDNA.

Using this model system, I investigated whether mtDAMPs mediated macrophage activation stimulated mtDNA release from myeloma cells. To do this, BMDMs were cultured from BM cells isolated from the CBA mouse strain. These BMDMs were treated with mtDAMPs for 24 hours or remained untreated, the conditioned media was then used to culture 5TGM1 cells for 24 hours. The media from the 5TGM1 cells was then analysed for 5TGM1 SNP mtDNA as described in section 2.8.5.4 (Figure 4.13).

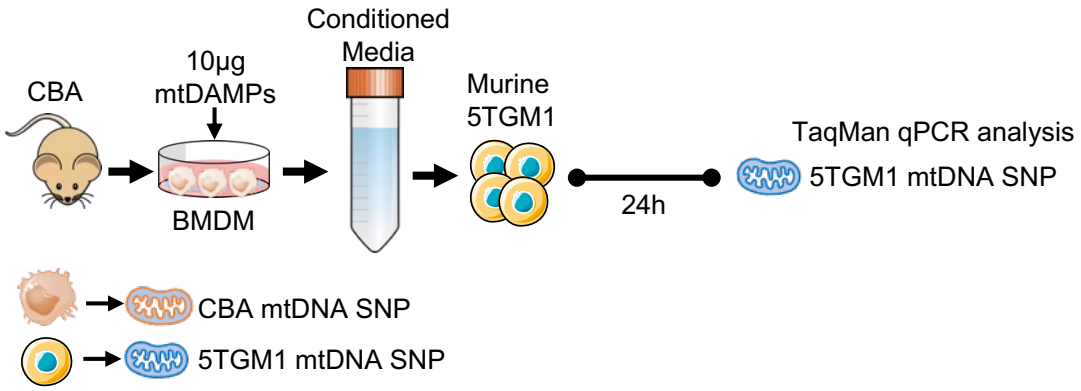

Figure 4.13. Schematic of experimental design.

CBA cells express a different mtDNA SNP than 5TGM1 cells. CBA mouse strain bone marrow-derived macrophages (BMDM) were cultured and activated via mtDAMPs (10 µg) for 24 hours. Cell-free CBA BMDM conditioned media, with or without mtDAMPs treatment, was harvested by centrifugation and 5TGM1 cells were cultured in the conditioned media for 24 hours. The 5TGM1 cells were removed by centrifugation and the media was analysed for 5TGM1 SNP mtDNA by TaqMan qPCR using COX3 probes.

Figure 4.14 shows that 5TGM1 mtDNA release is significantly increased (p = 0.0286) in 5TGM1 cells treated with mtDAMPs activated BMDM conditioned media in comparison to 5TGM1 cells treated with non-activated BMDM conditioned media. The fold change in mtDNA was normalised to mtDNA in the media of untreated 5TGM1 cells (Figure 4.14).

This data suggests that there is a positive feedback loop mechanism at play whereby mtDAMPs stimulation in macrophages induces further mtDAMPs release from MM cells.

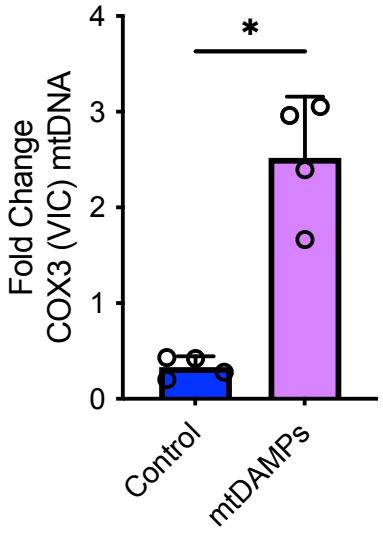

Figure 4.14. BMDMs activated by mtDAMPs induce mtDNA release from 5TGM1 cells.

*5TGM1 cells were cultured for 24 hours in cell-free CBA BMDM conditioned media, with or without mtDAMPs (10 μg) treatment. 5TGM1 cells were removed from the media by centrifugation and the media was analysed via TaqMan qPCR for the presence of 5TGM1 SNP mtDNA using the COX3 (VIC) probe. Untreated 5TGM1 cell SNP mtDNA was used to standardise mtDNA fold change and fold change was calculated based on the ΔΔCt value of the Ct value of control samples subtracted from the mtDAMPs samples. n=4. Data indicate mean ± SD. Statistics are presented as Mann-Whitney U test. *p < 0.05.*

4.6 Summary

In this chapter, I have explored the functional role that mtDAMPs play in the MM microenvironment. I have presented data to show that bone marrow macrophage pro-inflammatory cytokine gene expression is activated in MM. More specifically, I found that this activation was mediated by mtDAMPs exclusively.

Furthermore, the cGAS-STING pathway was shown to be the preferred mechanism of mtDAMPs signalling over TLR-9. Interestingly, the inhibition of the STING pathway in a MM microenvironment led to the suppression of MM tumour progression. Additionally, I report preliminary data that suggests that a positive feedback loop may be involved between myeloma cells and BM macrophages, whereby mtDAMPs activated macrophages stimulate mtDNA release from MM cells which would then feedback to further activate macrophages.

Overall, I show that MM-derived mtDAMPs are responsible for the activation of the STING signalling pathway in BM macrophages. This leads to the production of type I interferon and pro-inflammatory cytokines, which promote the progression of MM.

5 mtDAMPs induce a migratory signature in bone marrow macrophages that mediates MM cell homing and retention in the bone marrow microenvironment

5.1 Introduction

In chapters 3 and 4, I have established that interactions between myeloma-derived mtDAMPs and BM macrophages are important in promoting MM disease progression via cGAS-STING mediated activation. I then wanted to further examine other effects that mtDAMPs may have on BM macrophages.

Macrophages are highly plastic cells, that have been shown to play an important role in the cancer cell microenvironment. With specific regard to multiple myeloma, pro-inflammatory macrophages have been shown to promote drug resistance [337], cell proliferation, and mediate MM cell migration and homing to the bone marrow [328].

Macrophages secrete a range of chemotactic factors that are known to play a role in MM cell migration [338, 339]. The homing and establishment of MM cells within the BM niche is a crucial step in the initiation and subsequent progression of MM disease and metastasis.

In this chapter, I will explore the role of mtDAMPs in altering the cytokine expression profile of BM macrophages. Furthermore, I aim to examine the effects of these changes in the context of MM, and further elucidate the involvement of the mtDAMPs-STING signalling pathway in the promotion of MM disease progression.

5.2 mtDAMPs upregulate bone marrow macrophage chemotactic gene expression

Macrophages are well-known for producing various cytokines and chemokines in response to external stimuli. Whilst we previously show that mtDAMPs elicit a pro-inflammatory cytokine response from bone marrow macrophages in MM, we wanted to investigate what other mtDAMPs-dependent changes in cytokine gene expression were occurring.

To explore a large number of cytokines at once, the Proteome Profiler Mouse Cytokine Array Panel was used as described in section 2.8.6. BMDMs from C57BL/6-KaLwrij mice were cultured with mtDAMPs for 24 hours, and the cell supernatant was removed and used to incubate the cytokine array blot membranes (Figure 5.1A). Detection of each cytokine was quantified based on the mean pixel density of the blots, and mtDAMPs treatment appeared to upregulate several specific genes in BMDMs. However, most cytokines were not found to be upregulated in unstimulated BMDMs save for a few regulatory cytokines (MCP-1, IL-1ra, and TIMP-1) which suggests that BMDM cytokine release is tightly regulated and stimuli-specific (Figure 5.1B).

To further investigate this, cytokines expressed by mtDAMPs-stimulated BMDMs were grouped together depending on their key functions. Pro-inflammatory cytokines were found to be upregulated, particularly TNF-α which is indicative of STING activation via downstream NF-κB signalling [262] (Figure 5.2A). Whilst the pro-inflammatory cytokine IL-6 was not found to be upregulated, this may be due to IL-6 expression being diminished by the 24-hour timepoint as it has been reported *in vitro* that IL-6 expression levels in LPS-stimulated BMDMs peaks at 6 hours before decreasing [340]. Moreover, a cluster of chemotactic cytokines was found to be exclusively expressed upon mtDAMPs stimulation (Figure 5.2B).

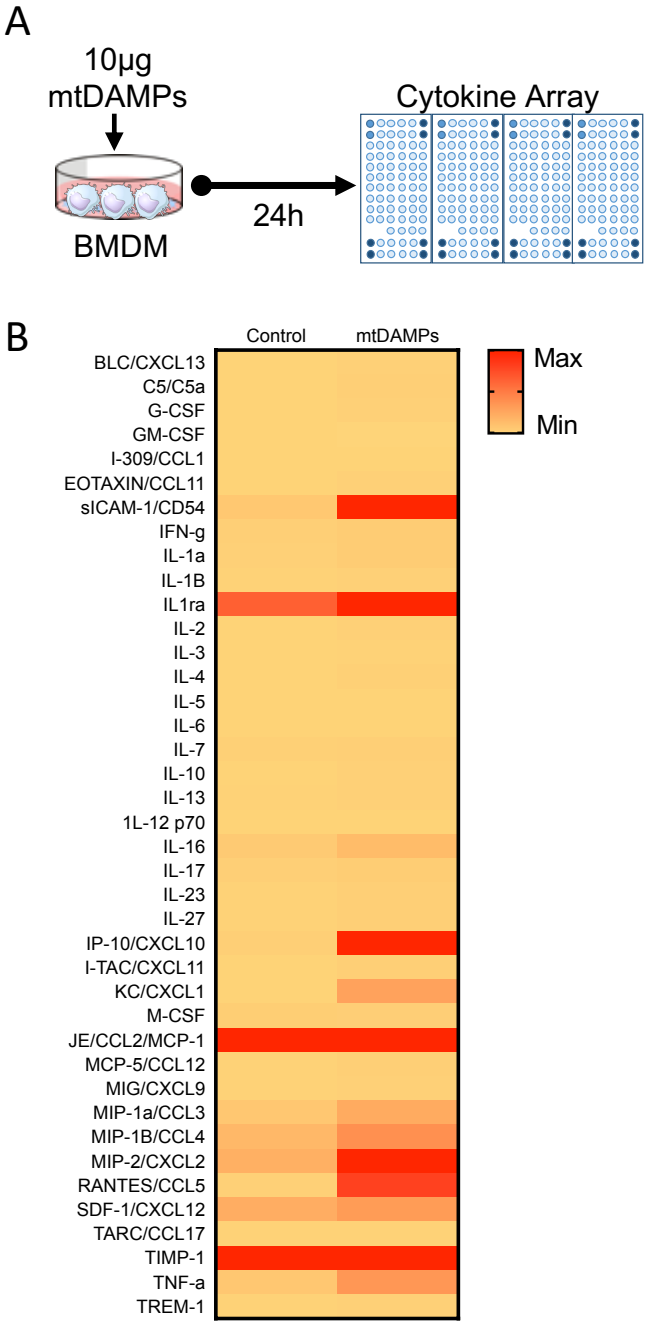

Figure 5.1. Cytokine array analysis of bone marrow-derived macrophages cultured with mtDAMPs.

(A) Schematic of experimental design. C57BL-KaLwRij bone marrow-derived macrophages (BMDM) were cultured with mtDAMPs (10 µg) for 24 hours. BMDM cell supernatant was cleared of cellular debris by centrifugation prior to cytokine array analysis. Cytokine array blots were analysed using the G:BOX Chemi XRQ (Syngene) and quantified using ImageJ software. (B) Heatmap of complete cytokine quantification of the mean pixel density.

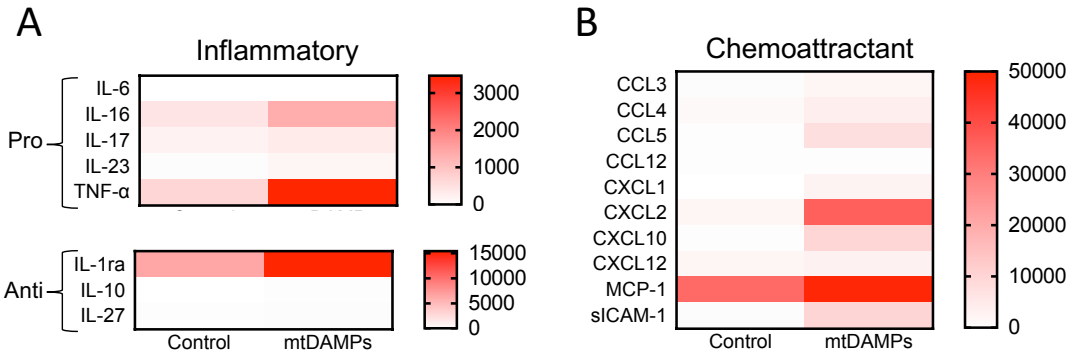

Figure 5.2. Clustered cytokine array analysis of bone marrow-derived macrophages cultured with mtDAMPs.

(A) Heatmap of pro- and anti-inflammatory related cytokines from bone marrow-derived macrophages (BMDM) cultured with or without mtDAMPs (10 µg) for 24 hours. (B) Heatmap of chemoattractant-related cytokines from BMDM cultured with or without mtDAMPs (10 µg) for 24 hours. Cytokine expression levels were quantified by mean pixel density and depicted by scale bars per panel.

Notably, *Ccl5*, *Cxcl2*, and *Cxcl10* were the most upregulated. *Cxcl2* and *Cxcl10* are cytokines directly linked to STING activation [341]. This data suggests that mtDAMPs stimulate bone marrow macrophages to produce chemokines that are involved in the recruitment of other cells and that this chemokine production is mediated by the STING signalling pathway.

To investigate this finding further and in an *in vivo* setting, C57BL/KaLwRij mice were engrafted with 5TGM1$^{(GFP+\ Luci+)}$ cells, and at 20 days post-engraftment a group of these mice were treated with STING inhibitor H-151. At the endpoint of the experiment, MM-associated macrophages were isolated via FACS purification, and their RNA was extracted and analysed for gene expression by qPCR (Figure 5.3A). Interestingly, the fold gene expression of *Cxcl10* (p = 0.0312) and *Cxcl2* (p = 0.0106) was significantly upregulated in the 5TGM1-engrafted mice when compared to the control non-engrafted group. Furthermore, the fold gene expression of *Cxcl2* (p = 0.0415) and *Ccl5* (p = 0.0061) was significantly downregulated in the STING-inhibited group. Overall, there was a general trend of increased *Cxcl10*, *Cxcl2*, and *Ccl5* gene expression in 5TGM1-engrafted mice which was attenuated with H-151 mediated STING inhibition (Figure 5.3B).

This data further corroborates that MM-derived mtDAMPs drive the activation of STING in bone marrow macrophages stimulating the production of cyto- and chemokines.

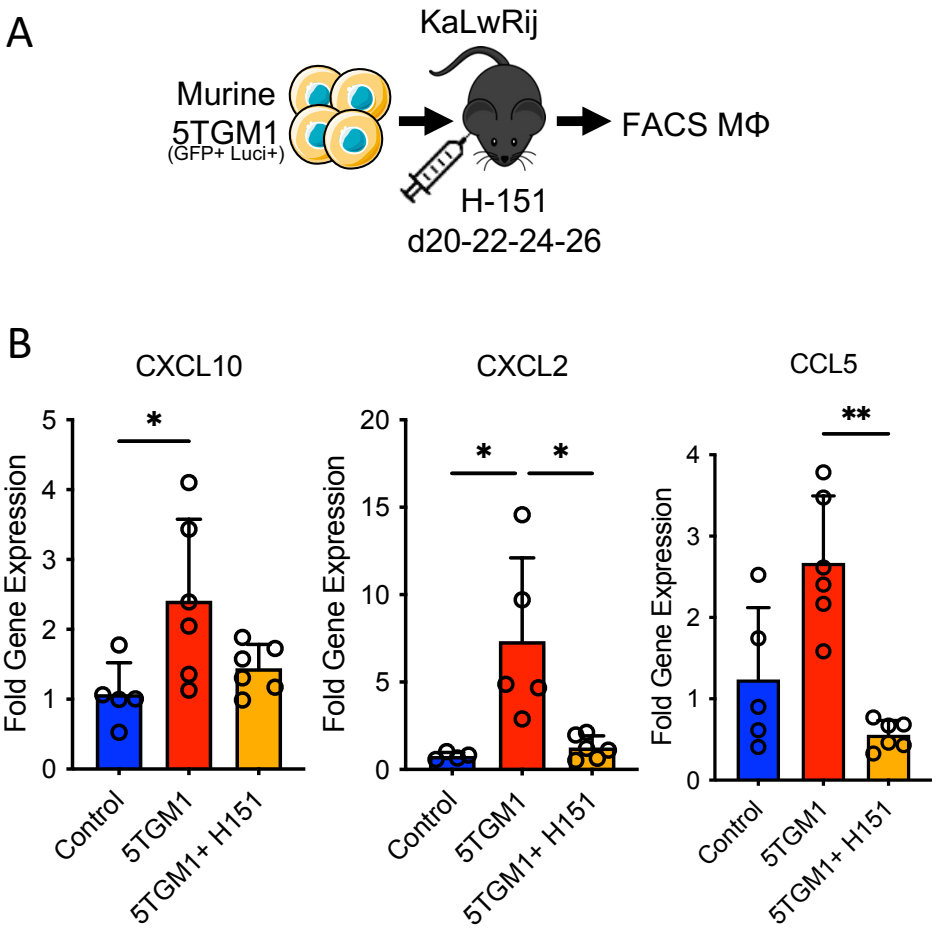

Figure 5.3. MM-induced chemoattractant cytokine expression in bone marrow macrophages is attenuated by STING inhibition.

*(A) Schematic of experimental design. Murine 5TGM1$^{(GFP+\ Luci+)}$ cells (1x10^6) were injected into C57BL/KaLwRij mice. On days 20, 22, 24, and 26 post-engraftment, mice were injected intraperitoneally (i.p.) with either 200 µl H-151 (750 nmol) or vehicle. Mice were sacrificed at 27 days; BM was harvested and myeloma-associated macrophages were isolated via FACS purification. (B) Relative gene expression of Cxcl10, Cxcl2, and Ccl5. n=6 in each treatment group. Fold change was calculated based on the ΔΔCt value obtained from the ΔCt value calculated from the Ct value of the housekeeping gene (GAPDH) subtracted from the Ct value of the gene of interest. Data indicate mean ± SD. Statistics presented as Kruskal-Wallis test with Dunn's post-hoc multiple comparisons test. *p < 0.05; *p < 0.01.*

5.3 mtDAMPs mediate MM cell homing and retention in the bone marrow via STING signalling in bone marrow macrophages

It has previously been shown that *Cxcl2* and *Cxcl10* are implicated in the homing of myeloma cells to the bone marrow [342, 343]. Additionally, *Ccl5* has also been shown to induce the migration of myeloma cells [188]. Given this, we wanted to determine whether the observed upregulation of these chemotactic cytokines in myeloma-associated macrophages affected the migration of 5TGM1 cells and ascertain the role of STING signalling in this process.

To do so, a transwell assay was designed to determine the chemotactic effect of mtDAMPs-stimulated and STING-inhibited BMDM-conditioned media on 5TGM1 cells in vitro (Figure 5.4).

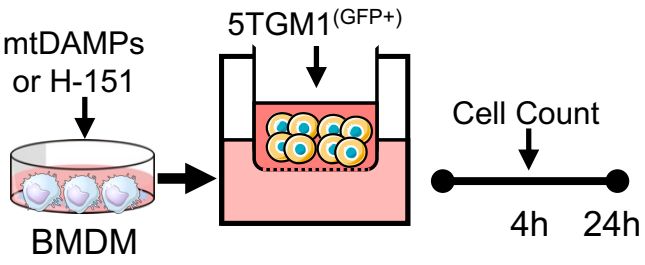

Figure 5.4. 5TGM1 in vitro migration assay.

Schematic of experimental design. Bone marrow-derived macrophages (BMDM) were cultured with either mtDAMPs (10 µg) or H-151 (10 µM) for 24 hours. BMDM-conditioned media was cleared of cellular debris by centrifugation and placed into the bottom chamber of transwell. 5TGM1$^{(GFP+)}$ cells were placed in the upper chamber and migrated 5TGM1$^{(GFP+)}$ cells were counted at 4 and 24 hours.

Figure 5.5 demonstrates that migration was increased in 5TGM1 cells towards mtDAMPs-stimulated macrophage-conditioned media, this migration was significantly reduced by STING inhibition in as little as 4 hours (p = 0.0286) and remained reduced at 24 hours (p = 0.0571).

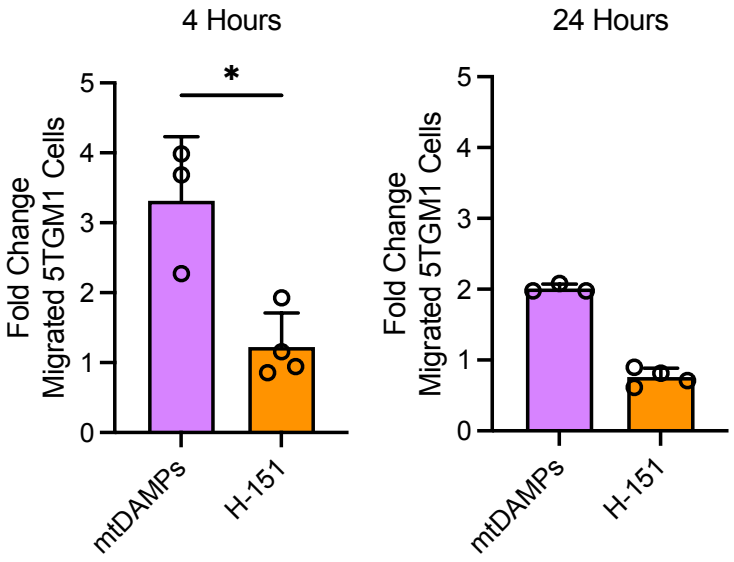

Figure 5.5. mtDAMPs increase 5TGM1 migration, whereas STING inhibition reduces migration.

*Fold change in migrated cells 5TGM1$^{(GFP+)}$ cells towards mtDAMPs activated BMDM conditioned media or H-151 treated BMDM conditioned media. Quantification was relative to control migration observed with 5TGM1$^{(GFP+)}$ cells towards untreated BMDM conditioned media at 4 and 24 hours. n=4 wells per condition. Data indicate mean ± SD. Statistics are presented as Mann-Whitney U test. *p < 0.05.*

In order to investigate this finding in an *in vivo* setting, C57BL/KaLwRij mice were engrafted with 5TGM1$^{(GFP+\ Luci+)}$ cells and allowed to engraft for 34 days. On day 34, peripheral blood samples were taken prior to treatment with H-151, after 24 hours another peripheral blood sample was taken to be analysed by flow cytometry (Figure 5.6).

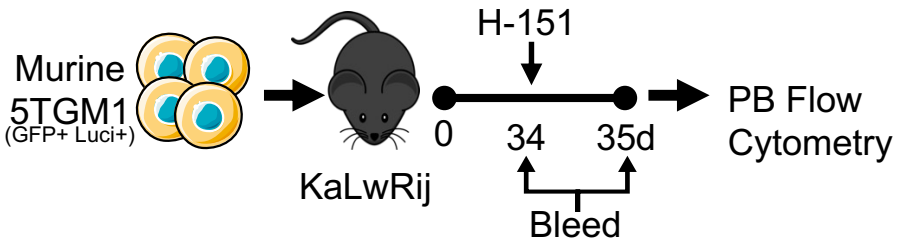

Figure 5.6. 5TGM1 in vivo migration assay with STING inhibition.

(A) Schematic of experimental design. Murine 5TGM1$^{(GFP+\ Luci+)}$ cells (1x10^6) were injected into C57BL/KaLwRij mice. At 34 days post-engraftment, peripheral blood (PB) samples were taken by tail vein bleed then mice were injected intraperitoneally (i.p.) with H-151 (750 nmol). On day 35, post-treatment blood samples were taken, and mice were sacrificed. The PB samples were analysed for 5TGM1$^{(GFP+)}$ cell presence via flow cytometry.

The peripheral blood samples were analysed by flow cytometry for the presence of 5TGM1$^{(GFP+)}$ cells before and after STING inhibition via H-151 treatment (Figure 5.7A). The frequency of 5TGM1$^{(GFP+)}$ cells in the peripheral blood of engrafted mice was significantly increased (p = 0.0078) after a single dose of H-151 treatment (Figure 5.7B). This data indicates that STING inhibition leads to the migration of 5TGM1 cells out of the BM and into the peripheral blood circulation.

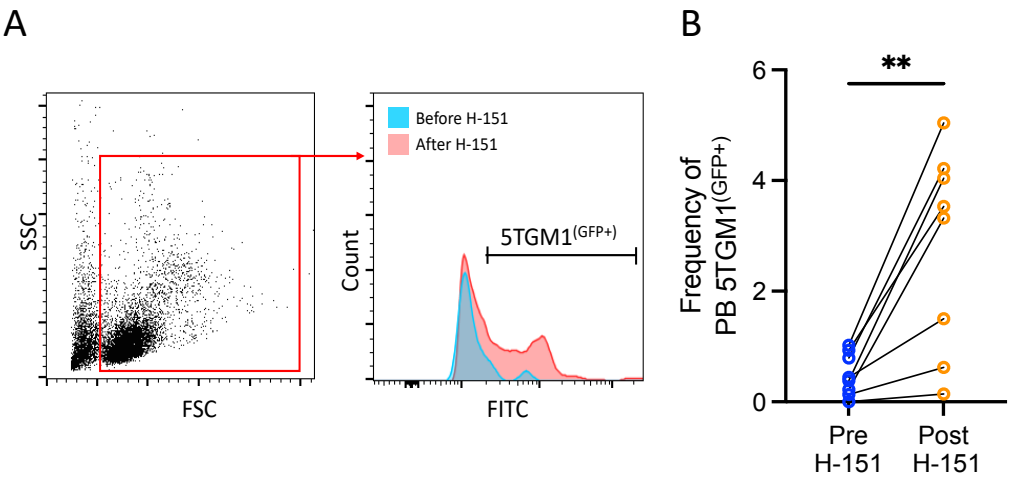

Figure 5.7. Inhibition of STING causes 5TGM1 migration into PB.

*(A) Gating strategy and representative flow plots of 5TGM1$^{(GFP+)}$ cells in the peripheral blood before and after H-151 (750 nmol) treatment. (B) Quantification of 5TGM1$^{(GFP+)}$ cells in the PB. n=8 mice. Data indicate mean ± SD. Statistics are presented as Wilcoxon matched-pairs signed rank test. **p < 0.01.*

The data shown in this chapter so far suggest that macrophages are involved in the process of 5TGM1 cell homing and retention in the bone marrow. To explore this role of macrophages we conducted an *in vivo* experiment whereby macrophages were depleted via clodronate liposome treatment, which causes the selective apoptosis of macrophages [344]. C57BL/KaLwRij mice were engrafted with 5TGM1$^{(GFP+\ Luci+)}$ cells. At 13 days post-engraftment, mice were injected with clodronate or control liposomes. Mice were sacrificed at 14 days and the bone marrow and peripheral blood were isolated for analysis via flow cytometry (Figure 5.8).

To confirm the depletion of macrophages in the bone marrow, the harvested bone marrow was analysed by flow cytometry to identify the BMMΦ population defined as GR1-, CD115$^{LO/INT}$, F4/80+ in the control and clodronate groups. Clodronate-treated mice had a significantly reduced BMMΦ population (p = 0.0286) compared to control-treated mice (Figure 5.9).

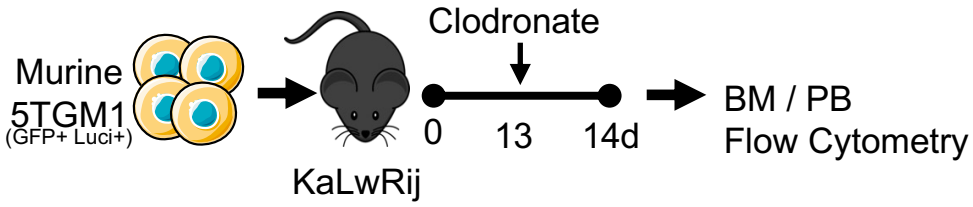

Figure 5.8. C57BL/KaLwRij BM macrophage depletion.

Schematic of experimental design. Murine 5TGM1$^{(GFP+\ Luci+)}$ cells (1x10^6) were injected into C57BL/KaLwRij mice. 13 days post-engraftment, mice were injected intraperitoneally (i.p.) with either, 150 µl clodronate liposomes or liposome controls. Mice were sacrificed on day 14, BM and PB was harvested for flow cytometry analysis.

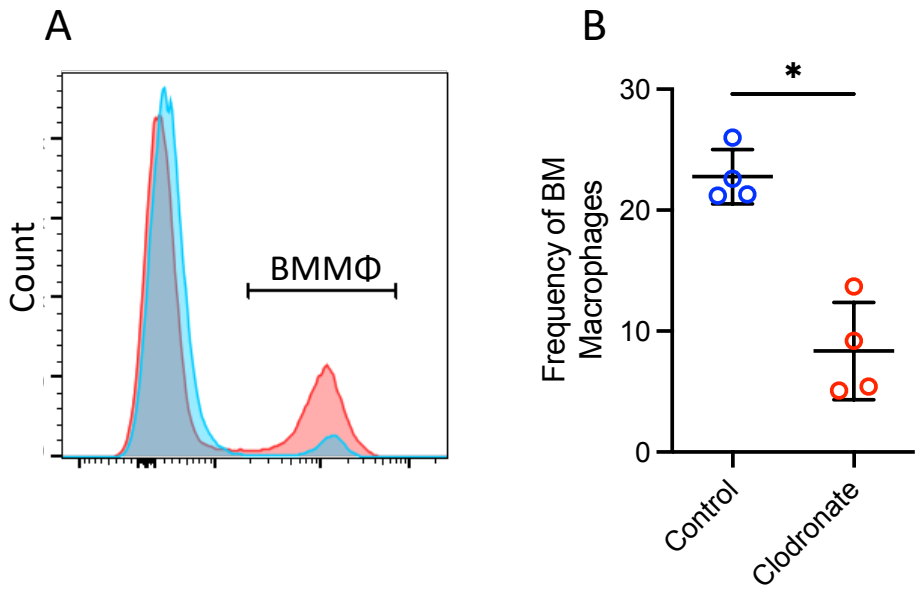

Figure 5.9. Clodronate mediates depletion of BM macrophage in vivo.

*(A) Representative flow cytometry plot of bone marrow macrophages (BMMΦ) (GR1-, CD115 lo/int, F4/80+) in both treatment groups. (B) Quantification of BMMΦ as analysed by flow cytometry. n=4 mice per treatment group. Data indicate mean ± SD. Statistics are presented as Mann-Whitney U test. *p < 0.05.*

As bone marrow macrophages were shown to be depleted, we next identified the frequency of 5TGM1$^{(GFP+)}$ cells in the bone marrow and in the peripheral blood via flow cytometry. Figure 5.10 shows that in the clodronate liposome treatment group, there was a significantly reduced frequency of 5TGM1 cells in the bone marrow (p = 0.0286) and a significantly increased frequency of 5TGM1 cells in the peripheral blood (p = 0.0286).

Together, these results show that bone marrow macrophages are important in the retention of 5TGM1 cells, as macrophage depletion led to the egress of 5TGM1 cells out of the bone marrow and into the peripheral blood circulation.

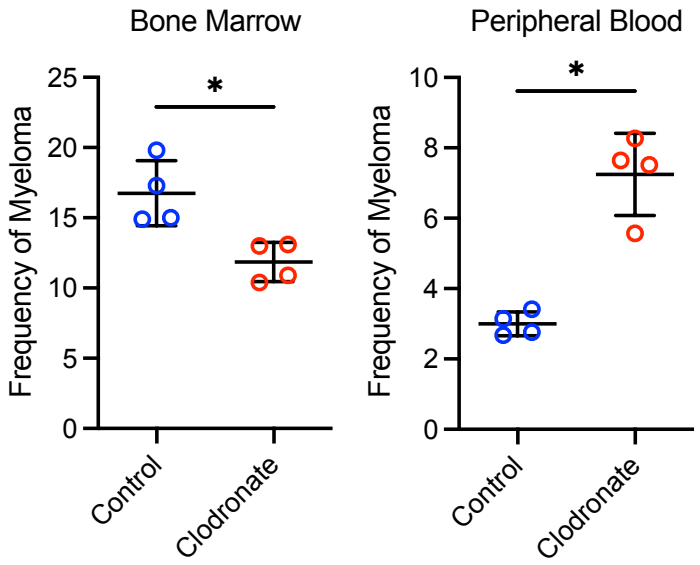

Figure 5.10. Macrophage depletion causes loss of MM retention in BM.

*(A) Quantification of 5TGM1$^{(GFP+)}$ cells in the bone marrow (BM) and in the peripheral blood (PB) as identified by flow cytometry analysis. n=4 mice per treatment group. Data indicate mean ± SD. Statistics are presented as Mann-Whitney U test. *p < 0.05.*

5.4 Summary

In this final results chapter, I have presented data to show that mtDAMPs induce a chemotactic signature in bone marrow macrophages through the upregulation of the chemokines CCL5, CXCL2, and CXCL10. Furthermore, I showed that this gene expression signature was present in myeloma-associated macrophages. Additionally, I identified that mtDAMPs caused increased migration of 5TGM1 cells *in vitro* and furthermore, this migratory effect was dampened by STING inhibition. In an *in vivo* setting, STING inhibition led to the migration of 5TGM1 cells into the peripheral blood. Macrophages were found to be the key mediators of this migration as depletion of macrophages led to the egress of 5TGM1 cells out of the bone marrow and into the peripheral blood. Overall, this data suggests that myeloma-derived mtDAMPs promote the production of chemokines from bone marrow macrophages, which act to attract and retain MM cells in the BM microenvironment. Moreover, the STING signalling pathway mediates this migratory signature.

6 Discussion and Conclusions

6.1 General Discussion

Multiple myeloma is a haematological malignancy that, despite substantial developments in treatment options, remains incurable and the majority of patients succumb to refractory disease [345, 346]. This unfortunate outcome is in part attributed to interactions within the BM microenvironment where MM cells reside. The BM microenvironment is a highly complex structure composed of haematopoietic and non-haematopoietic cells. In MM, the BM milieu forms a niche that is favourably supportive, promoting the differentiation, proliferation, survival, migration, and chemo-resistance of malignant plasma cells [129, 347, 348]. Macrophages are an essential regulator of BM homeostasis in normal physiology. However, macrophage infiltration is associated with poor prognosis in MM and its precursor stage MGUS, as they influence critical mechanisms of MM initiation and progression such as cell growth, angiogenesis, immune suppression, and BM homing [328, 329]. Therefore, targeting BM macrophage and MM-specific interactions may not only enhance the therapeutic efficacy of existing and novel therapies in overt malignancy but also potentially prevent disease progression from precursor stages. Moreover, circulating cell-free mtDAMPs have been implicated in the circulation of many cancer types [197]. However, mechanisms by which mtDAMPs influence cancer progression have not been sufficiently elucidated. Gaining a better understanding of the functional purpose of mtDAMPs in the malignant MM BM microenvironment can help to provide new insights into the promotion of MM disease development. In future, this may be able to be translated to better understand other the pathogenesis of malignancies. In this thesis, I have demonstrated that MM-derived mtDAMPs are released into the MM BM microenvironment. Additionally, I identify a signalling mechanism specifically mediated by mtDAMPs which results in the activation of macrophages. Moreover, I establish the important role that mtDAMPs-activated macrophages play in promoting MM progression and BM homing.

6.2 Key Findings

6.2.1 Cell-free circulating mtDNA is elevated in the serum of MM

In this thesis, I have shown that the levels of circulating mtDNA in the peripheral blood serum of MM patients are elevated compared to healthy controls and this is further increased in the serum of the bone marrow. This finding was corroborated in xenograft mouse models of MM.

The presence of circulating mtDNA has been reported in many cancer types as a promising biomarker for disease [313]. Despite the impact of circulating mtDNA on these cancers being less established, the volume of emerging literature describing this phenomenon indicates a clear association. However, it is important to note that the sample source analysed for mtDNA is a factor that can impact the interpretation of results. Where my data has observed mtDNA in the peripheral blood serum, other studies have used plasma or whole blood itself. This likely contributes to the variability in the current literature and is an important factor that should be taken into consideration. Furthermore, this highlights the need to establish a standardised methodology for analysing circulating mtDNA in each cancer type to achieve conclusive and comparable results. In this study, we chose to look at serum because it is considered the gold standard for research and is often used for diagnostic testing in clinical settings.

The same methodology was employed to analyse both human and mouse serum samples, using the same isolation techniques, volumes, reagents and methods to analyse the extracted DNA, therefore ensuring as little variation in the system as possible. Furthermore, as stated above, the elevated levels of mtDNA were observed in human patient samples and further corroborated in an *in vitro* study of cell lines where MM primary and immortalised cell lines had an increased level of mtDNA in their cell culture medium. Moreover, this finding was validated in the NSG, C57BL/6, and C57BL/KaLwRij mouse models of MM.

Interestingly, we also observed a significantly higher level of circulating mtDNA in the bone marrow serum of both human MM samples and *in vivo* in the NSG xenograft model of MM. Together, this data suggests a strong association between mtDNA and MM and highlights the potential of circulating mtDNA as a non-invasive diagnostic biomarker for MM.

6.2.2 Cell-free circulating mtDNA is derived from MM cells

An important aspect of this thesis was to ascertain the origin of circulating mtDNA. Establishing the source and form of release of circulating cell-free mtDNA is important in understanding the possible downstream effects and targets in MM. Potential forms of circulating cell-free mtDNA may include whole mitochondria, whole genome or DNA fragments either encapsulated in lipid-based vesicles or naked. Furthermore, it has been suggested that the release mechanism can be passive, from damaged cells via necrosis or apoptosis, or active through regulated processes such as lipid vesicle release [349]. In AML; another haematological malignancy, AML cells have been shown to actively release mitochondria in the form of apoptotic bodies [321].

In most cancers, a phenomenon called the Warburg effect is established. This effect describes a pattern whereby cancer cells rely on a combination of both oxidative phosphorylation and aerobic glycolysis, instead of relying solely on the more efficient process of oxidative phosphorylation [350]. Increased mtDNA copy number which reflects the abundance of mitochondria and correlates with energy production capacity [351, 352], has been attributed to the pathogenetic transformation of MM which contributes to disease progression [323]. Therefore, it is likely that this increased demand for ATP production is the reason behind the increased mitochondrial mass. In turn, this increases the likelihood of dysfunctional mitochondria, which ultimately leads to increased reactive oxygen species (ROS) which promotes the process of apoptosis [353].

In this study, I established that the elevated circulating mtDNA was derived from MM cells and not from the surrounding microenvironment. The central experiment in reaching this conclusion utilised the xenograft NSG mouse model where human MM cells were engrafted into immunocompromised mice. The circulating mtDNA could then be distinguished as either murine or human. We observed that levels of circulating murine mtDNA were unchanged in engrafted mice whilst human mtDNA was increased in a fashion that correlated with disease progression. This experiment could have benefitted from the addition of another treatment group receiving CD34+ haematopoietic stem cells as a negative control to confirm that the increased human mtDNA is MM-specific and not just due to human cells being introduced to the murine immune system. However, the substantiative data from numerous syngeneic mouse model experiments confirming this observation were deemed sufficient to reach the conclusion in this study. Furthermore, the observation that MM cells are responsible for releasing circulating mtDNA is further validated by the finding that significantly higher levels of mtDNA are present in the bone marrow serum of MM, as the BM niche is where MM cells reside.

Taken all together, whilst this study has determined the cell of origin of circulating mtDNA in MM, it would be interesting to examine the mechanism and form of mtDNA (and associated mtDAMPs) that is released. If we were to shed light on this, we may then be able to identify potential targets to prevent the release of mtDAMPs before they are able to initiate their downstream effects.

6.2.3 Macrophages are activated by mtDAMPs via STING signalling

MM is a disease that displays a high dependency on the BM niche and is characterised by a compromised immune microenvironment from the very early stages of disease onset [354]. This reliance on the BM microenvironment implies a crucial role for the cells of the BM microenvironment in supporting MM pathogenesis. One such cell type is the macrophage. Macrophages are abundant in MM and play a fundamental role in the initiation and progression of MM by supporting key pro-tumoral processes such as proliferation, drug resistance and angiogenesis [328, 355].

I have identified that MM-derived mtDAMPs stimulate macrophages via the activation of the cGAS-STING signalling pathway which results in a pro-inflammatory gene expression signature. This is not surprising as mtDAMPs are potent activators of the innate immune system [198, 261]. I found that levels of the pro-inflammatory cytokine IL-6 were increased both *in vitro* and *in vivo*. Genes indicative of type I interferon release were also upregulated confirming the activation of the STING pathway. Furthermore, STING inhibition was found to attenuate this gene expression profile in macrophages from MM engrafted mice and in BMDMs treated with mtDAMPs. Interestingly, using a molecular mimic of mtDNA (ODN 1826) did not elicit the same gene expression profile in BMDMs. This finding suggests that the STING activation response is mtDAMPs-specific.

Targeting of cGAS-STING has become one of the most investigated signalling pathways, its role as a cytosolic DNA sensor is recognised as an important regulator of the innate immune system and has been implicated in the pathogenesis of many diseases [262, 327]. STING activation has been shown to significantly extend survival in *in vivo* models of AML [321], and reduces the tumour burden in mouse models of pancreatic cancer [356].

As such, the use of STING agonists has currently come into focus as a promising avenue for the potential treatment of cancers. Their mode of action reignites immune responses causing type I interferon responses which mediate cytotoxic T-cell activity and result in tumour cell death [357, 358].
The synthetic cyclic dinucleotide ADU-S100 is currently being trialled clinically and has been shown to be a well-tolerated activator of STING in the treatment of advanced and metastatic solid tumours [359]. In my thesis, however, I crucially show data contradictory to this as inhibition of STING *in vivo* led to a reduction in MM progression. So far, the research community is focused on the antitumoral T-cell priming effects of STING activation in the context of cancer immunotherapy. Whereas the inhibition of STING has mainly been regarded as a potential treatment option for inflammatory diseases, where dampening cGAS-STING signalling and the consequent innate immune response would prove beneficial [326, 341].

However, the novel findings presented in my thesis demonstrate a strong association between mtDAMPs-mediated STING-driven inflammation and MM progression. Furthermore, inflammation has been regarded as a hallmark of various cancers [112, 311] and the pro-inflammatory BM microenvironment has proven to be instrumental in the promotion of MM [360]. Therefore, the role of STING antagonists in the treatment of cancers should also be taken into consideration as potential cancer immunotherapy options.

Additionally, I show data that suggests that mtDAMPs-activated macrophages cause mtDNA release from MM cells in a positive feedback loop mechanism which would exacerbate the pro-inflammatory effects of STING signalling. This finding highlights that interruption of the MM cell and BM macrophage interaction axis by targeting STING warrants further investigation.

6.2.4 MM homing and macrophages

Importantly in this study, I have shown that mtDAMPs induce a chemotactic signature in BM macrophages by the secretion of migratory chemokines which murine MM cells migrate towards. Furthermore, we found that macrophages play a vital role in the retention of MM cells in the BM microenvironment. This was demonstrated by the depletion of macrophages using clodronate, which resulted in the egress of MM cells from the BM to the peripheral blood. Another study identified that depletion of macrophages prior to engraftment of MM cells results in impaired engraftment of MM [190]. Together, this demonstrates the importance of macrophages in the BM homing capacity of MM. Additionally, my study highlights the important role that STING-mediated activation of macrophages plays in BM homing, as inhibition of STING resulted in a similar loss of MM cell retention in the BM.

It has been reported that MM cells have been shown to secrete the chemokines CCL3 and CCL5 [184], which are ligands for the receptors CCR1 and CCR5. Current observations have proposed that MM progression is supported by this signalling axis by promoting the BM homing of MM cells [188, 361]. These reports are corroborated by the data I present showing that CCL5 gene expression is upregulated in BMDMs stimulated with mtDAMPs. Moreover, this was also observed in BM macrophages isolated from MM-engrafted mice. This upregulated gene expression is subsequently downregulated upon STING inhibition which impairs MM disease progression.

Furthermore, CXCL2 and CXCL10 gene expression was also found to be upregulated. The CXCL2/CXCR2 signalling axis has been implicated in mediating the migration of colon cancer cells and is a key facilitator of metastasis in colorectal cancer [362]. Meanwhile, CXCL10 and its receptor have been associated with mediating tumour progression in MM [343]. Additionally, inhibition of CCR1 was demonstrated to reduce tumour burden in a mouse model of myeloma [174].

Overall, this demonstrates the importance of activated BM macrophages in the induction of a pro-chemotactic signature which promotes MM homing to the protective BM niche. Additionally, it implicates the need for further investigation into the inhibition of these chemokine signalling pathways as a potential therapeutic avenue in the treatment of cancer. However, as this function of mtDAMPs-mediated macrophage activation is downstream of initial STING signalling, the inhibition of the STING pathway is likely to be the most-effective line of therapeutic intervention in MM.

Nonetheless, the key findings of this thesis present multiple avenues of investigation that may be the key to MM research.

6.3 Limitations

Although the data presented in this study has furthered the understanding of the role of mtDAMPs in the MM microenvironment, as with any study, there are limitations that should be taken into account.

Firstly, due to the unprecedented Covid-19 pandemic, the scope and scale of the project involving the collection of primary MM samples were limited. Therefore, the data generated in this study investigated only a small sample size of newly diagnosed MM patients. Initially, MM patient samples were to be collected from patients at diagnosis, during treatment, and after treatment with the aim of monitoring serum mtDNA levels, which would have generated data of greater depth. Additionally, having a larger sample size would have allowed for a more compelling statistical analysis, due to the heterogeneity of the disease.

With regards to the *in vivo* data in this study, the number of mice used in each experiment was quite low and increasing the number of mice in each cohort may have provided greater statistical significance when comparing data sets. However, numbers were kept low in keeping with the 3Rs (Replacement, Reduction, and Refinement) to perform animal research in an efficient and humane manner. Another limitation of *in vivo* experiments was the variability in the engraftment of mouse strains. This could have been due to various factors such as the tail vein being missed during i.v. injections, poor cell viability, or a loss of signalling from the GFP and luciferase reporter-tagged cells. However, for each experiment involving MM engraftment, engraftment levels were confirmed prior to setting up the different treatment groups to ensure the cohorts were evenly split to allow for a fair comparison.

In my thesis, a key finding was the involvement of the STING signalling pathway in promoting the progression of MM. Through a combination of *in vitro* and *in vivo* experiments deploying RNA gene expression analysis, cytokine arrays and the use of a STING inhibitor, I showed that STING activation in macrophages played a crucial role in the response to mtDAMPs in stimulating pro-tumoral responses such as inflammation and homing. Though the use of the STING antagonist H-151 has proven to be a robust inhibitor *in vivo* [334], the use of pharmacological agents to inhibit receptor signalling can be of concern due to the possible off-target effects that may arise. Therefore, this data could have been further substantiated by using an shRNA knockdown method or better still, a STING knockout mouse model to ensure total inhibition of STING. However, due to time constraints and restrictions, these mouse models could not be made available for this study.

Furthermore, I briefly investigated the role of TLR-9 signalling in mtDAMPs-mediated macrophage activation and MM progression, however, the TLR-9 antagonist ODN 2088 did not prove effective *in vivo*. This suggested that ODN 2088 may not have been the best option to target TLR-9. Therefore, the use of a TLR-9 knockout model would have allowed me to better investigate the role of this signalling pathway.

Moreover, in this study, I only investigated 2 of the many receptor pathways implicated in the sensing of mtDAMPs, it would have been interesting to investigate other PRRs and their respective mtDAMPs ligands individually to ascertain their distinct roles. However, due to the vast time commitment that this would demand, this was beyond the scope of this project, but it does leave room for the expansion of this project.

Lastly, like many other researchers, this thesis was heavily impacted by the global Covid-19 pandemic which placed significant limitations on the amount of laboratory research that could be undertaken. Due to this, access to patient samples was severely affected for a prolonged period ultimately reducing the sample size of the study which would have allowed for more comparisons to be drawn from the data. Furthermore, the *in vivo* work in this study, particularly the C57BL/KaLwRij model could have benefitted from more time to be refined in order to achieve optimal engraftment levels and replicability. Additionally, time constraints meant that the investigation of the chemotactic profile of mtDAMPs activated macrophages in MM was not fully expounded. More research would be required to fully explore this interaction and resulting phenotype.

6.4 Future work

Although the primary aims of this study have been addressed in this thesis, there are questions that have been raised in the process that could require further investigation.

I have shown that mtDNA is associated with MM disease and has the potential to be used as a diagnostic biomarker due to its non-invasive and easy detection protocol. However, this finding could be expanded upon. It is well-known that MM follows a defined disease progression with precursor stages and relapsed/refractory disease. Therefore, it would be interesting to compare circulating cell-free mtDNA levels in the serum of patients with monoclonal gammopathy of undetermined significance (MGUS), smouldering myeloma (SMM) as well as MM patients in different stages of treatment. Furthermore, the sample size could be expanded and studied in a longitudinal project. This would allow us to stratify what levels of circulating mtDNA are significant prognostically as well as diagnostically.

In addition, we show that the circulating mtDNA is derived from MM cells, however, the mechanism and reasoning behind this have not been established. It could be hypothesised that excess mtDNA is actively expelled from the MM cell but there are many methods of cell-free mtDNA release that have been described [349]. Further research is warranted to determine the exact mechanism used by MM cells. As I have also shown that there is likely a positive feedback mechanism at play whereby mtDAMPs-activated macrophages stimulate mtDNA release from MM cells, investigating the means of this release could lead to the identification of a method to inhibit this process and the downstream pro-inflammatory effects of mtDAMPs signalling.

The pro-inflammatory and pro-chemotactic macrophage signatures identified have proven to be instrumental in the progression of MM disease via the cGAS-STING signalling pathway and we show that these interactions are vital in the retention of MM cells in the BM. In this thesis, I show a mtDAMPs-specific activation gene expression signature in BM macrophages using cytokine arrays and RT-qPCR analysis. However, the use of more sophisticated techniques such as RNA sequencing would be better equipped to characterise the transcriptional changes that occur in mtDAMPs-mediated macrophage activation. This could reveal other gene expression signatures that may shed light on how mtDAMPs manipulate the macrophage phenotype to promote MM disease progression. Furthermore, the novel finding that mtDAMPs-mediated STING pathway activation in macrophages promotes MM disease progression presents the potential therapeutic impact of STING pathway inhibitors in MM treatment. The pre-clinical development of effective small molecule inhibitors targeting the cGAS-STING pathway is ongoing with screening to identify potential clinical trial candidates [326]. STING inhibition could prove a valuable addition to the current conventional MM treatment options. A better understanding of the minimum level of inhibition required to achieve effective therapeutic benefits, potential side effects and, drug interactions will be crucial in the clinical implementation of STING antagonists in MM disease treatment.

The findings presented in this thesis could impact the way that circulating cell-free mtDNA is used as a biomarker in the detection and therapeutic monitoring of MM disease in a clinical setting. Circulating mtDNA is an attractive biomarker candidate as its means of detection in the peripheral blood serum are non-invasive, easily accessible, and cost-effective. However, in order for the clinical implementation of circulating mtDNA to be successful, further research is required to standardise protocols for sample collection, processing and analysis to establish reproducible and accurate results. Furthermore, a large patient population study would likely be required to determine and optimise cut-off detection levels of mtDNA. Nonetheless, in a clinical setting circulating mtDNA holds great promise as a biomarker of MM disease.

6.5 Conclusions

In summary, in this thesis, I have demonstrated that mtDNA is elevated in the MM tumour microenvironment and that this mtDNA is derived from malignant plasma cells. Furthermore, these MM-derived mtDAMPs function mechanistically via the STING signalling pathway to activate BM macrophages. Whilst mtDAMPs and MM were not shown to alter the composition and polarisation of BM macrophages in mouse models of MM, the STING activation did result in the induction of a pro-inflammatory and pro-chemotactic gene expression signature. This finding was confirmed by the attenuation of this phenotype by STING inhibition. The significance of this gene expression profile was shown by the mediation of MM disease progression. This again was evidenced by the inhibition of STING *in vivo,* which led to a reduction in MM tumour progression. Pathophysiologically, MM cells were shown *in vitro* to exhibit a chemotactic affinity for mtDAMPs-activated macrophages. Lastly, the mtDAMPs-mediated STING activation of BM macrophages was shown to drive the pro-chemotactic gene expression profile which functions to facilitate BM homing and retention of MM cells within the pro-tumoral BM microenvironment.

Overall, the data provided establishes the functional role that mtDAMPs play in the MM microenvironment. This identifies the important mechanism by which mtDAMPs activate BM macrophages in order to confer pro-tumoral responses that promote MM disease progression.

7 References

1. Clarke, B., *Normal Bone Anatomy and Physiology.* Clin J Am Soc Nephrol, 2008. **3**(Suppl 3): p. S131-9.
2. Birbrair, A. and P.S. Frenette, *Niche heterogeneity in the bone marrow.* Ann N Y Acad Sci, 2016. **1370**(1): p. 82-96.
3. Gurkan, U.A. and O. Akkus, *The Mechanical Environment of Bone Marrow: A Review.* Annals of Biomedical Engineering, 2008. **36**(12): p. 1978-1991.
4. Moerman, E.J., et al., *Aging activates adipogenic and suppresses osteogenic programs in mesenchymal marrow stroma/stem cells: the role of PPAR-γ2 transcription factor and TGF-β/BMP signaling pathways.* Aging Cell, 2004. **3**(6): p. 379-389.
5. Guerra, D.A.P., et al., *Adipocytes role in the bone marrow niche.* Cytometry Part A, 2018. **93**(2): p. 167-171.
6. Devlin, M.J., *Why does starvation make bones fat?* American Journal of Human Biology, 2011. **23**(5): p. 577-585.
7. Cao, J.J., L. Sun, and H. Gao, *Diet-induced obesity alters bone remodeling leading to decreased femoral trabecular bone mass in mice.* Ann N Y Acad Sci, 2010. **1192**: p. 292-7.
8. Zhang, J., et al., *Cross-talk between leukemic and endothelial cells promotes angiogenesis by VEGF activation of the Notch/Dll4 pathway.* Carcinogenesis, 2013. **34**(3): p. 667-77.
9. Gurevitch, O., S. Slavin, and A.G. Feldman, *Conversion of red bone marrow into yellow - Cause and mechanisms.* Med Hypotheses, 2007. **69**(3): p. 531-6.
10. Travlos, G.S., *Normal Structure, Function, and Histology of the Bone Marrow.* Toxicologic Pathology, 2006. **34**(5).
11. Calvo, W., *The innervation of the bone marrow in laboratory animals.* American Journal of Anatomy, 1968.
12. Jung, W.-C., J.-P. Levesque, and M.J. Ruitenburg, *It takes nerve to fight back: The significance of neural innervation of the bone marrow and spleen for immune function.* Seminars in Cell & Development Biology, 2016. **61**.
13. Park, M.H., J.K. Lee, and N. Kim, *Neuropeptide Y Induces Hematopoietic Stem/Progenitor Cell Mobilization by Regulating Matrix Metalloproteinase-9 Activity Through Y1 Receptor in Osteoblasts.* Stem Cells, 2016.
14. Hoggatt, J. and L.M. Pelus, *Mobilization of hematopoietic stem cells from the bone marrow niche to the blood compartment.* Stem Cell Research & Therapy, 2011. **2**(2): p. 13.
15. Kumar, R. and T. Evans, *Haematopoiesis.* eLS, John Wiley & Sons, Ltd, 2015.
16. Cooper, B., *The origins of bone marrow as the seedbed of our blood: from antiquity to the time of Osler.* Proc (Bayl Univ Med Cent), 2011. **24**(2): p. 115-8.
17. Fliedner, T.M., et al., *Structure and Function of Bone Marrow Hemopoiesis: Mechanisms of Response to Ionizing Radiation Exposure.* Cancer Biotherapy and Radiopharmaceuticals, 2002. **17**(4): p. 405-426.
18. Schofield, R., *The relationship between the spleen colony-forming cell and the haemopoietic stem cell.* Blood Cells, 1978. **4**(1-2): p. 7-25.

19. Jagannathan-Bogdan, M. and L.I. Zon, *Hematopoiesis.* Development, 2013. **140**(12): p. 2463-7.
20. Oda, A., et al., *Niche-induced extramedullary hematopoiesis in the spleen is regulated by the transcription factor Tlx1*, in *Scientific Reports*. 2018.
21. Yang, L., et al., *Identification of Lin(-)Sca1(+)kit(+)CD34(+)Flt3- short-term hematopoietic stem cells capable of rapidly reconstituting and rescuing myeloablated transplant recipients.* Blood, 2005. **105**(7): p. 2717-23.
22. Cheng, H., Z. Zheng, and T. Cheng, *New paradigms on hematopoietic stem cell differentiation.* Protein & Cell, 2019. **11**(1): p. 34-44.
23. Pietras, E.M., et al., *Functionally Distinct Subsets of Lineage-Biased Multipotent Progenitors Control Blood Production in Normal and Regenerative Conditions.* Cell Stem Cell, 2015. **17**(1): p. 35-46.
24. Paul, F., et al., *Transcriptional Heterogeneity and Lineage Commitment in Myeloid Progenitors.* Cell, 2015. **163**(7): p. 1663-1677.
25. Nestorowa, S., et al., *A single-cell resolution map of mouse hematopoietic stem and progenitor cell differentiation.* Blood, 2016. **128**(8): p. e20-31.
26. Laurenti, E. and B. Göttgens, *From haematopoietic stem cells to complex differentiation landscapes.* Nature, 2018. **553**(7689): p. 418-26.
27. Haas, S., A. Trumpp, and M.D. Milsom, *Causes and Consequences of Hematopoietic Stem Cell Heterogeneity.* Cell Stem Cell, 2018. **22**(5).
28. Quesenberry, P.J., et al., *Adult marrow hematopoiesis: a continuum of change.* Leukemia Supplements, 2014. **3**(1): p. S18-S18.
29. Muguruma, Y., et al., *Reconstitution of the functional human hematopoietic microenvironment derived from human mesenchymal stem cells in the murine bone marrow compartment.* Blood, 2006. **107**(5): p. 1878-87.
30. Kumar, R., P.S. Godavarthy, and D.S. Krause, *The bone marrow microenvironment in health and disease at a glance.* Journal of Cell Science, 2018.
31. Sugiyama, T., et al., *Maintenance of the Hematopoietic Stem Cell Pool by CXCL12-CXCR4 Chemokine Signaling in Bone Marrow Stromal Cell Niches.* Immunity, 2020. **25**(6): p. 977-988.
32. Sacchetti, B., et al., *Self-renewing osteoprogenitors in bone marrow sinusoids can organize a hematopoietic microenvironment.* Cell, 2007. **131**(2): p. 324-36.
33. Mendez-Ferrer, S., et al., *Mesenchymal and haematopoietic stem cells form a unique bone marrow niche.* Nature, 2010. **466**(7308): p. 829-34.
34. Ding, L., et al., *Endothelial and perivascular cells maintain haematopoietic stem cells.* Nature, 2012. **481**(7382): p. 457-462.
35. Ciciarello, M., et al., *The Yin and Yang of the Bone Marrow Microenvironment: Pros and Cons of Mesenchymal Stromal Cells in Acute Myeloid Leukemia.* Frontiers in Oncology, 2019. **9**.
36. Kunisaki, Y., et al., *Arteriolar niches maintain haematopoietic stem cell quiescence.* Nature, 2013. **502**(7473): p. 637-643.
37. Gimble, J.M., et al., *The function of adipocytes in the bone marrow stroma: an update.* Bone, 1996. **19**(5): p. 421-8.

38. Cawthorn, William P., et al., *Bone Marrow Adipose Tissue Is an Endocrine Organ that Contributes to Increased Circulating Adiponectin during Caloric Restriction.* Cell Metabolism, 2014. **20**(2): p. 368-375.
39. Fazeli, P.K., et al., *Marrow Fat and Bone—New Perspectives.* The Journal of Clinical Endocrinology & Metabolism, 2013. **98**(3): p. 935-945.
40. Justesen, J., et al., *Adipocyte tissue volume in bone marrow is increased with aging and in patients with osteoporosis.* Biogerontology, 2001. **2**(3): p. 165-171.
41. Botolin, S. and L.R. McCabe, *Bone Loss and Increased Bone Adiposity in Spontaneous and Pharmacologically Induced Diabetic Mice.* Endocrinology, 2007. **148**(1): p. 198-205.
42. Hardaway, A.L., et al., *Marrow adipocyte-derived CXCL1 and CXCL2 contribute to osteolysis in metastatic prostate cancer.* Clinical & Experimental Metastasis, 2015. **32**(4): p. 353-368.
43. Templeton, Z.S., et al., *Breast Cancer Cell Colonization of the Human Bone Marrow Adipose Tissue Niche.* Neoplasia, 2015. **17**(12): p. 849-861.
44. Tavassoli, M., *Marrow adipose cells. Histochemical identification of labile and stable components.* Arch Pathol Lab Med, 1976. **100**(1): p. 16-8.
45. Scheller, E.L. and C.J. Rosen, *What's the matter with MAT? Marrow adipose tissue, metabolism, and skeletal health.* Annals of the New York Academy of Sciences, 2014. **1311**(1): p. 14-30.
46. Scheller, E.L., et al., *Region-specific variation in the properties of skeletal adipocytes reveals regulated and constitutive marrow adipose tissues.* Nature Communications, 2015. **6**(1): p. 7808.
47. Attané, C., et al., *Human Bone Marrow Is Comprised of Adipocytes with Specific Lipid Metabolism.* Cell Reports, 2020. **30**(4): p. 949-958.e6.
48. Gimble, J.M., et al., *Peroxisome proliferator-activated receptor-gamma activation by thiazolidinediones induces adipogenesis in bone marrow stromal cells.* Mol Pharmacol, 1996. **50**(5): p. 1087-94.
49. Belaid-Choucair, Z., et al., *Human Bone Marrow Adipocytes Block Granulopoiesis Through Neuropilin-1-Induced Granulocyte Colony-Stimulating Factor Inhibition.* Stem Cells, 2009. **26**.
50. S., G.S., et al., *Neuropilin-1 Is an Important Niche Component and Exerts Context-Dependent Effects on Hematopoietic Stem Cells.* Stem Cells and Development, 2017. **26**(1).
51. Zhou, B.O., et al., *Bone marrow adipocytes promote the regeneration of stem cells and haematopoiesis by secreting SCF.* Nat Cell Biol, 2017. **19**(8): p. 891-903.
52. Scandura, J.M., et al., *Transforming growth factor β-induced cell cycle arrest of human hematopoietic cells requires p57KIP2 up-regulation.* 2004.
53. Miharada, K.-I., et al., *Lipocalin 2 functions as a negative regulator of red blood cell production in an autocrine fashion.* The FASEB Journal, 2005. **19**(13).
54. Broxmeyer, H.E., et al., *Dipeptidylpeptidase 4 negatively regulates colony-stimulating factor activity and stress hematopoiesis.* Nature Medicine, 2012. **18**(12): p. 1786-1796.

55. DiMascio, L., et al., *Identification of Adiponectin as a Novel Hemopoietic Stem Cell Growth Factor.* 2007.
56. Wang, H., Y. Leng, and Y. Gong, *Bone Marrow Fat and Hematopoiesis.* Frontiers in Endocrinology, 2018. **9**.
57. Asada, N. and Y. Katayama, *Regulation of hematopoiesis in endosteal microenvironments.* International Journal of Hematology, 2014. **99**(6): p. 679-684.
58. Taichman, R., et al., *Hepatocyte growth factor is secreted by osteoblasts and cooperatively permits the survival of haematopoietic progenitors.* British Journal of Haematology, 2001. **112**(2): p. 438-48.
59. Taichman, R.S. and S.G. Emerson, *Human osteoblasts support hematopoiesis through the production of granulocyte colony-stimulating factor.* Journal of Experimental Medicine, 1994. **179**(5).
60. Sebastian, S., et al., *Osteopontin is a hematopoietic stem cell niche component that negatively regulates stem cell pool size.* Journal of Experimental Medicine, 2005. **201**(11).
61. R., C.B., Y.-H. Cheng, and M.A. Kacena, *Hierarchical organization of osteoblasts reveals the significant role of CD166 in hematopoietic stem cell maintenance and function.* Bone, 2013. **54**(1).
62. Morrison, S.J. and D.T. Scadden, *The bone marrow niche for haematopoietic stem cells.* Nature, 2014. **505**(7483): p. 327-334.
63. Asada, N., et al., *Matrix-Embedded Osteocytes Regulate Mobilization of Hematopoietic Stem/Progenitor Cells.* Cell Stem Cell, 2013. **12**(6).
64. Sato, M., et al., *Osteocytes Regulate Primary Lymphoid Organs and Fat Metabolism.* Cell Metabolism, 2013. **18**(5).
65. Kissa, K. and P. Herbomel, *Blood stem cells emerge from aortic endothelium by a novel type of cell transition.* Nature, 2010. **464**(7285): p. 112-115.
66. Xu, C., et al., *Stem cell factor is selectively secreted by arterial endothelial cells in bone marrow.* Nature Communications, 2018. **9**(1): p. 1-13.
67. Rafii, S., et al., *Human bone marrow microvascular endothelial cells support long-term proliferation and differentiation of myeloid and megakaryocytic progenitors.* Blood, 1995. **86**(9): p. 3353-63.
68. Winkler, I.G., et al., *Vascular niche E-selectin regulates hematopoietic stem cell dormancy, self renewal and chemoresistance.* Nature Medicine, 2012. **18**(11): p. 1651-1657.
69. Rice, G.E. and M.P. Bevilacqua, *An inducible endothelial cell surface glycoprotein mediates melanoma adhesion.* Science, 1989. **246**(4935): p. 1303-6.
70. Osborn, L., et al., *Direct expression cloning of vascular cell adhesion molecule 1, a cytokine-induced endothelial protein that binds to lymphocytes.* Cell, 1989. **59**(6): p. 1203-11.
71. Papayannopoulou, T., et al., *The VLA4/VCAM-1 adhesion pathway defines contrasting mechanisms of lodgement of transplanted murine hemopoietic progenitors between bone marrow and spleen.* Proc Natl Acad Sci U S A, 1995. **92**(21): p. 9647-51.
72. Pinho, S., et al., *VCAM1 confers innate immune tolerance on haematopoietic and leukaemic stem cells.* Nature Cell Biology, 2022. **24**(3): p. 290-298.

73. Smith, A.O., et al., *A novel strategy for isolation of mice bone marrow endothelial cells (BMECs).* Stem Cell Research & Therapy, 2021. **12**(1): p. 267.
74. Gordon, S. and P.R. Taylor, *Monocyte and macrophage heterogeneity.* Nat Rev Immunol, 2005. **5**(12): p. 953-64.
75. Epelman, S., Kory J. Lavine, and Gwendalyn J. Randolph, *Origin and Functions of Tissue Macrophages.* Immunity, 2014. **41**(1): p. 21-35.
76. Manwani, D. and J.J. Bieker, *The Erythroblastic Islands.* Current Topics in Developmental Biology, 2008. **82**.
77. Koury, M.J. and M.C. Bondurant, *Maintenance by erythropoietin of viability and maturation of murine erythroid precursor cells.* J Cell Physiol, 1988. **137**(1): p. 65-74.
78. Li, W., et al., *Identification and transcriptome analysis of erythroblastic island macrophages.* Blood, 2019. **134**(5): p. 480-491.
79. Chow, A., et al., *Bone marrow CD169+ macrophages promote the retention of hematopoietic stem and progenitor cells in the mesenchymal stem cell niche.* Journal of Experimental Medicine, 2011. **208**(2).
80. Winkler, I.G., et al., *Bone marrow macrophages maintain hematopoietic stem cell (HSC) niches and their depletion mobilizes HSCs.* Blood, 2010. **116**(23): p. 4815-4828.
81. Mosmann, T.R. and R.L. Coffman, *TH1 and TH2 Cells: Different Patterns of Lymphokine Secretion Lead to Different Functional Properties.* Annual Review of Immunology, 1989. **7**(1): p. 145-173.
82. Mills, C.D., et al., *M-1/M-2 Macrophages and the Th1/Th2 Paradigm.* The Journal of Immunology, 2000. **164**(12): p. 6166.
83. Mantovani, A., et al., *The chemokine system in diverse forms of macrophage activation and polarization.* Trends in Immunology, 2004. **25**(12): p. 677-686.
84. Chen, Y. and X. Zhang, *Pivotal regulators of tissue homeostasis and cancer: macrophages.* Experimental Hematology & Oncology, 2017. **6**(1): p. 23.
85. Ivashkiv, L.B., *IFNγ: signalling, epigenetics and roles in immunity, metabolism, disease and cancer immunotherapy.* Nat Rev Immunol, 2018. **18**(9): p. 545-558.
86. Bonizzi, G. and M. Karin, *The two NF-kappaB activation pathways and their role in innate and adaptive immunity.* Trends Immunol, 2004. **25**(6): p. 280-8.
87. Hansen, G., et al., *The structure of the GM-CSF receptor complex reveals a distinct mode of cytokine receptor activation.* Cell, 2008. **134**(3): p. 496-507.
88. Martinez, F.O. and S. Gordon, *The M1 and M2 paradigm of macrophage activation: time for reassessment.* F1000Prime Rep, 2014. **6**: p. 13.
89. Atri, C., F.Z. Guerfali, and D. Laouini, *Role of Human Macrophage Polarization in Inflammation during Infectious Diseases.* Int J Mol Sci, 2018. **19**(6).
90. Wang, T., et al., *HIF1α-Induced Glycolysis Metabolism Is Essential to the Activation of Inflammatory Macrophages.* Mediators of Inflammation, 2017. **2017**: p. 9029327.
91. Kim, J., et al., *Synergistic Oxygen Generation and Reactive Oxygen Species Scavenging by Manganese Ferrite/Ceria Co-decorated Nanoparticles for Rheumatoid Arthritis Treatment.* ACS Nano, 2019. **13**(3): p. 3206-3217.

92. Wagener, J., et al., *Candida albicans Chitin Increases Arginase-1 Activity in Human Macrophages, with an Impact on Macrophage Antimicrobial Functions.* mBio, 2017. **8**(1).
93. Reales-Calderón, J.A., et al., *Proteomic characterization of human proinflammatory M1 and anti-inflammatory M2 macrophages and their response to Candida albicans.* Proteomics, 2014. **14**(12): p. 1503-18.
94. Gordon, S. and F.O. Martinez, *Alternative Activation of Macrophages: Mechanism and Functions.* Immunity, 2010. **32**(5): p. 593-604.
95. Stein, M., et al., *Interleukin 4 potently enhances murine macrophage mannose receptor activity: a marker of alternative immunologic macrophage activation.* J Exp Med, 1992. **176**(1): p. 287-92.
96. Sica, A. and A. Mantovani, *Macrophage plasticity and polarization: in vivo veritas.* The Journal of Clinical Investigation, 2012. **122**(3): p. 787-795.
97. Heller, N.M., et al., *Type I IL-4Rs selectively activate IRS-2 to induce target gene expression in macrophages.* Sci Signal, 2008. **1**(51): p. ra17.
98. Junttila, I.S., et al., *Tuning sensitivity to IL-4 and IL-13: differential expression of IL-4Rα, IL-13Rα1, and γc regulates relative cytokine sensitivity.* Journal of Experimental Medicine, 2008. **205**(11): p. 2595-2608.
99. Hershey, G.K.K., *IL-13 receptors and signaling pathways: An evolving web.* Journal of Allergy and Clinical Immunology, 2003. **111**(4): p. 677-690.
100. Lupardus, P.J., M.E. Birnbaum, and K.C. Garcia, *Molecular basis for shared cytokine recognition revealed in the structure of an unusually high affinity complex between IL-13 and IL-13Ralpha2.* Structure, 2010. **18**(3): p. 332-42.
101. Kawakami, K., et al., *The interleukin-13 receptor alpha2 chain: an essential component for binding and internalization but not for interleukin-13-induced signal transduction through the STAT6 pathway.* Blood, 2001. **97**(9): p. 2673-9.
102. Raes, G., et al., *Differential expression of FIZZ1 and Ym1 in alternatively versus classically activated macrophages.* Journal of Leukocyte Biology, 2002. **71**(4): p. 597-602.
103. Lopes, R.L., et al., *IL-10 is required for polarization of macrophages to M2-like phenotype by mycobacterial DnaK (heat shock protein 70).* Cytokine, 2016. **85**: p. 123-9.
104. Anthony, R.M., et al., *Memory T(H)2 cells induce alternatively activated macrophages to mediate protection against nematode parasites.* Nat Med, 2006. **12**(8): p. 955-60.
105. Zhao, A., et al., *Th2 cytokine-induced alterations in intestinal smooth muscle function depend on alternatively activated macrophages.* Gastroenterology, 2008. **135**(1): p. 217-225.e1.
106. Bleau, G., et al., *Mammalian chitinase-like proteins.* EXS, 1999. **87**: p. 211-221.
107. Hesse, M., et al., *Differential regulation of nitric oxide synthase-2 and arginase-1 by type 1/type 2 cytokines in vivo: granulomatous pathology is shaped by the pattern of L-arginine metabolism.* J Immunol, 2001. **167**(11): p. 6533-44.
108. Munitz, A., et al., *Distinct roles for IL-13 and IL-4 via IL-13 receptor alpha1 and the type II IL-4 receptor in asthma pathogenesis.* Proc Natl Acad Sci U S A, 2008. **105**(20): p. 7240-5.

109. Iqbal, S. and A. Kumar, *Characterization of in vitro generated human polarized macrophages.* J Clin Cell Immunol, 2015. **6**(06): p. 10.4172.
110. Duluc, D., et al., *Tumor-associated leukemia inhibitory factor and IL-6 skew monocyte differentiation into tumor-associated macrophage-like cells.* Blood, 2007. **110**(13): p. 4319-30.
111. Mantovani, A. and P. Allavena, *The interaction of anticancer therapies with tumor-associated macrophages.* Journal of Experimental Medicine, 2015. **212**(4): p. 435-445.
112. Mantovani, A., et al., *Cancer-related inflammation.* Nature, 2008. **454**(7203): p. 436-444.
113. Mantovani, A., et al., *Macrophage polarization: tumor-associated macrophages as a paradigm for polarized M2 mononuclear phagocytes.* Trends Immunol, 2002. **23**(11): p. 549-55.
114. Pan, Y., et al., *Tumor-Associated Macrophages in Tumor Immunity.* Frontiers in Immunology, 2020. **11**.
115. Muraoka, D., et al., *Antigen delivery targeted to tumor-associated macrophages overcomes tumor immune resistance.* J Clin Invest, 2019. **129**(3): p. 1278-1294.
116. Yin, M., et al., *Tumor-associated macrophages drive spheroid formation during early transcoelomic metastasis of ovarian cancer.* J Clin Invest, 2016. **126**(11): p. 4157-4173.
117. Trombetta, A.C., et al., *A circulating cell population showing both M1 and M2 monocyte/macrophage surface markers characterizes systemic sclerosis patients with lung involvement.* Respiratory Research, 2018. **19**(1): p. 186.
118. Hanahan, D. and R.A. Weinberg, *The hallmarks of cancer.* Cell, 2000. **100**(1): p. 57-70.
119. Gal-Yam, E.N., et al., *Cancer epigenetics: modifications, screening, and therapy.* Annu Rev Med, 2008. **59**: p. 267-80.
120. Sarkar, S., et al., *Demethylation and re-expression of epigenetically silenced tumor suppressor genes: sensitization of cancer cells by combination therapy.* Epigenomics, 2013. **5**(1): p. 87-94.
121. Hanahan, D. and R.A. Weinberg, *Hallmarks of cancer: the next generation.* Cell, 2011. **144**(5): p. 646-74.
122. Hallek, M., et al., *Guidelines for the diagnosis and treatment of chronic lymphocytic leukemia: a report from the International Workshop on Chronic Lymphocytic Leukemia updating the National Cancer Institute–Working Group 1996 guidelines.* Blood, 2008. **111**(12).
123. Dighiero, M. and T. Hamblin, *Chronic Lymphocytic Leukaemia.* The Lancet, 2008. **371**(9617).
124. Fayad, L., et al., *Interleukin-6 and interleukin-10 levels in chronic lymphocytic leukemia: correlation with phenotypic characteristics and outcome.* Blood, 2001. **97**.
125. Maffei, R., et al., *Physical Contact With Endothelial Cells Through B1- And B2-Integrins Rescues Chronic Lymphocytic Leukemia Cells From Spontaneous And Drug-Induced Apoptosis And Induces A Peculiar Gene Expression Profile In Leukemic Cells.* Haematologica, 2012. **97**(6).

126. Nguyen, P.-H., et al., *LYN Kinase in the Tumor Microenvironment Is Essential for the Progression of Chronic Lymphocytic Leukemia.* Cancer Cell, 2016. **30**(4).
127. Roberts, K.G., *Genetics and prognosis of ALL in children vs adults.* Hematology Am Soc Hematol Educ Program, 2018. **2018**(1): p. 137-145.
128. Dinner, S. and M. Liedtke, *Antibody-based therapies in patients with acute lymphoblastic leukemia.* Hematology Am Soc Hematol Educ Program, 2018. **2018**(1): p. 9-15.
129. Kotecha, R.S. and L.C. Cheung, *Targeting the bone marrow microenvironment: a novel therapeutic strategy for pre-B acute lymphoblastic leukemia.* Oncotarget, 2019. **10**(19): p. 1756-7.
130. Shin, W., et al., *The chemokine receptor CXCR4 enhances integrin-mediated in vitro adhesion and facilitates engraftment of leukemic precursor-B cells in the bone marrow.* Experimental Hematology, 2001. **29**(12).
131. Frazer, R., A.E. Irvine, and M.F. McMullin, *Chronic Myeloid Leukaemia in The 21st Century.* Ulster Med J, 2007. **76**(1): p. 8-17.
132. Goldman, J.M. and J.V. Melo, *Chronic myeloid leukemia--advances in biology and new approaches to treatment.* N Engl J Med, 2003. **349**(15): p. 1451-64.
133. Liersch, R., et al., *Expression of Osteopontin in the Bone Marrow of Patients with Acute Myeloid Leukemia.* Blood, 2009. **114**(22).
134. Kouchkovsky, I.D. and M. Abdul-Hay, *'Acute myeloid leukemia: a comprehensive review and 2016 update'.* Blood Cancer Journal, 2016. **6**(7).
135. Liersch, R., et al., *Prognostic factors for acute myeloid leukaemia in adults--biological significance and clinical use.* Br J Haematol, 2014. **165**(1): p. 17-38.
136. Battula, V.L., et al., *AML-induced osteogenic differentiation in mesenchymal stromal cells supports leukemia growth.* JCI Insight, 2017. **2**(13).
137. Kumar, S.K., et al., *Multiple myeloma.* Nat Rev Dis Primers, 2017. **3**: p. 17046.
138. Siegel, R.L., K.D. Miller, and A. Jemal, *Cancer statistics, 2016.* CA Cancer J Clin, 2016. **66**(1): p. 7-30.
139. UK, C.R. *Myeloma statistics*. 2015 2015-05-14 08/04/20]; Available from: https://www.cancerresearchuk.org/health-professional/cancer-statistics/statistics-by-cancer-type/myeloma.
140. Atkin, C., A. Richter, and E. Sapey, *What is the significance of monoclonal gammopathy of undetermined significance?* Clin Med (Lond), 2018. **18**(5): p. 391-6.
141. Kaufmann, H., et al., *Both IGH translocations and chromosome 13q deletions are early events in monoclonal gammopathy of undetermined significance and do not evolve during transition to multiple myeloma.* Leukemia, 2004. **18**(11): p. 1879-82.
142. Bianchi, G. and N.C. Munshi, *Pathogenesis beyond the cancer clone(s) in multiple myeloma.* Blood, 2015. **125**(20): p. 3049-58.
143. Rajkumar, S.V., *Updated Diagnostic Criteria and Staging System for Multiple Myeloma.* Am Soc Clin Oncol Educ Book, 2016. **35**: p. e418-23.
144. Rajkumar, S.V. and S. Kumar, *Multiple myeloma current treatment algorithms.* Blood Cancer Journal, 2020. **10**(9): p. 94.
145. Al Hamed, R., et al., *Current status of autologous stem cell transplantation for multiple myeloma.* Blood Cancer J, 2019. **9**(4): p. 44.

146. Kumar, S.K., et al., *Multiple Myeloma, Version 3.2021, NCCN Clinical Practice Guidelines in Oncology.* J Natl Compr Canc Netw, 2020. **18**(12): p. 1685-1717.
147. Teoh, P.J. and W.J. Chng, *CAR T-cell therapy in multiple myeloma: more room for improvement.* Blood Cancer Journal, 2021. **11**(4): p. 84.
148. Sadelain, M., R. Brentjens, and I. Rivière, *The basic principles of chimeric antigen receptor design.* Cancer Discov, 2013. **3**(4): p. 388-98.
149. Benmebarek, M.R., et al., *Killing Mechanisms of Chimeric Antigen Receptor (CAR) T Cells.* Int J Mol Sci, 2019. **20**(6).
150. Carpenter, R.O., et al., *B-cell maturation antigen is a promising target for adoptive T-cell therapy of multiple myeloma.* Clin Cancer Res, 2013. **19**(8): p. 2048-60.
151. Ghermezi, M., et al., *Serum B-cell maturation antigen: a novel biomarker to predict outcomes for multiple myeloma patients.* Haematologica, 2017. **102**(4): p. 785-795.
152. Munshi, N.C., et al., *Idecabtagene Vicleucel in Relapsed and Refractory Multiple Myeloma.* New England Journal of Medicine, 2021. **384**(8): p. 705-716.
153. Berdeja, J.G., et al., *Ciltacabtagene autoleucel, a B-cell maturation antigen-directed chimeric antigen receptor T-cell therapy in patients with relapsed or refractory multiple myeloma (CARTITUDE-1): a phase 1b/2 open-label study.* The Lancet, 2021. **398**(10297): p. 314-324.
154. Martin, T., et al., *Ciltacabtagene Autoleucel, an Anti–B-cell Maturation Antigen Chimeric Antigen Receptor T-Cell Therapy, for Relapsed/Refractory Multiple Myeloma: CARTITUDE-1 2-Year Follow-Up.* Journal of Clinical Oncology, 2022: p. JCO.22.00842.
155. Martino, M., et al., *CART-Cell Therapy: Recent Advances and New Evidence in Multiple Myeloma.* Cancers (Basel), 2021. **13**(11).
156. Samur, M.K., et al., *Biallelic Loss of BCMA Triggers Resistance to Anti-BCMA CAR T Cell Therapy in Multiple Myeloma.* Blood, 2020. **136**(Supplement 1): p. 14-14.
157. Yan, Z., et al., *Characteristics and Risk Factors of Cytokine Release Syndrome in Chimeric Antigen Receptor T Cell Treatment.* Frontiers in Immunology, 2021. **12**.
158. Cohen, A.D., et al., *Incidence and management of CAR-T neurotoxicity in patients with multiple myeloma treated with ciltacabtagene autoleucel in CARTITUDE studies.* Blood Cancer J, 2022. **12**(2): p. 32.
159. García-Ortiz, A., et al., *The Role of Tumor Microenvironment in Multiple Myeloma Development and Progression.* Cancers, 2021. **13**(2): p. 217.
160. Guillerey, C., et al., *Immune responses in multiple myeloma: role of the natural immune surveillance and potential of immunotherapies.* Cell Mol Life Sci, 2016. **73**(8): p. 1569-89.
161. Roccaro, A.M., et al., *SDF-1 inhibition targets the bone marrow niche for cancer therapy.* Cell Rep, 2014. **9**(1): p. 118-128.
162. Nefedova, Y., et al., *Involvement of Notch-1 signaling in bone marrow stroma-mediated de novo drug resistance of myeloma and other malignant lymphoid cell lines.* Blood, 2004. **103**(9): p. 3503-10.

163. Nefedova, Y., et al., *Inhibition of Notch signaling induces apoptosis of myeloma cells and enhances sensitivity to chemotherapy.* Blood, 2008. **111**(4): p. 2220-9.
164. Wang, J., et al., *Bone marrow stromal cell-derived exosomes as communicators in drug resistance in multiple myeloma cells.* Blood, 2014. **124**(4): p. 555-66.
165. Zhu, D., et al., *The Cyclophilin A-CD147 complex promotes the proliferation and homing of multiple myeloma cells.* Nat Med, 2015. **21**(6): p. 572-80.
166. Piddock, R.E., et al., *Myeloma-derived macrophage inhibitory factor regulates bone marrow stromal cell-derived IL-6 via c-MYC*, in *J Hematol Oncol*. 2018.
167. Zheng, Y., et al., *Role of Myeloma-Derived MIF in Myeloma Cell Adhesion to Bone Marrow and Chemotherapy Response.* J Natl Cancer Inst, 2016. **108**(11).
168. Sanderson, R.D. and Y. Yang, *Syndecan-1: A dynamic regulator of the myeloma microenvironment.* Clin Exp Metastasis, 2008. **25**(2): p. 149-59.
169. Hazlehurst, L.A., et al., *Adhesion to fibronectin via beta1 integrins regulates p27kip1 levels and contributes to cell adhesion mediated drug resistance (CAM-DR).* Oncogene, 2000. **19**(38): p. 4319-27.
170. Jelinek, T., B. Paiva, and R. Hajek, *Update on PD-1/PD-L1 Inhibitors in Multiple Myeloma.* Front Immunol, 2018. **9**.
171. Benson, D.M., Jr., et al., *The PD-1/PD-L1 axis modulates the natural killer cell versus multiple myeloma effect: a therapeutic target for CT-011, a novel monoclonal anti-PD-1 antibody.* Blood, 2010. **116**(13): p. 2286-94.
172. Gordon, S.R., et al., *PD-1 expression by tumour-associated macrophages inhibits phagocytosis and tumour immunity.* Nature, 2017. **545**(7655): p. 495-499.
173. Tai, Y.T., S.F. Cho, and K.C. Anderson, *Osteoclast Immunosuppressive Effects in Multiple Myeloma: Role of Programmed Cell Death Ligand 1.* Front Immunol, 2018. **9**.
174. Dairaghi, D.J., et al., *CCR1 blockade reduces tumor burden and osteolysis in vivo in a mouse model of myeloma bone disease.* Blood, 2012. **120**(7): p. 1449-57.
175. Liu, H., et al., *Reprogrammed marrow adipocytes contribute to myeloma-induced bone disease.* Science Translational Medicine, 2019. **11**(494): p. eaau9087.
176. Ruan, J., et al., *Heparanase inhibits osteoblastogenesis and shifts bone marrow progenitor cell fate in myeloma bone disease.* Bone, 2013. **57**(1): p. 10-17.
177. Trotter, T.N., et al., *Adipocyte-Lineage Cells Support Growth and Dissemination of Multiple Myeloma in Bone.* The American Journal of Pathology, 2016. **186**(11): p. 3054-3063.
178. Liu, Z., et al., *Mature adipocytes in bone marrow protect myeloma cells against chemotherapy through autophagy activation.* Oncotarget, 2015. **6**(33): p. 34329-41.
179. Hu, Y.L., et al., *Tumor cell autophagy as an adaptive response mediating resistance to treatments such as antiangiogenic therapy.* Cancer Res, 2012. **72**(17): p. 4294-9.

180. Urashima, M., et al., *The Development of a Model for the Homing of Multiple Myeloma Cells to Human Bone Marrow.* Blood, 1997. **90**(2): p. 754-765.
181. Butcher, E.C. and L.J. Picker, *Lymphocyte homing and homeostasis.* Science, 1996. **272**(5258): p. 60-6.
182. Sanz-Rodríguez, F., A. Hidalgo, and J. Teixidó, *Chemokine stromal cell-derived factor-1alpha modulates VLA-4 integrin-mediated multiple myeloma cell adhesion to CS-1/fibronectin and VCAM-1.* Blood, 2001. **97**(2): p. 346-51.
183. Okada, T., et al., *Significance of VLA-4-VCAM-1 interaction and CD44 for transendothelial invasion in a bone marrow metastatic myeloma model.* Clin Exp Metastasis, 1999. **17**(7): p. 623-9.
184. Möller, C., et al., *Expression and function of chemokine receptors in human multiple myeloma.* Leukemia, 2003. **17**(1): p. 203-10.
185. Broek, I.V., et al., *Chemokine receptor CCR2 is expressed by human multiple myeloma cells and mediates migration to bone marrow stromal cell-produced monocyte chemotactic proteins MCP-1, -2 and -3.* British Journal of Cancer, 2003. **88**(6): p. 855-862.
186. Alsayed, Y., et al., *Mechanisms of regulation of CXCR4/SDF-1 (CXCL12)-dependent migration and homing in multiple myeloma.* Blood, 2007. **109**(7): p. 2708-17.
187. Giuliani, N., et al., *CXCR3 and its binding chemokines in myeloma cells: expression of isoforms and potential relationships with myeloma cell proliferation and survival.* Haematologica, 2006. **91**(11): p. 1489-97.
188. Menu, E., et al., *Role of CCR1 and CCR5 in homing and growth of multiple myeloma and in the development of osteolytic lesions: a study in the 5TMM model.* Clin Exp Metastasis, 2006. **23**(5-6): p. 291-300.
189. Vande Broek, I., et al., *Extravasation and homing mechanisms in multiple myeloma.* Clinical & Experimental Metastasis, 2008. **25**(4): p. 325-334.
190. Opperman, K., et al., *Macrophages as a potential therapeutic target: Clodronate-liposome treatment inhibits multiple myeloma tumour establishment in vivo.* Clinical Lymphoma, Myeloma and Leukemia, 2019. **19**(10): p. e96.
191. Siekevitz, P., *Powerhouse of the Cell.* Scientific American, 1957. **197**(1): p. 131-144.
192. Sjostrand, F.S., *Electron Microscopy of Mitochondria and Cytoplasmic Double Membranes: Ultra-Structure of Rod-shaped Mitochondria.* Nature, 1953. **171**(4340): p. 30-31.
193. Zhao, R.Z., et al., *Mitochondrial electron transport chain, ROS generation and uncoupling (Review).* Int J Mol Med, 2019. **44**(1): p. 3-15.
194. Pebay-Peyroula, E., et al., *Structure of mitochondrial ADP/ATP carrier in complex with carboxyatractyloside.* Nature, 2003. **426**(6962): p. 39-44.
195. Davies, K.M., et al., *Macromolecular organization of ATP synthase and complex I in whole mitochondria.* Proc Natl Acad Sci U S A, 2011. **108**(34): p. 14121-6.
196. Sagan, L., *On the origin of mitosing cells.* J Theor Biol, 1967. **14**(3): p. 255-74.
197. Grazioli, S. and J. Putin, *Mitochondrial Damage-Associated Molecular Patterns: From Inflammatory Signaling to Human Diseases.* Frontiers in Immunology, 2018. **9**.

198. Zhang, Q., et al., *Circulating mitochondrial DAMPs cause inflammatory responses to injury.* Nature, 2010. **464**(7285): p. 104-7.
199. Palikaras, K., E. Lionaki, and N. Tavernarakis, *Mechanisms of mitophagy in cellular homeostasis, physiology and pathology.* Nature Cell Biology, 2018. **20**(9): p. 1013-1022.
200. Taanman, J.-W., *The mitochondrial genome: structure, transcription, translation and replication.* Biochimica et Biophysica Acta, 1999. **1410**(2).
201. Ngo, H.B., et al., *Distinct structural features of TFAM drive mitochondrial DNA packaging versus transcriptional activation.* Nature Communications, 2014. **5**(1): p. 1-12.
202. Wai, T., et al., *The Role of Mitochondrial DNA Copy Number in Mammalian Fertility1.* Biology of Reproduction, 2010. **83**(1): p. 52-62.
203. Hemmi, H., et al., *A Toll-like receptor recognizes bacterial DNA.* Nature, 2000. **408**(6813): p. 740-745.
204. Rongvaux, A., et al., *Apoptotic caspases prevent the induction of type I interferons by mitochondrial DNA.* Cell, 2014. **159**(7): p. 1563-77.
205. White, M.J., et al., *Apoptotic caspases suppress mtDNA-induced STING-mediated type I IFN production.* Cell, 2014. **159**(7): p. 1549-62.
206. Gordon, J.L., *Extracellular ATP: effects, sources and fate.* Biochemical Journal, 1986. **233**(2): p. 309-319.
207. Idzko, M., D. Ferrari, and H.K. Eltzschig, *Nucleotide signalling during inflammation.* Nature, 2014. **509**(7500): p. 310-317.
208. Elliott, M.R., et al., *Nucleotides released by apoptotic cells act as a find-me signal to promote phagocytic clearance.* Nature, 2009. **461**(7261): p. 282-286.
209. Chen, Y., et al., *ATP release guides neutrophil chemotaxis via P2Y2 and A3 receptors.* Science, 2006. **314**(5806): p. 1792-1795.
210. Kouzaki, H., et al., *The danger signal, extracellular ATP, is a sensor for an airborne allergen and triggers IL-33 release and innate Th2-type responses.* The Journal of Immunology, 2011. **186**(7): p. 4375-4387.
211. Idzko, M., et al., *Extracellular ATP triggers and maintains asthmatic airway inflammation by activating dendritic cells.* Nature medicine, 2007. **13**(8): p. 913-919.
212. Di Virgilio, F., et al., *Extracellular ATP and P2 purinergic signalling in the tumour microenvironment.* Nature Reviews Cancer, 2018. **18**(10): p. 601-618.
213. Hewinson, J., et al., *A key role for redox signaling in rapid P2X7 receptor-induced IL-1β processing in human monocytes.* The Journal of Immunology, 2008. **180**(12): p. 8410-8420.
214. Fairbairn, I.P., et al., *ATP-mediated killing of intracellular mycobacteria by macrophages is a P2X7-dependent process inducing bacterial death by phagosome-lysosome fusion.* The Journal of Immunology, 2001. **167**(6): p. 3300-3307.
215. Placido, R., et al., *P2X(7) purinergic receptors and extracellular ATP mediate apoptosis of human monocytes/macrophages infected with Mycobacterium tuberculosis reducing the intracellular bacterial viability.* Cell Immunol, 2006. **244**(1): p. 10-8.

216. Ghiringhelli, F., et al., *Activation of the NLRP3 inflammasome in dendritic cells induces IL-1beta-dependent adaptive immunity against tumors.* Nat Med, 2009. **15**(10): p. 1170-8.
217. Vénéreau, E., C. Ceriotti, and M.E. Bianchi, *DAMPs from Cell Death to New Life.* Frontiers in Immunology, 2015. **6**(422).
218. Campbell, C.T., J.E. Kolesar, and B.A. Kaufman, *Mitochondrial transcription factor A regulates mitochondrial transcription initiation, DNA packaging, and genome copy number.* Biochim Biophys Acta, 2012. **1819**(9-10): p. 921-9.
219. Chaung, W.W., et al., *Mitochondrial transcription factor A is a proinflammatory mediator in hemorrhagic shock.* Int J Mol Med, 2012. **30**(1): p. 199-203.
220. Crouser, E.D., et al., *Monocyte activation by necrotic cells is promoted by mitochondrial proteins and formyl peptide receptors.* Crit Care Med, 2009. **37**(6): p. 2000-9.
221. Julian, M.A., et al., *Mitochondrial Transcription Factor A, an Endogenous Danger Signal, Promotes TNFα Release via RAGE- and TLR9-Responsive Plasmacytoid Dendritic Cells.* PLoS ONE, 2013. **8**(8).
222. Scaffidi, P., T. Misteli, and M.E. Bianchi, *Release of chromatin protein HMGB1 by necrotic cells triggers inflammation.* Nature, 2002. **418**(6894): p. 191-195.
223. Pandolfi, F., et al., *Key Role of DAMP in Inflammation, Cancer, and Tissue Repair.* Clinical Therapeutics, 2016. **38**(5): p. 1017-1028.
224. Frank, M.G., et al., *Stress sounds the alarmin: the role of the danger-associated molecular pattern HMGB1 in stress-induced neuroinflammatory priming.* Brain, behavior, and immunity, 2015. **48**: p. 1-7.
225. Kokkola, R., et al., *RAGE is the major receptor for the proinflammatory activity of HMGB1 in rodent macrophages.* Scandinavian journal of immunology, 2005. **61**(1): p. 1-9.
226. Fiuza, C., et al., *Inflammation-promoting activity of HMGB1 on human microvascular endothelial cells.* Blood, The Journal of the American Society of Hematology, 2003. **101**(7): p. 2652-2660.
227. Tian, J., et al., *Toll-like receptor 9–dependent activation by DNA-containing immune complexes is mediated by HMGB1 and RAGE.* Nature immunology, 2007. **8**(5): p. 487-496.
228. Urbonaviciute, V., et al., *Induction of inflammatory and immune responses by HMGB1–nucleosome complexes: implications for the pathogenesis of SLE.* The Journal of experimental medicine, 2008. **205**(13): p. 3007-3018.
229. Yang, H., H. Wang, and U. Andersson, *Targeting Inflammation Driven by HMGB1.* Frontiers in Immunology, 2020. **11**(484).
230. Panaro, M.A., et al., *Biological role of the N-formyl peptide receptors.* Immunopharmacol Immunotoxicol, 2006. **28**(1): p. 103-27.
231. Czapiga, M., et al., *Human platelets exhibit chemotaxis using functional N-formyl peptide receptors.* Exp Hematol, 2005. **33**(1): p. 73-84.
232. Wenceslau, C.F., et al., *Mitochondrial N-formyl peptides cause airway contraction and lung neutrophil infiltration via formyl peptide receptor activation.* Pulm Pharmacol Ther, 2016. **37**: p. 49-56.
233. Dudek, J., *Role of Cardiolipin in Mitochondrial Signaling Pathways.* Frontiers Cell and Developmental Biology, 2017. **5**.

234. Iyer, S.S., et al., *Mitochondrial cardiolipin is required for Nlrp3 inflammasome activation.* Immunity, 2013. **39**(2): p. 311-323.
235. Dieude, M., et al., *Cardiolipin binds to CD1d and stimulates CD1d-restricted gammadelta T cells in the normal murine repertoire.* J Immunol, 2011. **186**(8): p. 4771-81.
236. Ott, M., B. Zhivotovsky, and S. Orrenius, *Role of cardiolipin in cytochrome c release from mitochondria.* Cell Death Differ, 2007. **14**(7): p. 1243-7.
237. Kuhlbrandt, W., *Structure and function of mitochondrial membrane protein complexes.* BMC Biol, 2015. **13**: p. 89.
238. Shakeri, R., A. Kheirollahi, and J. Davoodi, *Apaf-1: Regulation and function in cell death.* Biochimie, 2017. **135**: p. 111-125.
239. Li, P., et al., *Cytochrome c and dATP-dependent formation of Apaf-1/caspase-9 complex initiates an apoptotic protease cascade.* Cell, 1997. **91**(4): p. 479-89.
240. Adachi, N., et al., *Serum cytochrome c level as a prognostic indicator in patients with systemic inflammatory response syndrome.* Clin Chim Acta, 2004. **342**(1-2): p. 127-36.
241. Takeda, K. and S. Akira, *Toll-like receptors in innate immunity.* Int Immunol, 2005. **17**(1): p. 1-14.
242. Medzhitov, R., P. Preston-Hurlburt, and C.A. Janeway, Jr., *A human homologue of the Drosophila Toll protein signals activation of adaptive immunity.* Nature, 1997. **388**(6640): p. 394-7.
243. Kawasaki, T. and T. Kawai, *Toll-like receptor signaling pathways.* Front Immunol, 2014. **5**: p. 461.
244. Deguine, J. and G.M. Barton, *MyD88: a central player in innate immune signaling*, in *F1000Prime Rep*. 2014.
245. Zhang, Q., I. , Kiyoshi, and C.J. Hauser, *Mitochondrial DNA is released by shock and activates neutrophils via P38 MAP Kinase.* Shock, 2010. **34**(1).
246. Nakayama, H. and K. Otsu, *Mitochondrial DNA as an inflammatory mediator in cardiovascular diseases | Biochemical Journal | Portland Press.* Biochemical Journal, 2018. **475**(5).
247. Broz, P. and V.M. Dixit, *Inflammasomes: mechanism of assembly, regulation and signalling.* Nat Rev Immunol, 2016. **16**(7): p. 407-20.
248. Lamkanfi, M. and V.M. Dixit, *Mechanisms and functions of inflammasomes.* Cell, 2014. **157**(5): p. 1013-22.
249. Gross, O., et al., *The inflammasome: an integrated view.* Immunol Rev, 2011. **243**(1): p. 136-51.
250. Nakahira, K., et al., *Autophagy proteins regulate innate immune responses by inhibiting the release of mitochondrial DNA mediated by the NALP3 inflammasome.* Nat Immunol, 2011. **12**(3): p. 222-30.
251. Shimada, K., et al., *Oxidized mitochondrial DNA activates the NLRP3 inflammasome during apoptosis.* Immunity, 2012. **36**(3): p. 401-14.
252. Zhou, R., et al., *A role for mitochondria in NLRP3 inflammasome activation.* Nature, 2011. **469**(7329): p. 221-5.
253. Hornung, V., et al., *AIM2 recognizes cytosolic dsDNA and forms a caspase-1-activating inflammasome with ASC.* Nature, 2009. **458**(7237): p. 514-8.

254. Neeper, M., et al., *Cloning and expression of a cell surface receptor for advanced glycosylation end products of proteins.* J Biol Chem, 1992. **267**(21): p. 14998-5004.
255. Watanabe, H. and M. Son, *The Immune Tolerance Role of the HMGB1-RAGE Axis.* Cells, 2021. **10**(3).
256. Sakaguchi, M., et al., *TIRAP, an adaptor protein for TLR2/4, transduces a signal from RAGE phosphorylated upon ligand binding.* PLoS One, 2011. **6**(8): p. e23132.
257. Wenceslau, C.F., et al., *Mitochondrial-derived N-formyl peptides: Novel links between trauma, vascular collapse and sepsis.* Medical Hypotheses, 2013. **81**(4): p. 532-535.
258. Hazeldine, J., et al., *N-Formyl peptides drive mitochondrial damage associated molecular pattern induced neutrophil activation through ERK1/2 and P38 MAP kinase signalling pathways.* Injury, 2015. **46**(6): p. 975-84.
259. Dorward, D.A., et al., *The Role of Formylated Peptides and Formyl Peptide Receptor 1 in Governing Neutrophil Function during Acute Inflammation*, in *Am J Pathol*. 2015. p. 1172-84.
260. Sun, L., et al., *Cyclic GMP-AMP synthase is a cytosolic DNA sensor that activates the type I interferon pathway.* Science, 2013. **339**(6121): p. 786-91.
261. Rodriguez-Nuevo, A. and A. Zorzano, *The sensing of mitochondrial DAMPs by non-immune cells.* Cell Stress, 2019. **3**(6): p. 195-207.
262. Ishikawa, H. and G.N. Barber, *STING is an endoplasmic reticulum adaptor that facilitates innate immune signalling.* Nature, 2008. **455**(7213): p. 674-678.
263. Tanaka, Y. and Z.J. Chen, *STING specifies IRF3 phosphorylation by TBK1 in the cytosolic DNA signaling pathway.* Sci Signal, 2012. **5**(214): p. ra20.
264. Zhang, J., et al., *Guanylate-binding protein 2 regulates Drp1-mediated mitochondrial fission to suppress breast cancer cell invasion.* Cell Death & Disease, 2017. **8**(10): p. e3151-e3151.
265. Chikhalya, A., et al., *Human IFIT3 Protein Induces Interferon Signaling and Inhibits Adenovirus Immediate Early Gene Expression.* mBio, 2021. **12**(6): p. e02829-21.
266. Davies, M.G. and P.-O. Hagen, *Systemic inflammatory response syndrome.* British Journal of Surgery, 2005. **84**(7): p. 920-935.
267. Itagaki, K., et al., *Role of Mitochondria-Derived Danger Signals Released After Injury in Systemic Inflammation and Sepsis.* Antioxidants & Redox Signaling, 2021. **35**(15): p. 1273-1290.
268. Kung, C.-T., et al., *Plasma nuclear and mitochondrial DNA levels as predictors of outcome in severe sepsis patients in the emergency room.* Journal of Translational Medicine, 2012. **10**(1): p. 130.
269. Schneck, E., et al., *Blood Levels of Free-Circulating Mitochondrial DNA in Septic Shock and Postsurgical Systemic Inflammation and Its Influence on Coagulation: A Secondary Analysis of a Prospective Observational Study.* Journal of Clinical Medicine, 2020. **9**(7).
270. Hu, Q., et al., *Elevated Levels of Plasma Mitochondrial DNA Are Associated with Clinical Outcome in Intra-Abdominal Infections Caused by Severe Trauma.* Surgical Infections, 2017. **18**(5): p. 610-618.

271. Gu, X., et al., *The plasma mitochondrial DNA is an independent predictor for post-traumatic systemic inflammatory response syndrome.* PLoS One, 2013. **8**(8): p. e72834.
272. Yamanouchi, S., et al., *Plasma mitochondrial DNA levels in patients with trauma and severe sepsis: time course and the association with clinical status.* J Crit Care, 2013. **28**(6): p. 1027-31.
273. Simmons, J.D., et al., *Elevated levels of plasma mitochondrial DNA DAMPs are linked to clinical outcome in severely injured human subjects.* Ann Surg, 2013. **258**(4): p. 591-6; discussion 596-8.
274. Pullerits, R., et al., *Extracellular cytochrome c, a mitochondrial apoptosis-related protein, induces arthritis.* Rheumatology, 2005. **44**(1): p. 32-39.
275. McInnes, I.B. and G. Schett, *The pathogenesis of rheumatoid arthritis.* N Engl J Med, 2011. **365**(23): p. 2205-19.
276. Hajizadeh, S., et al., *Extracellular mitochondrial DNA and oxidatively damaged DNA in synovial fluid of patients with rheumatoid arthritis.* Arthritis Res Ther, 2003. **5**(5): p. R234-40.
277. Goldstein, R.S., et al., *Cholinergic anti-inflammatory pathway activity and High Mobility Group Box-1 (HMGB1) serum levels in patients with rheumatoid arthritis.* Mol Med, 2007. **13**(3-4): p. 210-5.
278. Andersson, U., et al., *High mobility group 1 protein (HMG-1) stimulates proinflammatory cytokine synthesis in human monocytes.* J Exp Med, 2000. **192**(4): p. 565-70.
279. Schierbeck, H., et al., *Monoclonal anti-HMGB1 (high mobility group box chromosomal protein 1) antibody protection in two experimental arthritis models.* Mol Med, 2011. **17**(9-10): p. 1039-44.
280. Abdulahad, D.A., et al., *High mobility group box 1 (HMGB1) and anti-HMGB1 antibodies and their relation to disease characteristics in systemic lupus erythematosus.* Arthritis Res Ther, 2011. **13**(3): p. R71.
281. Tumburu, L., et al., *Circulating mitochondrial DNA is a proinflammatory DAMP in sickle cell disease.* Blood, 2021. **137**(22): p. 3116-3126.
282. Barbu, E.A., et al., *Neutrophils remain detrimentally active in hydroxyurea-treated patients with sickle cell disease.* PLOS ONE, 2019. **14**(12): p. e0226583.
283. Calfee, C.S., et al., *Acute respiratory distress syndrome subphenotypes and differential response to simvastatin: secondary analysis of a randomised controlled trial.* Lancet Respir Med, 2018. **6**(9): p. 691-698.
284. Hernandez-Beeftink, T., et al. *Mitochondrial DNA in peripheral blood as a prognostic biomarker of acute respiratory distress syndrome*. in *EUROPEAN JOURNAL OF HUMAN GENETICS*. 2020. SPRINGERNATURE CAMPUS, 4 CRINAN ST, LONDON, N1 9XW, ENGLAND.
285. Mao, J.-y., et al., *Plasma mitochondrial DNA levels are associated with acute lung injury and mortality in septic patients.* BMC Pulmonary Medicine, 2021. **21**(1): p. 66.
286. Ray, N.B., et al., *Dynamic regulation of cardiolipin by the lipid pump Atp8b1 determines the severity of lung injury in experimental pneumonia.* Nat Med, 2010. **16**(10): p. 1120-1127.
287. Lusuardi, M., et al., *Role of Surfactant in Chronic Obstructive Pulmonary Disease: Therapeutic Implications.* Respiration, 1992. **59**(1): p. 28-32.

288. Garg, M., et al., *Cardiolipin-mediated PPARγ S112 phosphorylation impairs IL-10 production and inflammation resolution during bacterial pneumonia.* Cell Rep, 2021. **34**(6): p. 108736.
289. Remels, A.H., et al., *Peroxisome proliferator-activated receptor expression is reduced in skeletal muscle in COPD.* 2007.
290. Lommatzsch, M., et al., *Extracellular adenosine triphosphate and chronic obstructive pulmonary disease.* Am J Respir Crit Care Med, 2010. **181**(9): p. 928-34.
291. Lucattelli, M., et al., *P2X7 receptor signaling in the pathogenesis of smoke-induced lung inflammation and emphysema.* Am J Respir Cell Mol Biol, 2011. **44**(3): p. 423-9.
292. Alleyne, T., J. Joseph, and V. Sampson, *Cytochrome-c detection: a diagnostic marker for myocardial infarction.* Appl Biochem Biotechnol, 2001. **90**(2): p. 97-105.
293. Kang, D., S.H. Kim, and N. Hamasaki, *Mitochondrial transcription factor A (TFAM): roles in maintenance of mtDNA and cellular functions.* Mitochondrion, 2007. **7**(1-2): p. 39-44.
294. Tsai, N.W., et al., *The value of serial plasma nuclear and mitochondrial DNA levels in patients with acute ischemic stroke.* Clin Chim Acta, 2011. **412**(5-6): p. 476-9.
295. Bliksoen, M., et al., *Increased circulating mitochondrial DNA after myocardial infarction*, in *Int J Cardiol*. 2012: Netherlands. p. 132-4.
296. Stachon, P., et al., *Extracellular ATP Induces Vascular Inflammation and Atherosclerosis via Purinergic Receptor Y2 in Mice.* Arterioscler Thromb Vasc Biol, 2016. **36**(8): p. 1577-86.
297. Pinti, M., D. Ferraro, and M. Nasi, *Microglia activation: a role for mitochondrial DNA?* Neural Regeneration Research, 2021. **16**(12): p. 2393-2394.
298. Wilkins, H.M., et al., *Mitochondria-Derived Damage-Associated Molecular Patterns in Neurodegeneration.* Front Immunol, 2017. **8**: p. 508.
299. Venegas, C. and M.T. Heneka, *Danger-associated molecular patterns in Alzheimer's disease.* J Leukoc Biol, 2017. **101**(1): p. 87-98.
300. Festoff, B.W., et al., *HMGB1 and thrombin mediate the blood-brain barrier dysfunction acting as biomarkers of neuroinflammation and progression to neurodegeneration in Alzheimer's disease.* J Neuroinflammation, 2016. **13**(1): p. 194.
301. Herrero, M.T., et al., *Inflammation in Parkinson's disease: role of glucocorticoids.* Front Neuroanat, 2015. **9**: p. 32.
302. Yang, Y., et al., *High expression of the HMGB1-TLR4 axis and its downstream signaling factors in patients with Parkinson's disease and the relationship of pathological staging.* Brain Behav, 2018. **8**(4): p. e00948.
303. Sasaki, T., et al., *Anti-high mobility group box 1 antibody exerts neuroprotection in a rat model of Parkinson's disease.* Exp Neurol, 2016. **275 Pt 1**: p. 220-31.
304. Gao, X., et al., *Formyl-methionyl-leucyl-phenylalanine-induced dopaminergic neurotoxicity via microglial activation: a mediator between peripheral*

infection and neurodegeneration? Environ Health Perspect, 2008. **116**(5): p. 593-8.
305. Medzhitov, R., *Origin and physiological roles of inflammation.* Nature, 2008. **454**(7203): p. 428-435.
306. Greten, F.R. and S.I. Grivennikov, *Inflammation and Cancer: Triggers, Mechanisms, and Consequences.* Immunity, 2019. **51**(1): p. 27-41.
307. Greten, F.R., et al., *IKKβ Links Inflammation and Tumorigenesis in a Mouse Model of Colitis-Associated Cancer.* Cell, 2004. **118**(3): p. 285-296.
308. Liu, T., et al., *NF-κB signaling in inflammation.* Signal Transduction and Targeted Therapy, 2017. **2**(1): p. 17023.
309. Suarez-Carmona, M., et al., *EMT and inflammation: inseparable actors of cancer progression.* Molecular Oncology, 2017. **11**(7): p. 805-823.
310. López-Novoa, J.M. and M.A. Nieto, *Inflammation and EMT: an alliance towards organ fibrosis and cancer progression.* EMBO Mol Med, 2009. **1**(6-7): p. 303-14.
311. Aran, D., et al., *Widespread parainflammation in human cancer.* Genome Biology, 2016. **17**(1): p. 145.
312. Pesic, M. and F.R. Greten, *Inflammation and cancer: tissue regeneration gone awry.* Curr Opin Cell Biol, 2016. **43**: p. 55-61.
313. Afrifa, J., T. Zhao, and J. You, *Circulating Mitochondria DNA, a non-invasive cancer diagnostic biomarker candidate.* Mitochondrion, 2019. **47**.
314. Ellinger, J., et al., *Circulating mitochondrial DNA in serum: a universal diagnostic biomarker for patients with urological malignancies.* Urol Oncol, 2012. **30**(4): p. 509-15.
315. Mehra, N., et al., *Circulating mitochondrial nucleic acids have prognostic value for survival in patients with advanced prostate cancer.* Clin Cancer Res, 2007. **13**(2 Pt 1): p. 421-6.
316. Zachariah, R.R., et al., *Levels of circulating cell-free nuclear and mitochondrial DNA in benign and malignant ovarian tumors.* Obstet Gynecol, 2008. **112**(4): p. 843-50.
317. Yu, M., Y.F. Wan, and Q.H. Zou, *Cell-free circulating mitochondrial DNA in the serum: a potential non-invasive biomarker for Ewing's sarcoma.* Arch Med Res, 2012. **43**(5): p. 389-94.
318. Kohler, C., et al., *Levels of plasma circulating cell free nuclear and mitochondrial DNA as potential biomarkers for breast tumors.* Mol Cancer, 2009. **8**: p. 105.
319. Osaka, A., et al., *A novel role of serum cytochrome c as a tumor marker in patients with operable cancer.* J Cancer Res Clin Oncol, 2009. **135**(3): p. 371-7.
320. Javid, J., et al., *Extracellular cytochrome c as a biomarker for monitoring therapeutic efficacy and prognosis of non-small cell lung cancer patients.* Tumour Biol, 2015. **36**(6): p. 4253-60.
321. Moore, J.A., et al., *LC3-associated phagocytosis in bone marrow macrophages suppresses acute myeloid leukemia progression through STING activation.* Journal of Clinical Investigation, 2022. **132**(5).

322. Perdas, E., et al., *Altered levels of circulating nuclear and mitochondrial DNA in patients with Papillary Thyroid Cancer.* Scientific Reports, 2019. **9**(1): p. 1-7.
323. Ruiz-Heredia, Y., et al., *Pathogenetic and Prognostic Implications of Increased Mitochondrial Content in Multiple Myeloma.* Cancers (Basel), 2021. **13**(13).
324. Radl, J., et al., *Idiopathic Paraproteinemia. II. Transplantation of the Paraprotein-Producing Clone From Old to Young C57BL/KaLwRij Mice.* Journal of immunology (Baltimore, Md. : 1950), 1979. **122**(2).
325. Radl, J., et al., *Animal model of human disease. Multiple myeloma.* Am J Pathol, 1988. **132**(3): p. 593-7.
326. Decout, A., et al., *The cGAS–STING pathway as a therapeutic target in inflammatory diseases.* Nature Reviews Immunology, 2021. **21**(9): p. 548-569.
327. Barber, G.N., *Innate immune DNA sensing pathways: STING, AIMII and the regulation of interferon production and inflammatory responses.* Curr Opin Immunol, 2011. **23**(1): p. 10-20.
328. Opperman, K.S., et al., *Macrophages in multiple myeloma: key roles and therapeutic strategies.* Cancer Metastasis Rev, 2021. **40**(1): p. 273-284.
329. Berardi, S., et al., *Multiple myeloma macrophages: pivotal players in the tumor microenvironment.* J Oncol, 2013. **2013**: p. 183602.
330. Chen, H., et al., *Increase in M2 Macrophage Polarization in Multiple Myeloma Bone Marrow is Inhibited with the JAK2 Inhibitor Ruxolitinib Which Shows Anti-MM Effects.* Clinical Lymphoma, Myeloma and Leukemia, 2017. **17**(1): p. e93.
331. Honda, K., et al., *IRF-7 is the master regulator of type-I interferon-dependent immune responses.* Nature, 2005. **434**(7034): p. 772-777.
332. Hong, C., et al., *cGAS–STING drives the IL-6-dependent survival of chromosomally instable cancers.* Nature, 2022. **607**(7918): p. 366-373.
333. Krieg, A.M., et al., *CpG motifs in bacterial DNA trigger direct B-cell activation.* Nature, 1995. **374**(6522): p. 546-549.
334. Haag, S.M., et al., *Targeting STING with covalent small-molecule inhibitors.* Nature, 2018. **559**(7713): p. 269-273.
335. Yu, X., et al., *Dissecting the effects of mtDNA variations on complex traits using mouse conplastic strains.* Genome Res, 2009. **19**(1): p. 159-65.
336. Mistry, J.J., *'Investigation of the metabolic changes in the haematopoietic stem cell compartment in response to stress'*, in *Norwich Medical School*. 2021, University of East Anglia.
337. Beyar-Katz, O., et al., *Proinflammatory Macrophages Promote Multiple Myeloma Resistance to Bortezomib Therapy.* Molecular Cancer Research, 2019. **17**(11): p. 2331-2340.
338. Sica, A., P. Allavena, and A. Mantovani, *Cancer related inflammation: the macrophage connection.* Cancer Lett, 2008. **267**(2): p. 204-15.
339. Green, C.E., et al., *Chemoattractant Signaling between Tumor Cells and Macrophages Regulates Cancer Cell Migration, Metastasis and Neovascularization.* PLOS ONE, 2009. **4**(8): p. e6713.
340. Wongchana, W. and T. Palaga, *Direct regulation of interleukin-6 expression by Notch signaling in macrophages.* Cellular & Molecular Immunology, 2012. **9**(2): p. 155-162.

341. Ou, L., et al., *The cGAS-STING Pathway: A Promising Immunotherapy Target.* Front Immunol, 2021. **12**: p. 795048.
342. Jafari, A., et al., *Myeloma-bone marrow adipocyte axis in tumour survival and treatment response.* British Journal of Cancer, 2021. **125**(6): p. 775-777.
343. Pellegrino, A., et al., *CXCR3-binding chemokines in multiple myeloma.* Cancer Lett, 2004. **207**(2): p. 221-7.
344. van Rooijen, N. and E. Hendrikx, *Liposomes for specific depletion of macrophages from organs and tissues.* Methods Mol Biol, 2010. **605**: p. 189-203.
345. Hemminki, K., A. Försti, and M. Hansson, *Incidence, mortality and survival in multiple myeloma compared to other hematopoietic neoplasms in Sweden up to year 2016.* Scientific Reports, 2021. **11**(1): p. 17272.
346. Mohty, M., et al., *Understanding mortality in multiple myeloma: Findings of a European retrospective chart review.* European Journal of Haematology, 2019. **103**(2): p. 107-115.
347. Kawano, Y., et al., *Targeting the bone marrow microenvironment in multiple myeloma.* Immunol Rev, 2015. **263**(1): p. 160-72.
348. Vo, J.N., et al., *The genetic heterogeneity and drug resistance mechanisms of relapsed refractory multiple myeloma.* Nature Communications, 2022. **13**(1): p. 3750.
349. Trumpff, C., et al., *Stress and circulating cell-free mitochondrial DNA: A systematic review of human studies, physiological considerations, and technical recommendations.* Mitochondrion, 2021. **59**: p. 225-245.
350. Koppenol, W.H., P.L. Bounds, and C.V. Dang, *Otto Warburg's contributions to current concepts of cancer metabolism.* Nat Rev Cancer, 2011. **11**(5): p. 325-37.
351. Rosa, H.S., et al., *A case for measuring both cellular and cell-free mitochondrial DNA as a disease biomarker in human blood.* The FASEB Journal, 2020. **34**(9): p. 12278-12288.
352. Lindqvist, D., et al., *Circulating cell-free mitochondrial DNA, but not leukocyte mitochondrial DNA copy number, is elevated in major depressive disorder.* Neuropsychopharmacology, 2018. **43**(7): p. 1557-1564.
353. Zhan, X., et al., *Alteration of mitochondrial biogenesis promotes disease progression in multiple myeloma.* Oncotarget, 2017. **8**(67): p. 111213-111224.
354. Zavidij, O., et al., *Single-cell RNA sequencing reveals compromised immune microenvironment in precursor stages of multiple myeloma.* Nat Cancer, 2020. **1**(5): p. 493-506.
355. Zheng, Y., et al., *Macrophages are an abundant component of myeloma microenvironment and protect myeloma cells from chemotherapy drug-induced apoptosis.* Blood, 2009. **114**(17): p. 3625-8.
356. Jing, W., et al., *STING agonist inflames the pancreatic cancer immune microenvironment and reduces tumor burden in mouse models.* Journal for ImmunoTherapy of Cancer, 2019. **7**(1): p. 115.
357. Guerini, D., *STING Agonists/Antagonists: Their Potential as Therapeutics and Future Developments.* Cells, 2022. **11**(7): p. 1159.
358. Ding, C., et al., *Small molecules targeting the innate immune cGAS–STING–TBK1 signaling pathway.* Acta Pharm Sin B, 2020. **10**(12): p. 2272-2298.

359. Meric-Bernstam, F., et al., *Phase I Dose-Escalation Trial of MIW815 (ADU-S100), an Intratumoral STING Agonist, in Patients with Advanced/Metastatic Solid Tumors or Lymphomas.* Clin Cancer Res, 2022. **28**(4): p. 677-688.
360. de Jong, M.M.E., et al., *The multiple myeloma microenvironment is defined by an inflammatory stromal cell landscape.* Nature Immunology, 2021. **22**(6): p. 769-780.
361. Aldinucci, D. and A. Colombatti, *The inflammatory chemokine CCL5 and cancer progression.* Mediators Inflamm, 2014. **2014**: p. 292376.
362. Lepsenyi, M., et al., *CXCL2-CXCR2 axis mediates αV integrin-dependent peritoneal metastasis of colon cancer cells.* Clin Exp Metastasis, 2021. **38**(4): p. 401-410.

8 Appendix

Table 8.1. MM patient information from MM samples used

PATIENT NO.	AGE (YEARS)	SEX	DIAGNOSIS
MM1	59	F	Myeloma (s)
MM2	74	F	Myeloma (s)
MM3	72	F	Myeloma (s)
MM4	80	M	Myeloma (a)
MM5	37	M	Myeloma (s)
MM6	79	F	Myeloma (s)
MM7	69	M	Myeloma (a)
MM8	57	M	Myeloma (s)
MM9	66	F	Myeloma (s)
MM10	82	F	Myeloma (a)
MM11	74	M	Myeloma (a)
MM12	53	F	Myeloma (s)
MM13	64	M	Myeloma (s)
MM14	73	M	Myeloma (s)
MM15	75	F	Myeloma (s)
MM16	55	M	Myeloma (s)
MM17	75	F	Myeloma (s)
MM18	86	M	Myeloma (a)
MM19	83	F	Myeloma (a)

F, Female; M, Male; a, Asymptomatic; s, Symptomatic.